FREE FALL IMPACT PENETRATION TESTS ON SOILS

CENTRE FOR NEWFOUNDLAND STUDIES

TOTAL OF 10 PAGES ONLY
MAY BE XEROXED

(Without Author's Permission)

SAURENDRANATH CHAUDHURI

000230


CENTRE FOR REGL. STUDIES
JAN 29 1981
MEMORIAL UNIVERSITY
OF NEWFOUNDLAND

National Library of Canada

Cataloguing Branch
Canadian Theses Division

Ottawa, Canada
K1A 0N4

Bibliothèque nationale du Canada

Direction du catalogage
Division des thèses canadiennes

NOTICE

The quality of this microfiche is heavily dependent upon the quality of the original thesis submitted for microfilming. Every effort has been made to ensure the highest quality of reproduction possible.

If pages are missing, contact the university which granted the degree.

Some pages may have indistinct print especially if the original pages were typed with a poor typewriter ribbon or if the university sent us a poor photocopy.

Previously copyrighted materials (journal articles, published tests, etc.) are not filmed.

Reproduction in full or in part of this film is governed by the Canadian Copyright Act, R.S.C. 1970, c. C-30. Please read the authorization forms which accompany this thesis.

THIS DISSERTATION
HAS BEEN MICROFILMED
EXACTLY AS RECEIVED

AVIS

La qualité de cette microfiche dépend grandement de la qualité de la thèse soumise au microfilmage. Nous avons tout fait pour assurer une qualité supérieure de reproduction.

S'il manque des pages, veuillez communiquer avec l'université qui a conféré le grade.

La qualité d'impression de certaines pages peut laisser à désirer, surtout si les pages originales ont été dactylographiées à l'aide d'un ruban usé ou si l'université nous a fait parvenir une photocopie de mauvaise qualité.

Les documents qui font déjà l'objet d'un droit d'auteur (articles de revue, examens publiés, etc.) ne sont pas microfilmés.

La reproduction, même partielle, de ce microfilm est soumise à la Loi canadienne sur le droit d'auteur, SRC 1970, c. C-30. Veuillez prendre connaissance des formules d'autorisation qui accompagnent cette thèse.

LA THÈSE A ÉTÉ
MICROFILMÉE TELLE QUE
NOUS L'AVONS REÇUE

FREE FALL IMPACT PENETRATION TESTS ON SOILS

Saurendranath Chaudhuri, B.E. (Civil) ©

A Thesis submitted in partial fulfillment

of the requirements for the degree of

Master of Engineering

Faculty of Engineering

Memorial University of Newfoundland

August 1979

St. John's Newfoundland

Canada

FREE FALL IMPACT PENETRATION TESTS ON SOILS

TO MY PARENTS

ABSTRACT

The hydrosphere which is still the unexplored frontier of our planet is receiving the special attention of scientists and engineers because of its vast potential. A comprehensive knowledge of the properties of marine sediments is essential for most engineering activities in the oceans. A free fall penetrometer designed and developed at Memorial University is a potential tool for a quick and economical evaluation of the geotechnical properties of the top few metres of surficial ocean sediments.

In addition to measuring the cone resistance and sleeve friction, the deceleration is measured by an accelerometer mounted within the penetrometer. These quantities are then used for correlating the shear strength of the soil at different depths of penetration. Laboratory experiments were conducted with two types of soil targets.

Test results show that an increase in soil strength and roughness of the penetrometer cone material would cause a substantial increase in cone resistance and decrease in maximum penetration depth. Cone angles and weight per unit area of the penetrometer have also significant influence on the cone resistance and penetration depth. The effect of all these parameters on penetration behaviour are discussed.

The mode of soil failure at low velocity penetration was assumed to be similar to a conventional quasi-static case as proposed by

Meyerhof (1961). It was observed that results of free fall penetration tests showed a greater penetration resistance, compared to the standard quasi-static tests. However, when the results were translated into computation of the angle of shear resistance, the difference was insignificant. For cohesive soils penetration resistance is dependent on the penetration velocity. 'Strain-rate effect' was found to influence the results. 'Static' strength for clays from 'dynamic' strength profiles can, however, be obtained taking the 'strain-rate effect' into account.

ACKNOWLEDGEMENTS

This dissertation was completed at the Faculty of Engineering, Memorial University of Newfoundland. The writer wishes to acknowledge with thanks the receipt of a Memorial University Fellowship during the period of this study.

The writer is deeply indebted to Dr. T.R. Chari, Associate Professor of Engineering, for his constant advice and guidance in the progress of this study. Thanks are due to Dr. R.T. Dempster, Dean of Engineering, for the facilities provided.

As with nearly all research, many individuals contributed to this study. In particular, the writer wishes to express his appreciation to Mr. Austin Bursey for his assistance in the instrumentation, Mr. P. Robinson and his colleagues at the University Technical Services for their cooperation and Mrs. Dallas Strange in typing this thesis within a short period of time.

This study at Memorial University would not have been possible without the leave of absence granted by the Calcutta Metropolitan Development Authority, Government of West Bengal, India, which is gratefully acknowledged.

TABLE OF CONTENTS

	Page
ABSTRACT	iv
ACKNOWLEDGEMENTS	vi
LIST OF TABLES	x
LIST OF FIGURES	xi
NOTATION	xvi
CHAPTER	
I. INTRODUCTION	1
II. THE STATE-OF-THE-ART AND LITERATURE REVIEW	4
2.1 Q-Static Penetration Test	4
2.1.1 Penetration Theory for Q-CPT	5
2.2 Dynamic Penetration Test	8
2.1.1 High Velocity and Low Velocity Penetration	8
2.2.2 Dynamic Penetration Theory	9
2.3 Analysis	14
2.3.1 Mode of Shear Failure	16
2.3.2 Computation of Soil Properties - Cohesionless Soils	16
2.3.2.1 Estimation of Soil Strength from Deceleration Record	18
2.3.3 Depth of Penetration	19
2.3.4 Computation of Soil Properties - Cohesive Soils	20

CHAPTER		Page
III.	LABORATORY EXPERIMENTAL PROGRAM	23
	3.1 General	23
	3.2 Apparatus - Penetrometers	23
	3.2.1 Instrumentation	24
	3.3 Recording System	30
	3.4 Experimental Method	30
	3.5 Roughness of the Cone Material	31
	3.6 Target Preparation	32
	3.6.1 Silica-70 Sand	32
	3.6.2 Modelling Clay	38
	3.6.3 Target Properties	39
	3.6.4 Shear Tests	39
	3.6.4.1 Penetrometers to Soil Friction Angle	40
	3.7 Summary	55
IV.	ANALYSIS OF RESULTS AND DISCUSSION	56
	4.1 General	56
	4.2 Computation of Penetration Depth	58
	4.3 Velocity Variation with Depth	60
	4.4 Free Fall Penetration Tests on Silica-70 Sand	61
	4.4.1 Cone Resistance using the Soil Properties	61
	4.4.1.1 Theoretical Cone Resistance from Deceleration Record	62
	4.4.1.2 Cone Resistance using Meyerhof's Bearing Capacity Theory	62

CHAPTER Page

4.4.2 Effects of Penetrometer Diameter and Weight . . . 74

4.4.3 Effects of the Nose Shape 75

4.4.4 Effects of the Surface Roughness 84

4.4.5 Target Strength 84

4.4.6 Free Fall Tests on Wet Sand 85

4.5 Summary of Test Results - Silica-70 Sand 100

4.6 Free Fall Penetration Tests on Modelling Clay 101

4.6.1 Sleeve Friction and Soil Adhesion 102

4.6.2 Effects of Cone Shape 112

4.6.3 Effects of Water Content 112

4.6.4 Effects of Strait-rate 112

4.7 Summary of Test Results - Modelling Clay 115

V. CONCLUSIONS AND RECOMMENDATIONS 116

5.1 Summary and Conclusions 116

5.2 Recommendations for Further Studies 117

REFERENCES 118

APPENDICES:

A. FIGURES SHOWING TALYSURF ROUGHNESS MEASUREMENTS 123

B. FIGURES SHOWING TYPICAL OUTPUT FROM FREE FALL PENETRATION TESTS 128

C. COMPUTER PROGRAM FOR PENETRATION VELOCITY AND DEPTH . . . 133

LIST OF TABLES

TABLE		Page
1.	Description of the Penetrometers	25
2.	Details of Penetrometer Tips	25
3a.	Surface Roughness of Different Cone Material	35
3b.	Direct Shear Test Results for Determination of Roughness	36
4a.	Properties of Sand Targets	45
4b.	Properties of Clay Targets	46
4c.	Direct Shear Test Results for Determination of Adhesion (c_a)	47
5a.	Comparison of Predicted and Measured Penetration Depth	63
5b.	Comparison of Predicted and Measured Penetration Depth	64
6.	Comparison of Angle of Shear Resistance (ϕ)	73
7a.	Test Results for Dense Sand Target	91
7b.	Test Results for Medium Dense Sand Target	92
7c.	Test Results for Loose Sand Target	93
8.	Comparison of Sleeve Resistance and Adhesion	110
9.	Cone Resistance for Different Nose Shapes	111

LIST OF FIGURES

FIGURE		Page
1.	Assumed Failure Pattern by Meyerhof (1961)	7
2.	Dynamic Free Body Diagram of a Penetrometer	15
3.	Photograph Showing Different Types of Cone Shape	26
4.	Circuit Diagram of Strain Gage Arrangements (Dayal, 1974)	27
5a.	Details of Loan Cell Arrangement	28
5b.	Photograph Showing Details of Loan Cell Arrangement	29
6a.	Photograph Showing Experimental Facility	33
6b.	Taylor Hobson No. 4 Talysurf Machine	34
7.	Standard Proctor Compaction Test for Modelling Clay	41
8.	Equipment for Mixing Clay Samples	42
9a.	Grain Size Distribution for Silica-70 Sand	43
9b.	Grain Size Distribution for Modelling Clay	44
10a.	Triaxial Test Results for Silica-70 Sand (S1 Type Soil)	48
10b.	Triaxial Test Results for Silica-70 Sand (S2 Type Soil)	49
10c.	Triaxial Test Results for Silica-70 Sand (S3 Type Soil)	50
10d.	Triaxial Test Results for Modelling Clay	51
10e.	Triaxial Test Results for Modelling Clay	52

FIGURE		Page
11.	Constant Rate of Strain Shear Box - WF 25000	53
12a.	Variation of ϕ with e for Silica 70 Sand as Determined by Direct Shear and Triaxial Tests . . .	54
12b.	Variation of ϕ with I_D for Silica 70 Sand as Determined by Direct Shear and Triaxial Tests . . .	54
13.	Typical Output from a Free Fall Penetration Test . . .	57
14a.	Comparison of Predicted and Experimental Velocity of Penetration for 3.56 cms dia Penetrometer (S1, S2 and S3 Types of Soil)	65
14b.	Comparison of Predicted and Experimental Velocity of Penetration for 7.62 cms dia Penetrometer (S1, S2 and S3 Types of Soil)	66
14c.	Comparison of Predicted and Experimental Velocity of Penetration for 3.56 cms dia Penetrometer ($\alpha = 15^0$, 30^0 and 90^0)	67
14d.	Comparison of Predicted and Experimental Velocity of Penetration for 7.62 cms dia Penetrometer ($\alpha = 15^0$, 30^0 and 90^0)	68
15a.	Comparison of Analytical and Measured Unit Cone Resistance for 3.56 cms dia Penetrometer (Wang, 1971)	69
15b.	Comparison of Analytical and Measured Unit Cone Resistance for 3.56 cms dia Penetrometer (Orrje & Broms, 1970)	70

FIGURE Page

15c. Comparison of Analytical and Measured Unit Cone Resistance for 7.62 cms dia Penetrometer (Orrje & Broms, 1970) 71

15d. Comparison of Analytical and Measured Unit Cone Resistance for 3.56 cms dia Penetrometer (Meyerhof, 1961) 72

16. Plot of Deceleration vs. Penetration Depth 76

17. Plot of Unit Cone Resistance vs. Penetration Depth . . 77

18. Plot of Relative Density vs. Maximum Penetration Depth 78

19a. Plot of Deceleration vs. Penetration Depth 79

19b. Plot of Deceleration vs. Penetration Depth 80

20a. Plot of Unit Cone Resistance vs. Penetration Depth for 3.56 cms dia Penetrometer (α = 15°, 30° & 90°) . 81

20b. Plot of Unit Cone Resistance vs. Penetration Depth for 7.62 cms dia Penetrometer (α = 15°, 30° & 90°) . 82

20c. Plot of $q_c/\gamma D$ vs. Cone Semi-apex Angle (α) 83

21a. Plot of Unit Cone Resistance vs. Penetration Depth for 3.56 cms dia Penetrometer (δ/ϕ = 0.5, 0.6 & 0.75) 86

21b. Plot of Unit Cone Resistance vs. Penetration Depth for 7.62 cms dia Penetrometer (δ/ϕ = 0.5, 0.6 & 0.75) 87

21c. Plot of $q_c/\gamma D$ vs. Roughness (δ/ϕ) of Cone Material for 3.56 cms dia Penetrometer (S1, S2 &S3 Types of Soil) . 88

21d. Plot of $q_c/\gamma D$ vs. Roughness (δ/ϕ) of Cone Material for 7.62 cms dia Penetrometer (S1, S2 &S3 Types of Soil). 89

FIGURE Page

22a. Plot of Deceleration vs. Penetration Depth for 3.56 cms dia Penetrometer 93

22b. Plot of Deceleration vs. Penetration Depth for 7.62 cms dia Penetrometer 94

23a. Plot of Unit Cone Resistance vs. Penetration Depth for 3.56 cms dia Penetrometer 95

23b. Plot of Unit Cone Resistance vs. Penetration Depth for 7.62 cms dia Penetrometer 96

24. Plot of $q_c/\gamma D$ vs. Angle of Shear Resistance (ϕ) 97

25a. Plot of Unit Cone Resistance vs. Penetration Depth for 3.56 cms dia Penetrometer (Wet Sand Target) 98

25b. Plot of Unit Cone Resistance vs. Penetration Depth for 7.62 cms dia Penetrometer (Wet Sand Target) 99

26a. Plot of Deceleration vs. Penetration Depth Varying Soil Properties and Penetrometer dia 103

26b. Plot of Deceleration vs. Penetration Depth for 3.56 cms dia Penetrometer ($\alpha = 15^\circ, 30^\circ$ & 90°) 104

26c. Plot of Deceleration vs. Penetration Depth for 7.62 cms dia Penetrometer ($\alpha = 15^\circ, 30^\circ$ & 90°) 105

27a. Comparison of Analytical and Measured Unit Cone and Unit Sleeve Resistance for 3.56 cms dia Penetrometer 106

27b. Plot of Unit Cone Resistance and Unit Sleeve Resistance vs. Penetration Depth for 3.56 cms dia Penetrometer . . . 107

27c. Comparison of Analytical and Measured Unit Cone Resistance and Unit Sleeve Resistance for 7.62 cms dia Penetrometer. . 108

FIGURE Page

27d. Plot of Unit Cone Resistance and Unit Sleeve Resistance vs. Penetration Depth for 7.62 cms dia Penetrometer 109

A1. Talysurf Roughness Measurements for Cone ($\alpha = 15^0$) . . . 124

A2. Talysurf Roughness Measurements for Cone ($\alpha = 30^0$) . . . 125

A3. Talysurf Roughness Measurements for Cone ($\alpha = 90^0$) 126

A4. Talysurf Roughness Measurements for Plate 127

B1. Typical Output for Dense Sand Target 129

B2. Typical Output for Medium Dense Sand Target 130

B3. Typical Output for Loose Sand Target 131

B4. Typical Output for Clay Target 132

NOTATION

A = Pile tip area; cross-sectional area of penetrometer; constant.

a = Projectile cross-sectional area.

A_1, A_2, A_3 = Constants depending on soil strength and projectile properties.

A_s = Pile shaft area.

B = Foundation width; factor depending on the unit weight of soil and projectile cross-sectional area.

c = Cohesion, constant.

C_1 = Constant.

c_a = Adhesion.

CI_x = Cone index at penetration rate, r_x with cone diameter d_x.

CI_s = Cone index of a standard cone with penetration rate r_s and cone diameter d_s.

D = Depth of foundation; projectile penetration depth; projectile diameter.

D_r = Relative density of sand.

e = Void ratio.

f = Constant.

F = Soil resistance.

f_s = Shear strength of soil-pile interface.

G = Specific gravity.

g = Acceleration due to gravity.

G.F	= Gage factor.
K	= Constant.
M, m, M_p	= Mass of projectile.
M_c	= Mass of soil moving with projectile.
mV	= Milli volt.
N	= Nose performance co-efficient.
N_c, N_q, N_γ	= Dimensionless bearing capacity factors.
NL	= Projectile nose length.
P	= Maximum penetration depth.
q	= Overburden pressure.
Q_c	= Load transmitted through normal stress at the pile point.
Q_s	= Load transmitted through shear of the pile.
q_c	= Unit cone resistance; bearing capacity of soil.
q_d	= Ultimate bearing capacity.
Q_u	= Ultimate bearing capacity.
q_{cd}	= Theoretical cone resistance for impact velocity V_o and penetrometer diameter d.
R	= Gage resistance.
S	= Soil constant.
t	= Time of penetration.
V	= Penetration velocity.
v	= Projectile velocity.
, V_o	= Impact velocity at zero penetration.
V_c	= Critical velocity.

$V(t)$ = Velocity at time t.

V_n = Velocity at time t_n.

W = Weight of projectile; weight of penetrometer.

w = Water content.

x = Depth of penetration.

X_{max} = Maximum penetration depth.

Z = Depth of penetration.

Z_o = Displacement at time $t = 0$.

Z_n = Displacement at time t_n.

$Z(t)$ = Displacement at time t.

$\ddot{Z}$ = Acceleration.

α = Constant; semi-apex angle of cone.

β = Constant.

γ = Constant; unit weight of soil.

γ_d = Dry unit weight of soil.

ϕ = Angle of internal friction; angle of shear resistance.

δ = Friction angle between penetrometer material and soil.

δ/ϕ = Roughness.

σ_m = Average contact pressure.

μV = Micro volt.

CHAPTER I

INTRODUCTION

Activities related to the design and construction of offshore structures have gained great momentum in the last decade. Detailed information on the strength properties of sea floor soils is essential for safe and economical design of foundations on the ocean floor. Conventional sampling procedures used on land are generally not effective in the oceans because of the presence of the water column and the high degree of disturbance of the samples. Laboratory testing of such samples are therefore to be substantiated by other methods. In-situ testing thus forms an integral part of any offshore soil investigation.

Among the several devices in use at present for in-situ testing of marine soils, the standard (ASTM D3441-75T) electric cone penetrometer has been widely used in the static mode, either with a sea bed rig called the "seacalf" (De Ruiter, 1975; Zuidberg, 1975) or with a bore hole attachment called the "stingray" (Ferguson et al., 1977). It is estimated that a typical site investigation including drilling bore holes and in-situ testing with a standard penetrometer costs upward of $1 million (Hitchings et al., 1976). Such a detailed investigation may not be necessary in geotechnical surveys or for investigation of large tracts for locating pipe line routes, etc. The concept of a free fall penetrometer was initiated at Memorial University (Dayal, 1974) with the intention of using it as a tool for a quick and economical

testing of marine soil immediately below the mud line.

A free fall penetrometer is a cone tipped right circular cylindrical projectile which is allowed to fall on soil target from a preadjusted height of free fall. It is instrumented with load cells for measuring the cone tip resistance and friction on the side sleeve during penetration. An accelerometer is also mounted within the penetrometer for recording deceleration profile, up to the full depth of penetration. Integration of the deceleration-time record provides velocity versus time curve which can then be used to obtain the displacement versus time curve. By cross plotting, the record of penetration resistance versus depth profile is obtained. The data thus obtained is used for the final analysis of the soil strength properties.

Initial attempts with a field penetrometer (Jones, 1976) showed that the standard penetrometer (cross sectional area = 10.00 sq. cms.) was structurally inadequate in the free fall mode. A completely redesigned version of the free fall penetrometer (cross section area = 45.62 sq. cms.) was successfully tested during sea trials in Placentia Bay, off Newfoundland, in May, 1978 (Chari et al., 1978).

Laboratory tests with this redesigned penetrometer and an analysis of the results are presented in this dissertation. Free fall penetration tests were conducted using the standard "Fugro" type penetrometer and the redesigned "Memorial University" penetrometer. Two types of soil targets were used. Abdel-Gawad (1979) conducted a parallel project, in carrying out quasi-static tests with the two types of penetrometer and the results are published in a companion

dissertation.

The major factors which influence the penetration resistance in any cone penetration test are (i) cone apex angle; (ii) cone diameter; (iii) roughness of the cone material; (iv) rate of penetration; (v) soil properties (angle of shearing resistance, cohesion, degree of saturation, etc.). In the case of the free fall penetrometer, its weight is an additional influencing factor. The importance of these factors are studied in this experimental investigation.

The basic aims of this study are:

1. To study the influence of the different characteristics of the penetrometer.
2. To study the penetration phenomenon in different soil types.
3. To compare the results obtained from free fall tests with those for quasi-static tests.
4. To propose appropriate methods of interpreting the results in the light of theories currently available in the literature.

CHAPTER II

THE STATE-OF-THE-ART AND LITERATURE REVIEW

In-situ devices generally measure a characteristic property of soil in its natural environment which is then related to the shear strength and bearing capacity by semi-empirical formulation. Among a variety of techniques for in-place testing of soils, the use of penetrometers has been found to be satisfactory and reliable.

According to the mode of operation penetration could broadly be classified as: (i) static or quasi-static penetration, and (ii) dynamic penetration.

2.1. Q-Static Penetration Test

The idea of static or quasi-static penetration test (QCPT) is simple—a rod is advanced into soil at a constant rate (1-2 cm/sec) and the load required to produce such an advance is measured. The "Fugro" electrical cone penetrometer (De Ruiter, 1971) capable of measuring the tip resistance and sleeve friction through load cells is now popularly used as a standard tool. The forces measured, which are expressed as the unit cone resistance and the unit sleeve friction resistance are correlated with the soil density, shear strength, etc.

The static penetration test has been extensively used in Europe for more than fifty years. The use of the penetrometer and interpretation of the results is widely published in soil mechanics literature.

Plantema (1957), Meyerhof (1956, 1961), Begemann (1965), Ladanyi and Eden (1969), Mitchell and Durgunoglu (1973) used the test results for predicting soil type and strength.

Van der Veen (1957), Bogdanovic (1961), Artikoglue (1961) interpreted the results as a basis for pile bearing capacity.

Meyerhof (1956), Meigh and Nixon (1961), Schultze and Melzer (1965) performed experiments with cone penetrometers to estimate the compressibility and in-situ density of cohesionless soils.

De Beer and Martens (1957), Schmertmann (1970) used the test results to calculate settlement of footings on sand. A recent conference proceedings (ESOPT, 1974) provides comprehensive information on penetrometers. State-of-the-art summaries have also been presented recently by Durgunoglu and Mitchell (1975) and Schmertmann (1975).

2.1.1. Penetration Theory for Q-CPT

The penetration phenomenon could be correlated with the problem of resistance and bearing capacity of piles. When an object such as a pile, penetrates into soil, the force required to achieve penetration is the ultimate load Q_u, made up of two components; the load transmitted through tip of the pile Q_c and the load Q_s transmitted through resistance on the sides of the pile. If the area of the pile tip and pile shaft area are defined as A and A_s respectively, the ultimate load can be expressed as:

$$Q_u = Q_c + Q_s \quad \ldots\ldots\ldots\ldots\ldots\ldots\ldots\ldots (1)$$

$$= A\, q_c + A_s\, f_s \quad \ldots\ldots\ldots\ldots\ldots\ldots (2)$$

where q_c is the ultimate bearing capacity of the soil at the tip of pile and f_s is the frictional resistance of the soil-pile interface.

The general formulation for bearing capacity of soils was given by Terzaghi (1943) as:

$$q_d = c\,N_c + p_o\,N_q + \tfrac{1}{2}\gamma B N_\gamma \quad \ldots\ldots\ldots\ldots (3)$$

where q_d is the ultimate bearing capacity, c is the cohesion, γ is the unit weight of the soil, p_o is the overburden pressure at the tip of the foundation and B is the foundation width. N_c, N_q and N_γ are dimensionless bearing capacity factors, primarily dependent on ϕ, the angle of shear resistance of the soil.

Meyerhof has shown that the bearing capacity values obtained by using Terzaghi's formulation are conservative. Meyerhof (1961) suggested a modified type of failure surface (Fig. 1) and while keeping the basic form of the bearing capacity equation similar to that of Terzaghi, prepared a set of values for N_c, N_q and N_γ which depend not only on the angle of shearing resistance but also on the depth and shape of foundation, and roughness of its base.

It is generally assumed that the penetrometer is similar to a pile foundation loaded to its ultimate bearing pressure and theoretically the following relations exist:

$$q_c = f_1\,(\phi, c) \quad \ldots\ldots\ldots\ldots (4)$$

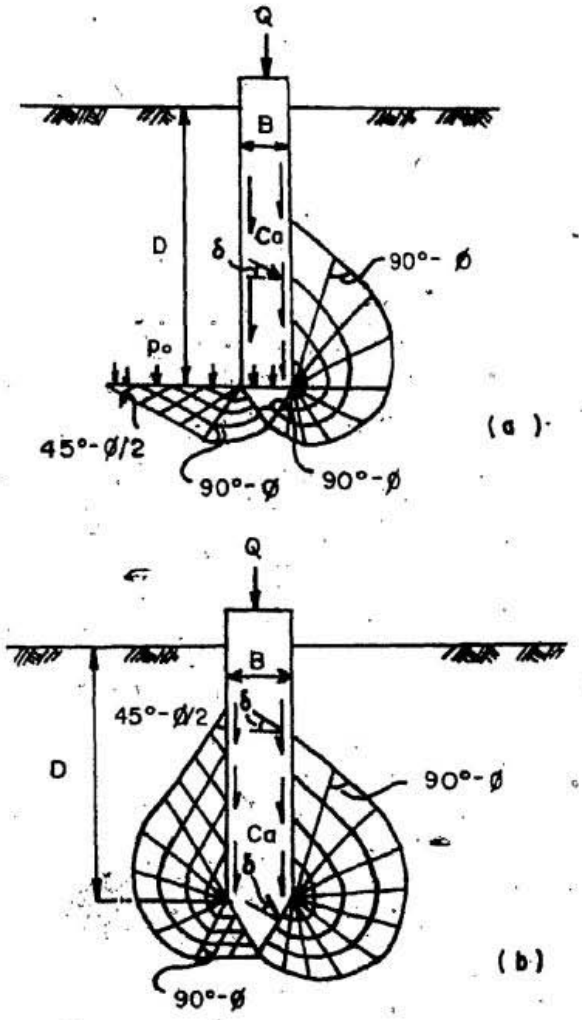
$$f_s = f_2\,(\phi, c) \quad \ldots\ldots\ldots\ldots (5)$$

For the case of purely cohesionless soil and purely cohesive soils, equation (4) and (5) may be greatly simplified.

In equation (3), the term $\frac{1}{2}\gamma B N_\gamma$ is usually small and negligible for pile foundations.

Equation (4) may therefore be written as:

(Text continued page 8)



SMOOTH BASE ROUGH BASE

(a) FOR FLAT TIP PILE

(b) FOR WEDGE OR CONICAL TIP PILE

FIG 1. ASSUMED FAILURE PATTERN BY MEYERHOF (1961)

For cohesionless soils: $q_c = \gamma D N_q$ . . . . . (6)

For cohesive soils: $q_c = \gamma D + cN_c$ . . . . . (7)

Conversely, if q_c and f_s can be measured, the ultimate bearing capacity and hence the soil shear properties can be determined.

2.2. Dynamic Penetration Test

A type of dynamic penetration test that has been part of any borehole investigation is the Standard Penetration Test (SPT), where a split spoon sampler is driven by repeated blows of a freely falling standard weight. In the recent past, the usefulness of this test has been questioned (Schmertmann, 1975). It appears to be the consensus that the interpretation of this type of test requires not only a lot of experience, but is to be done with caution. The other type of dynamic penetration test which is discussed in this thesis uses a penetrometer which has the same or similar configuration to that described under the cone penetration test.

2.2.1. High Velocity and Low Velocity Penetration

In connection with the study of projectile penetration into earth media, research has been going on since the early 1960's (Young, 1972) at the Sandia Laboratories in Albuquerque, New Mexico. Projectiles of different shapes, instrumented with an accelerometer have been tested with velocities of penetration up to 790 m/sec (2570 ft/sec).

In such dynamic tests, penetration is caused by virtue of the energy at the time of impact. Upon impact on a soil mass the projectile pushes against the soil particles, ruptures the soil

structure and comes to rest when the projectile energy is totally dissipated. Depending on the impact velocity with which the projectile strikes the soil target the penetration phenomenon has been classified as low velocity or high velocity. The basis for this demarcation is the type of soil failure. The term 'low velocity' is used to describe the events for which soil failure pattern is similar to the quasi-static cases (Wang, 1971; Murff and Coyle, 1972; Dayal, 1974).

Wang (1971) has suggested that the soil shear zone is similar to static case for velocities up to 152 m/sec (500 fps) but has conducted studies only to a maximum impact velocity of 7.6 m/sec (25 fps). Murff and Coyle (1972) investigated projectile penetration in velocity range of 9.1 m/sec to 91 m/sec (30 to 300 fps) and classified these tests as low velocity tests. Although a discussion of the exact limit for the low velocity mechanism is out of context, it can be seen from the published reports that velocities in the order of 9.1 m/sec (30 fps) are clearly a low velocity phenomenon. The velocity obtained for the free fall cone penetration tests reported in this thesis is in the order of 7.75 m/sec and is classified as low velocity penetration.

2.2.2. Dynamic Penetration Theory

The basic assumptions for deriving the expressions for projectile penetration are (Young, 1972; Dayal, 1974):

1. The soil target is homogeneous and isotropic.
2. The penetrometer is an unpowered projectile of a simple configuration having a cylindrical body and nose.
3. There is no significant angle between the axis of the penetrometer and its velocity vector.

Allen et al. (1957) conducted a series of penetration tests on sand with different nose shapes. They proposed the following theory:

$$-\frac{dv}{dt} = \alpha V^2 \quad \text{for} \quad V_o > V > V_c \qquad (8)$$

$$-\frac{dv}{dt} = \beta V^2 + \gamma \quad \text{for} \quad V_c > V > 0 \qquad (9)$$

where V_o is the impact velocity at zero penetration and V_c is the critical velocity.

Based on experimental results, the critical velocity, V_c (defined later) was calculated to be 96.5 m/sec. They concluded that an impact at a velocity greater than V_c is largely inelastic and at a velocity less than V_c the projectile simply pushes the sand elastically.

Schmid (1969) assumed the penetration equation as

$$-m\frac{dv}{dt} = \alpha + \beta V + \gamma V^2 \qquad (10)$$

where m is the mass of the projectile, V is the projectile velocity and α, β, γ are constants.

Depending upon the relative magnitude of α, β and γ, the solutions of equation (10) are:

(i) for the case where $\beta^2 < 4\alpha\gamma$

$$X = \frac{m}{2\gamma} \ln \frac{\gamma V_o^2 + \beta V_o + \alpha}{\gamma V^2 + \beta V + \alpha} - \frac{m\beta}{\gamma} A\,(4\alpha\gamma - \beta^2)^{-\frac{1}{2}} \qquad (11)$$

$$t = 2 A m (4\alpha\gamma - \beta^2)^{-\frac{1}{2}} \quad \ldots\ldots\ldots\ldots\ldots \quad (12)$$

where X is the instantaneous penetration at time t and velocity V;

V_o is the velocity of impact.

$$A = \tan^{-1} (2\gamma V_o + \beta)(4\alpha\gamma - \beta^2)^{-\frac{1}{2}} - \tan^{-1} (2\gamma V + \beta)(4\alpha\gamma - \beta^2)^{-\frac{1}{2}} \quad \ldots\ldots \quad (13)$$

(ii) for the case where $\beta^2 > 4\alpha\gamma$

$$X = \frac{m}{2\gamma} \ln \frac{\gamma V_o^2 + \beta V_o + \alpha}{\gamma V^2 + \beta V + \alpha} - \frac{m\beta}{\gamma} B (\beta^2 - 4\alpha\gamma)^{-\frac{1}{2}} \quad \ldots\ldots \quad (14)$$

$$t = 2BM (\beta^2 - 4\alpha\gamma)^{-\frac{1}{2}} \quad \ldots\ldots\ldots\ldots\ldots \quad (15)$$

where

$$B = \frac{1}{2} \ln \frac{\{2\gamma V + \beta + (\beta^2 - 4\alpha\gamma)^{\frac{1}{2}}\} \{2\gamma V_o + \beta - (\beta^2 - 4\alpha\gamma)^{\frac{1}{2}}\}}{\{2\gamma V + \beta - (\beta^2 - 4\alpha\gamma)^{\frac{1}{2}}\} \{2\gamma V_o + \beta + (\beta^2 - 4\alpha\gamma)^{\frac{1}{2}}\}} \quad \ldots\ldots \quad (16)$$

(iii) for the special case where $\beta^2 = 4\alpha\gamma$

$$X = \frac{m}{\gamma} \ln \frac{\beta + 2\gamma V_o}{\beta + 2\gamma V} - \frac{\beta C m}{\gamma} \quad \ldots\ldots \quad (17)$$

$$t = 2Cm \quad \ldots\ldots\ldots\ldots\ldots \quad (18)$$

where $$C = (2\gamma V + \beta)^{-1} - (2\gamma V_o + \beta)^{-1} \quad \ldots\ldots\ldots \quad (19)$$

Starting from Newton's equation of motion, Thompson et al. (1969) derived the following relationships for acceleration (A), velocity (V) and penetration depth (Z)

$$A = \frac{F}{M_p + M_c} + g \quad \ldots\ldots\ldots\ldots\ldots\ldots (20)$$

where F is the soil resistance, M_p is mass of projectile, M_c is mass of soil moving with the projectile and g is the acceleration due to gravity.

$$V = \int \left(\frac{F}{M_p + M_c} + g\right) dt \quad \ldots\ldots\ldots\ldots\ldots\ldots (21)$$

$$Z = \int \left(\int \left(\frac{F}{M_p + M_c} + g\right) dt\right) dt \quad \ldots\ldots\ldots\ldots\ldots\ldots (22)$$

They conducted laboratory experiments with the objective of demonstrating the influence of physical soil parameters, impact velocity and the projectile property. Thompson et al. (1969) concluded that the soil strength parameters have a strong influence on the depth of penetration.

Young (1969) presented the penetration prediction equation as

$$X_{max} = 530\ SN(W/A)^{\frac{1}{2}}\ 10^{-3}\ \ln(1+20\times10^{-6}V_o^2) \quad \ldots\ldots\ldots\ldots (23)$$

for $V_o < 200$ ft/sec

$$X_{max} = 3100\ SN(W/A)^{\frac{1}{2}}\ 10^{-6}\ (V_o - 100) \quad \ldots\ldots\ldots\ldots (24)$$

for $V_o > 200$ ft/sec

where X_{max} is the maximum penetration depth, S is the soil constant, N is the nose performance co-efficient, W is the weight of projectile and A is the cross-sectional area of the projectile.

Values of S lie within a wide range from 0.2 to 50. For solving the above equations, it is necessary to assume that S is constant for a given target. Thus, for penetration in a layered medium of widely different properties the correct value of S will depend on the total depth penetrated. Based on a detailed analysis of over 500 full scale tests, Young (1972) concluded that predictions are accurate within approximately ±20%.

Orrje and Broms (1970) conducted laboratory and field tests to investigate soil density effects on penetration event. They observed that an increase in soil density yields the following: a decrease in the total penetration, an increase in measured deceleration and a decrease in characteristic times. Furthermore, from load-settlement curves they concluded that dynamic bearing capacity was higher than the static bearing capacity.

Wang (1971) investigated the effects of low velocity penetration on sand targets. Varying the soil properties and the impact velocity (V_o < 25 fps) he showed that low velocity penetration results could be used for determining the angle of shear resistance of sand. Murff and Coyle (1972) conducted experimental studies on the nose shape and sharpness of the penetrometer tip and found that an increase in nose sharpness causes an increase in the total penetration With the help of a simple analytical model, they indicated that penetration depth is proportional to the ratio of the weight to

cross-sectional area of the penetrometer.

Murff and Coyle (1973) also conducted penetration tests by varying soil parameters, penetrometer characteristics and impact velocity. Prediction equations were suggested in which the soil resistance was assumed to be a linear function of the velocity and depth. Good fit was reported both for clay and sand.

Turnage and Freitag (1969) and Turnage (1973) conducted experiments to examine the viscous effects and inertial forces on soil penetration resistance for a wide variety of probe sizes, shapes and penetration velocities. Their data show that the cone penetration resistance of fine grained soils was proportional to velocity and inversely proportional to cone diameter. An exponential equation was developed to describe the interrelationship.

Varying the soil properties, penetrometer characteristics and impact velocity, Dayal (1974) performed laboratory studies for determining geotechnical properties of soils using an instrumented impact cone penetrometer and the results showed good agreement with the theoretical model. The impact velocities of those tests were in the range of 4.55 to 9.1 m/sec (15 to 30 ft/sec).

2.3. Analysis

During a free fall penetration, the penetrometer experiences resistance by the soil from the instant of entry until the conclusion of penetration event. The dynamic free body diagram of a penetrometer during penetration is shown in Fig. 2. The analytical relationship of different parameters (i.e., soil properties, impact velocity,

(Text continued page 16)

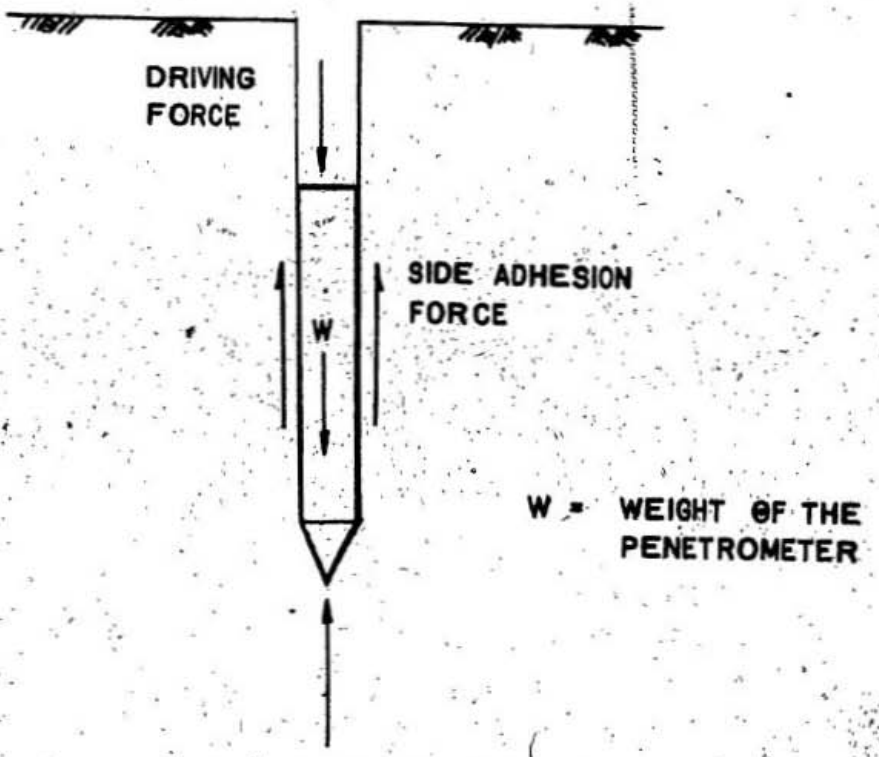


FIG 2. DYNAMIC FREE BODY DIAGRAM OF A PENETROMETER

penetrometer characteristics, etc.) governing the dynamic soil properties at low velocity penetration are discussed below.

2:3.1. Mode of Soil Shear Failure

As described earlier, the behaviour of soil under low velocity penetration would be similar to the quasi-static case. Accordingly, the failure mode during the free fall penetration is assumed to be that proposed by Meyerhof (1961) for deep cone tipped pile foundation. The reasons for adopting Meyerhof's failure pattern were summarized by Dayal (1974) as follows:

(i) Meyerhof's theory takes into account the shape and surface roughness of the penetrometer.

(ii) Failure pattern as observed experimentally for plane-strain model impact penetration tests could be approximated to that of Meyerhof's failure pattern.

(iii) Experimental results were found to be in good agreement with the analytical value obtained by Meyerhof's method.

Although different theories are available from recent publications (Durgunoglu and Mitchell, 1973) which also take into account the penetrometer shape, size and roughness, Meyerhof's theory is preferred by virtue of its ease of application and its wide acceptance.

2.3.2. Computation of Soil Properties - Cohesionless Soils

From the results of a series of low velocity penetration tests on sands, Wang (1971) expressed the following relationship for the ultimate bearing capacity:

$$Q_u = A + C_1 x \quad \ldots\ldots\ldots\ldots\ldots\ldots \quad (25)$$

where Q_u = ultimate bearing capacity

A and C_1 = constants depending on soil property, penetrometer shape and size

x = depth of penetration.

According to the principle of conservation of energy, Wang (1971) derived the following relationship:

$$M\, v\, dv = -(A + B\, v^2 + C_1\, x)dx \quad \ldots\ldots\ldots\ldots \quad (26)$$

where v = penetrometer velocity

$B = (\frac{\gamma}{g})a\,f \quad (f = 1)$

M = mass of the penetrometer

Solution of equation (26) was given as:

$$v = \{[V_o^2 - \frac{M}{2B}(\frac{C_1}{B} - \frac{2A}{M})]e^{-\frac{2B}{M}x} - (\frac{C_1}{B})x + \frac{M}{2B}(\frac{C_1}{B} - \frac{2A}{M})\}^{\frac{1}{2}} \quad \ldots \quad (27)$$

where V_o is the impact velocity.

The penetration depth is a maximum when projectile stops; i.e., x = P when v = 0; P = maximum depth of penetration.

$$V_o = \{\frac{M}{2B}(\frac{C_1}{B} - \frac{2A}{M}) + [(\frac{C_1}{B})P - (\frac{M}{2B})(\frac{C_1}{B} - \frac{2A}{M})]e^{\frac{2B}{M}P}\}^{\frac{1}{2}} \quad \ldots\ldots \quad (28)$$

Knowing the maximum penetration depth (P) for a certain impact velocity (V_o), C_1 could be calculated from equation (28). As the contribution of A is very small (Wang, 1971) in comparison to C_1, A is neglected while determining the value of C_1. Again, equation

(25) could be re-written as (Neglecting A),

$$Q_u = C_1 x \quad \ldots\ldots\ldots\ldots\ldots \quad (29)$$

Considering equation (6) as valid for low velocity penetration, it can be re-written as:

$$Q_u = \pi R^2 (\gamma' D N_q) \quad \ldots\ldots\ldots\ldots\ldots \quad (30)$$

where R is the radius of foundation.

From equations (29) and (30)

$$C_1 = \pi R^2 \gamma' N_q \quad \ldots\ldots\ldots\ldots\ldots \quad (31)$$

Knowing C_1, N_q could be calculated from equation (31). This, in turn, would give the value of ϕ.

It was already stated in equation (6) that the quasi-static value of q_c can be expressed as

$$q_c = \gamma' D N_q \quad \ldots\ldots\ldots\ldots\ldots \text{(eqn. 6)}$$

From Meyerhof's (1961) theory, Mitchell et al. (1978) have interpolated and given the value of ϕ as a function of N_q for a standard penetrometer (base area = 10 cm^2, cone apex angle = 60^0 and $\delta/\phi = 0.5$). Thus knowing q_c, N_q and ϕ could be calculated. This will provide the basis for comparing the values of ϕ obtained by the two methods of analysis.

2.3.2.1. Estimation of Soil Strength from Deceleration Record

Orrje and Broms (1970) derived the relationship between deceleration and average contact pressure of a free falling object as

$$\sigma_m = \frac{mg}{A} - \frac{m}{A}\ddot{Z} \quad \ldots\ldots\ldots\ldots\ldots\ldots \quad (32)$$

where σ_m = average contact pressure

$\ddot{Z}$ = acceleration

A = cross-sectional area of the object

By measuring deceleration at different penetration depths, corresponding soil resistance can be calculated from the above equation. The measured penetration resistance could thus be compared with the computed values using Orrje and Broms (1970) equation.

2.3.3. Depth of Penetration

Assuming the equation for motion for projectile penetration as

$$m\frac{d^2x}{dt^2} = A_1 + A_2x + A_3\frac{dx}{dt} \quad \ldots\ldots\ldots\ldots \quad (33)$$

where m = mass of the projectile

x = penetration depth at time t

A_1, A_2, A_3 = constants depending on soil strength and projectile property.

Murff and Coyle (1973) derived the following relationship based on the results of a series of controlled laboratory experiments

$$m\frac{d^2x}{dt^2} = -238\,D^2D_r - 162\,D\,D_r\,x + [37.3\,(\frac{NL}{D}) - 86.6]D^2\,D_r\frac{dx}{dt}$$

$$\ldots\ldots\ldots\ldots \quad (34)$$

where D = diameter of the projectile

D_r = relative density of sand

NL = projectile nose length.

Single and double integration of equation (34) would give expressions for velocity and depth of penetration. Using this approach and measuring actual penetration depths comparison can be made of the velocity profiles and penetration depths.

2.3.4. Computation of Soil Properties - Cohesive Soils

It is generally understood that 'strain-rate effect' is an important factor to be considered in cohesive soils. Casagrande and Wilson (1951), Whitman (1957), Richardson et al. (1963), Roy et al. (1976) have studied this effect on the shear strength of soils and concluded that shear strength gradually increases with an increasing rate of strain. The phenomenon controlling the shear rate effect is too complex to permit mathematical definition and prediction.

Extensive work by Casagrande and Wilson (1951), Whitman (1957), Vesic et al. (1965) dealing with the shear strength of sands indicated insignificant effect of the rate of strain on the shear strength in the range of the velocities tested by them. Whitman (1957) reported a change in the compressive strength of sand of about 10-15% due to strain rate.

However, for clays, this difference appears to be more significant. Based on laboratory test results, Berre and Bjerrum (1973) concluded that the stress-strain property of clay depends on the rate at which the stresses are applied. The critical shear stress is thus not a constant, but depends on the rate at which the load is applied. Most of the reported studies of the influence of shear speed have been confined to the determination of undrained strength

of saturated clays. Whitman (1957) has further shown that the strength is considerably increased under very rapid rates of loading. Whitman (1960) suggested that the rate effect upon strength might be caused by a change in excess pore pressure generated during the shear process. Data reported by O'Neill (1962) indicated that his hypothesis was substantially correct.

In connection with tests on bulldozer blades, Wismer and Luth (1972) attempted to quantify the strain rate effects and used the equation of Turnage and Freitag (1969) and suggested:

$$\frac{CI_x}{CI_s^*} = \left[\frac{(\frac{r}{d})_x}{(\frac{r}{d})_s} \right]^K \quad \ldots\ldots\ldots\ldots\ldots\ldots \quad (35)$$

where CI_x = cone index at penetration rate r_x with cone diameter dx.

CI_s = cone index of a standard cone with penetration rate r_s and cone diameter ds.

K = exponent of shear rate factor.

Based on experimental results, Wismer and Luth suggested a value of 0.1 for the exponential K.

From equation (35), theoretical value of cone resistance for different impact velocity and cone diameter can be calculated with the quasi-static penetration test as the reference or vice-versa.

Again for purely cohesive soils

$$q_c = c \cdot N_c + \gamma D \quad \ldots\ldots\ldots\ldots \quad \text{(eqn. 7)}.$$

Meyerhof (1976) has given N_c values for different soil types and relative depth of foundation. Knowing q_c, cohesion (c) could be calculated.

In summary, it may be stated that free fall projectile penetration at low velocity is influenced by various factors. These are different for cohesionless and cohesive soils. Different methods currently available can be used to evaluate the soil properties and compared with each other and also with the triaxial and direct shear test results.

CHAPTER III

LABORATORY EXPERIMENTAL PROGRAM

3.1. General

The experimental program was designed with the objective of studying the mechanics of free fall penetration resistance of soils and its correlation to the static penetration mechanism. The influence of cone angle, cone roughness and the type of soil target on static penetration resistance is recognized and reported in literature. These variables are examined in the free fall penetration tests conducted. The free fall penetrometer that was designed and successfully used at sea is 7.62 cms diameter while the standard penetrometer used in most static penetration tests is 3.56 cms diameter. In this work, tests were done with both types of penetrometers so that appropriate comparisons and correlations could be made.

3.2. Apparatus - Penetrometer

A detailed physical description of the two types of penetrometers used is given in Table 1. Tips for both penetrometers were detachable from the shaft and had various apex angle and roughness. A complete listing of the penetrometer tips used in this investigation is given in Table 2. Shapes and sizes of different cones together with the nose assembly for the two penetrometers are shown in Fig. 3.

3.2.1. Instrumentation

The penetrometers were instrumented with three sensors: accelerometer, cone load cell and friction sleeve load cell.

The accelerometer was mounted inside the penetrometer and aligned in the direction of the penetrometer axis. The accelerometer used in this investigation had the following specifications:

ENDEVCO:	Model 2262-25
Type:	Full bridge piezoresistive
Rated range:	±25 g
Useful range:	±50 g
Sensitivity:	16.7 mV/g (at 10V DC excitation)
Maxm. transverse sensitivity:	1.2%

Strain gages were used for measuring cone and sleeve friction loads. Each load cell contains four pairs of strain gages arranged in such a manner that compensation is made for bending stress and only the axial load is measured. Four strain gages were arranged in the axial direction and the remaining four in the circumferential direction, equidistant, on the periphery of the tube. The circuit diagram is shown in Fig. 4.

Cone and friction load cells were calibrated on an 'Instron' testing machine. For the calibration of load cells special jigs were designed and fabricated so that only axial load was applied during compression of the tube. The cells were loaded up to 635 Kg (1400 lbs) for cone and 272 Kg (600 lbs) for friction sleeve at 22.68 Kg (50 lbs) increment. The results of the calibration tests

(Text continued page 30)

TABLE 1. DESCRIPTION OF THE PENETROMETERS

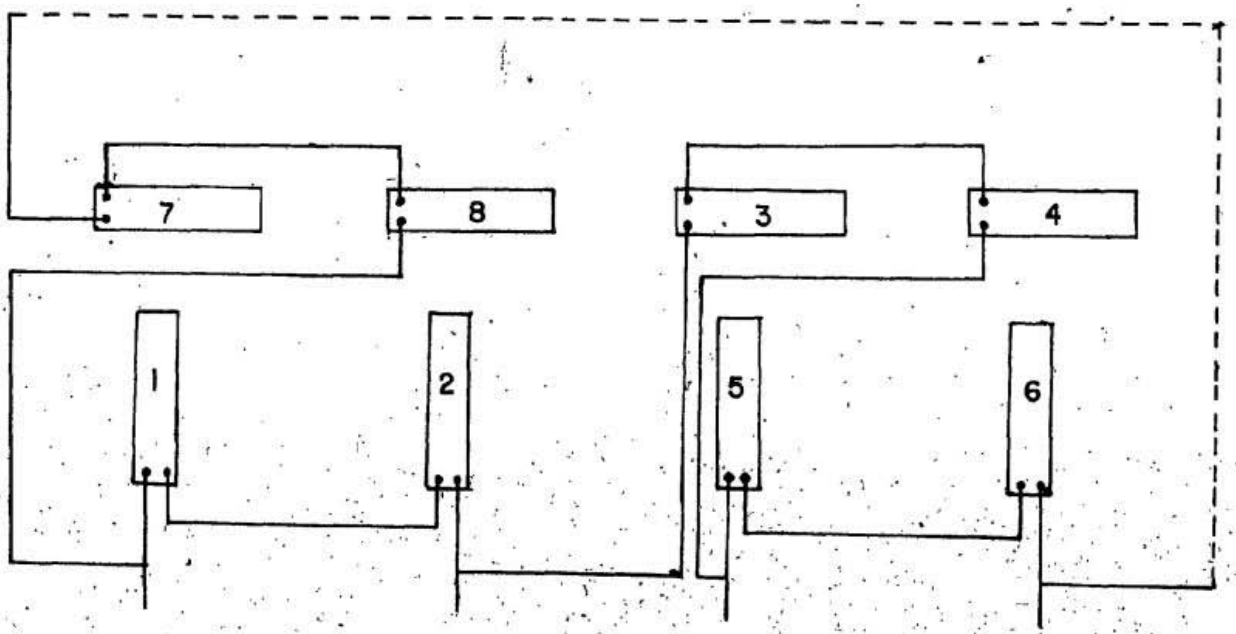
Details of penetrometer	"Fugro" type penetrometer	Memorial penetrometer
Diameter	3.56 cms (1.4 in.)	7.62 cms (3.0 in.)
Base area of the cone	10.00 cm^2 (1.55 $in.^2$)	45.62 cm^2 (7.07 $in.^2$)
Cone angles	30^o, 60^o and 180^o	30^o, 60^o and 180^o
Sleeve diameter	3.56 cms (1.4 in.)	7.62 cms (3.0 in.)
Area of sleeve	150 cm^2 (23.25 $in.^2$)	645.2 cm^2 (100 $in.^2$)

TABLE 2. DETAILS OF PENETROMETER TIPS

Penetrometer diameter (cms)	Penetrometer tip material	Roughness of cone material (δ/ϕ)	Base semi-apex angle (α)
3.56	Stainless steel Polished aluminium Sanded aluminium	0.5 0.6 0.75	15^o, 30^o and 90^o 15^o, 30^o and 90^o 15^o, 30^o and 90^o
7.62	Stainless steel Polished aluminium Sanded aluminium	0.5 0.6 0.75	15^o, 30^o and 90^o 15^o, 30^o and 90^o 15^o, 30^o and 90^o



FIG 3. PHOTOGRAPH SHOWING DIFFERENT TYPES OF CONE SHAPE



1, 2, 5, 6 = AXIAL STRAIN GAGES
3, 4, 7, 8 = CIRCUMFERENTIAL STRAIN GAGES

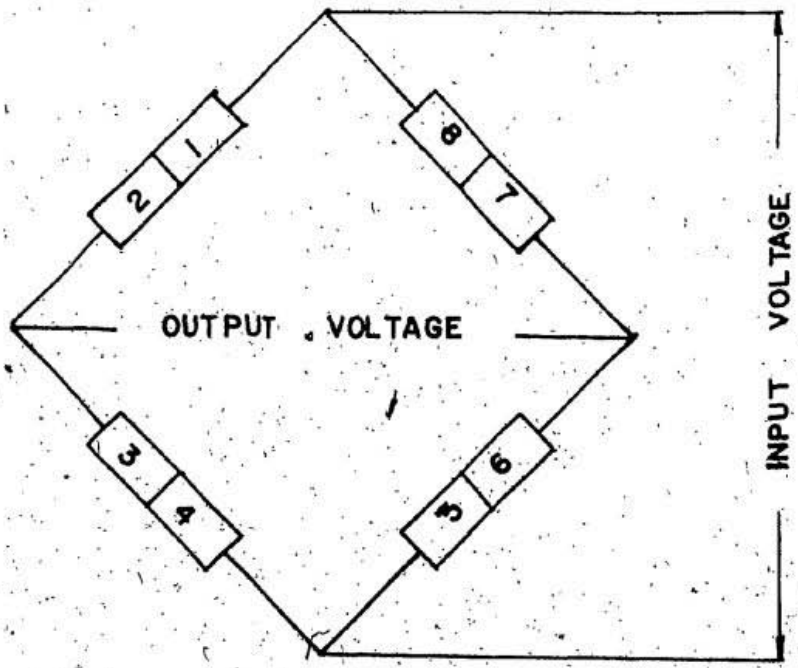
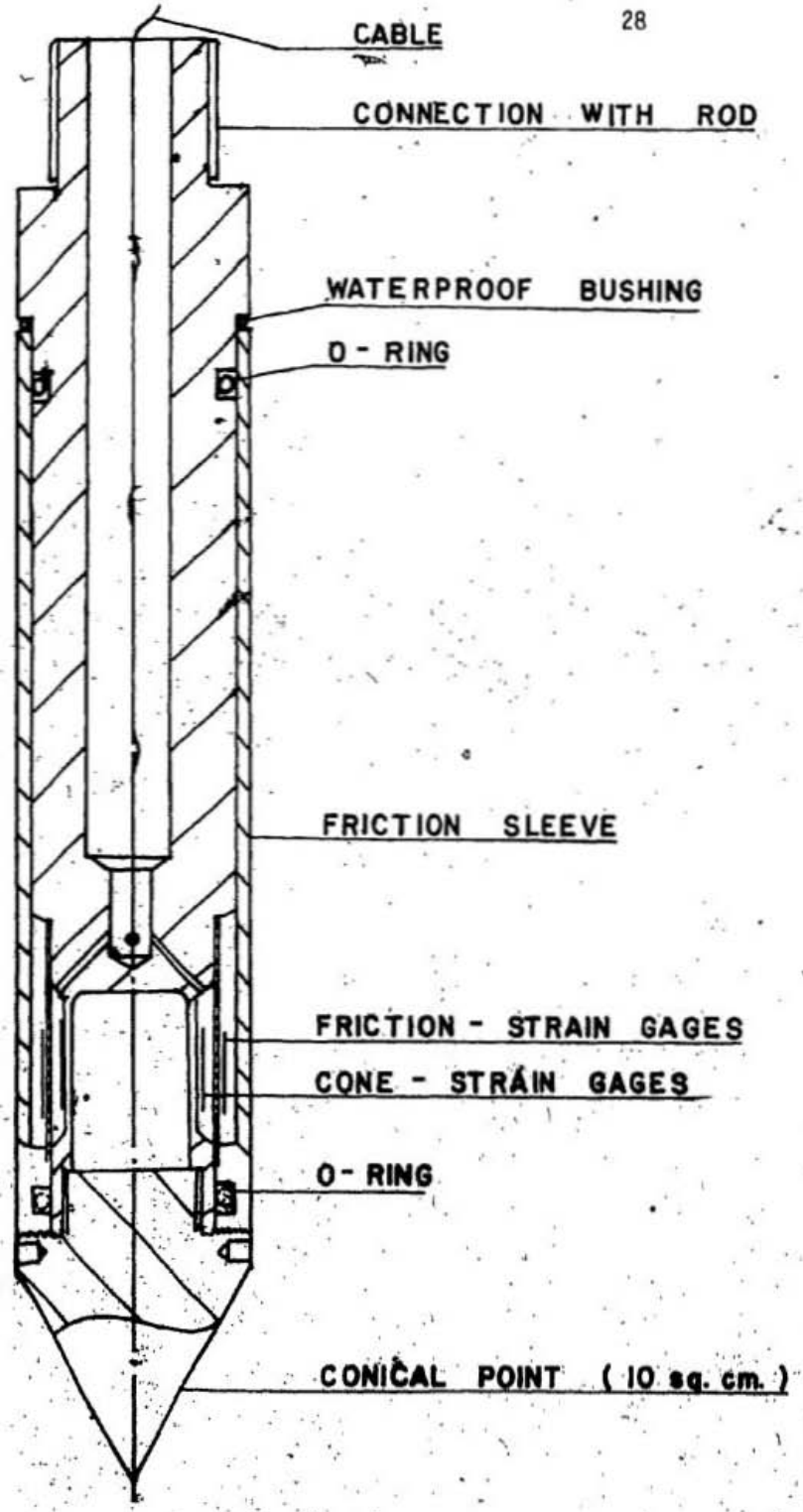


FIG 4. CIRCUIT DIAGRAM OF STRAIN GAGE ARRANGEMENTS (Dayal, 1974)



NOT TO SCALE

FIG 5a. DETAILS OF LOAD CELL ARRANGEMENT

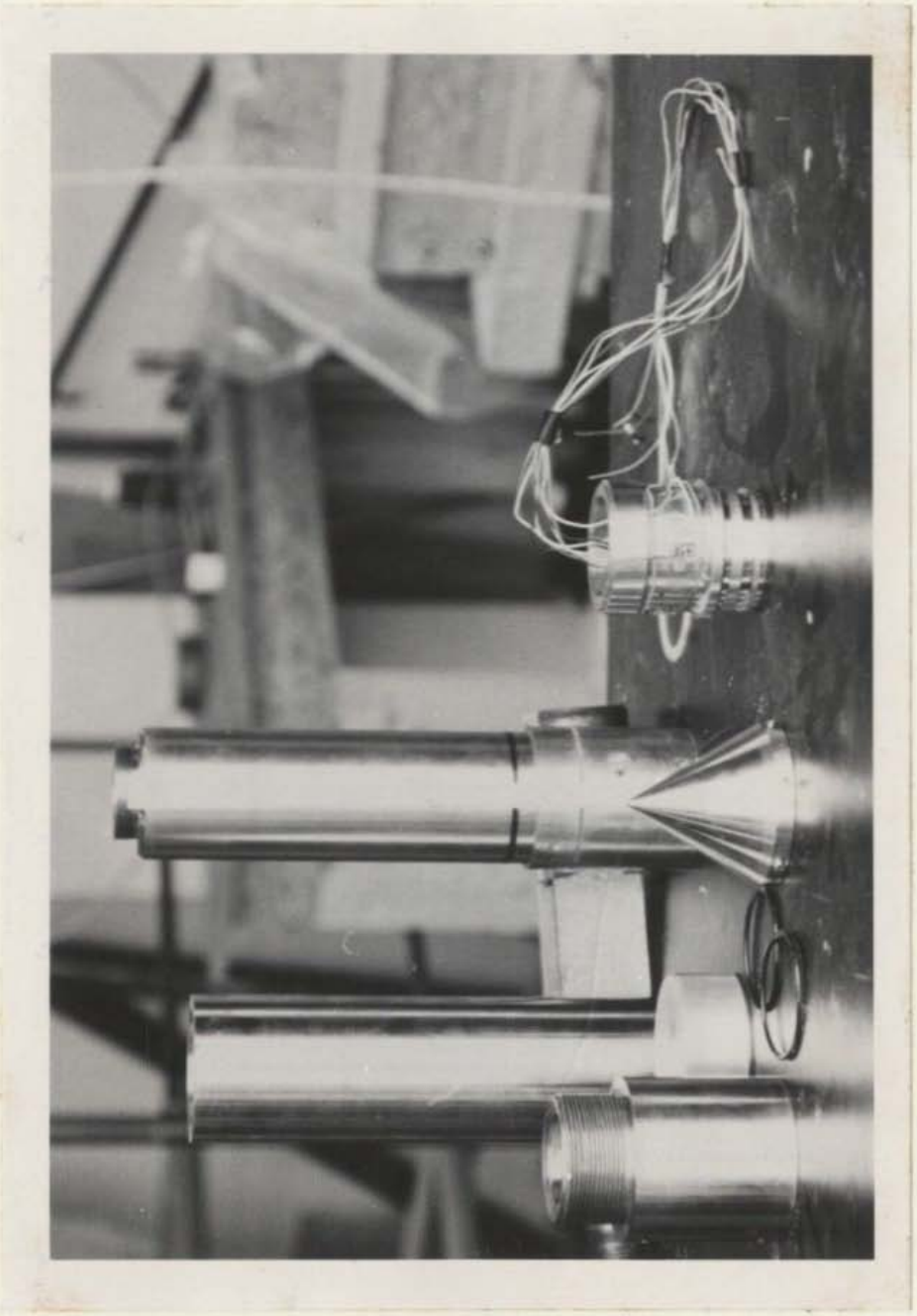


FIG 5b. PHOTOGRAPH SHOWING DETAILS OF LOAD CELL ARRANGEMENT

were plotted and the load versus strain indicator reading curves were obtained for the load cells. The strain gage bridges exhibited excellent linearity. These calibration curves were used to reduce the data from penetrometer tests. Details of load cell arrangements is shown in Figs. 5a and 5b. The following are the specifications of cone and friction sleeve load cells:

Gage resistance:	120 Ohms
Gage factor (G.F)	2.1
Sensitivity:	200 Kg/mV (3.56 cms dia. penetrometer) and 329 Kg/mV (7.62 cms dia. penetrometer)

3.3. Recording System

The output signals of the acclerometer, cone load cell and friction sleeve load cells were recorded on a high speed chart recorder (GOULD 2000), and also a tape recorder (HP 3968 A). The signals were amplified by selecting suitable gain on the amplifier before feeding into the recorder. The chart recorder is a self-contained unit housed in 250 mm main-frame chassis to accommodate three isolated recording channels. The chart speed used in this investigation was 200 mm/sec. The recorded data on the tapes will be used for permanent record and further reference when required.

3.4. Experimental Method

Before starting each test, the following calibration checks were made:

1. The actual gain of all amplifier including that of the tape recorder.
2. Balancing of the amplifiers.

3. The calibration of the acclerometer by turnover method, i.e., by orienting its sensitive axis in vertical direction and then turning over 180^{0} resulting in a change of '2g'.
4. Balancing the bridge of the cone and friction sleeve load cells.

The penetrometer was attached to a releasing mechanism which was in turn attached to a nylon rope. Thus the penetrometer can be pulled up to a certain fixed height and released by a quick release mechanism located at that height.

The height of free fall was kept constant at 3.06 metres for this investigation and corresponding velocity of impact was 7.75 m/sec. Care was taken to maintain the verticality of the penetrometer before every experiment. The complete set-up (frame, releasing mechanism, pullies, etc.) for free fall impact penetration tests is shown in Fig. 6a.

3.5. Roughness of the Cone Material

Surface roughness of the penetrometer has significant effect on the penetration resistance (Meyerhof, 1961; Karafiath, 1972). Careful consideration was given while determining the roughness of the cone material.

For tests in soils roughness is generally expressed as the ratio of the angle of friction between the penetrometer material (δ) and the soil friction angle (ϕ), i.e., relative roughness (δ/ϕ). In this investigation absolute roughness values were also determined in terms of the centre line average (CLA). Taylor-Hobson No. 4 Talysurf

(Fig. 6b) and a rectilinear recorder were used to evaluate surface roughness of three different cone tips used in this investigation. The results are shown in Appendix A. The roughness (CSA B95; 1962) is expressed in terms of centre line average (CLA) in microns over a cut-off length of 0.254 mm. The measured roughness values are presented in Table 3a. From these results it is seen that there is some difference in the CLA values of the plates and cones. Thus, the value of δ obtained for the plates from direct shear tests would be slightly different for the cones actually used in the penetration tests. A correction factor was therefore applied to calculate the final values of roughness for different cone materials.

3.6. Target Preparation

Two types of soil target materials were selected for this investigation:

(i) Silica-70 sand

(ii) Modelling clay

The materials were readily available and samples could be prepared easily. Besides, these were chosen as representative of purely non-cohesive (silica-70 sand) and purely cohesive (modelling clay) targets.

3.6.1. Silica-70 Sand

Sufficient care was taken while preparing samples of sand in view of the fact that preparation of homogeneous samples of cohesionless soil is difficult. Although sufficient accuracy could be achieved for dense and medium dense sand samples, it was difficult

(Text continued page 37)



FIG 6a. PHOTOGRAPH SHOWING EXPERIMENTAL FACILITY

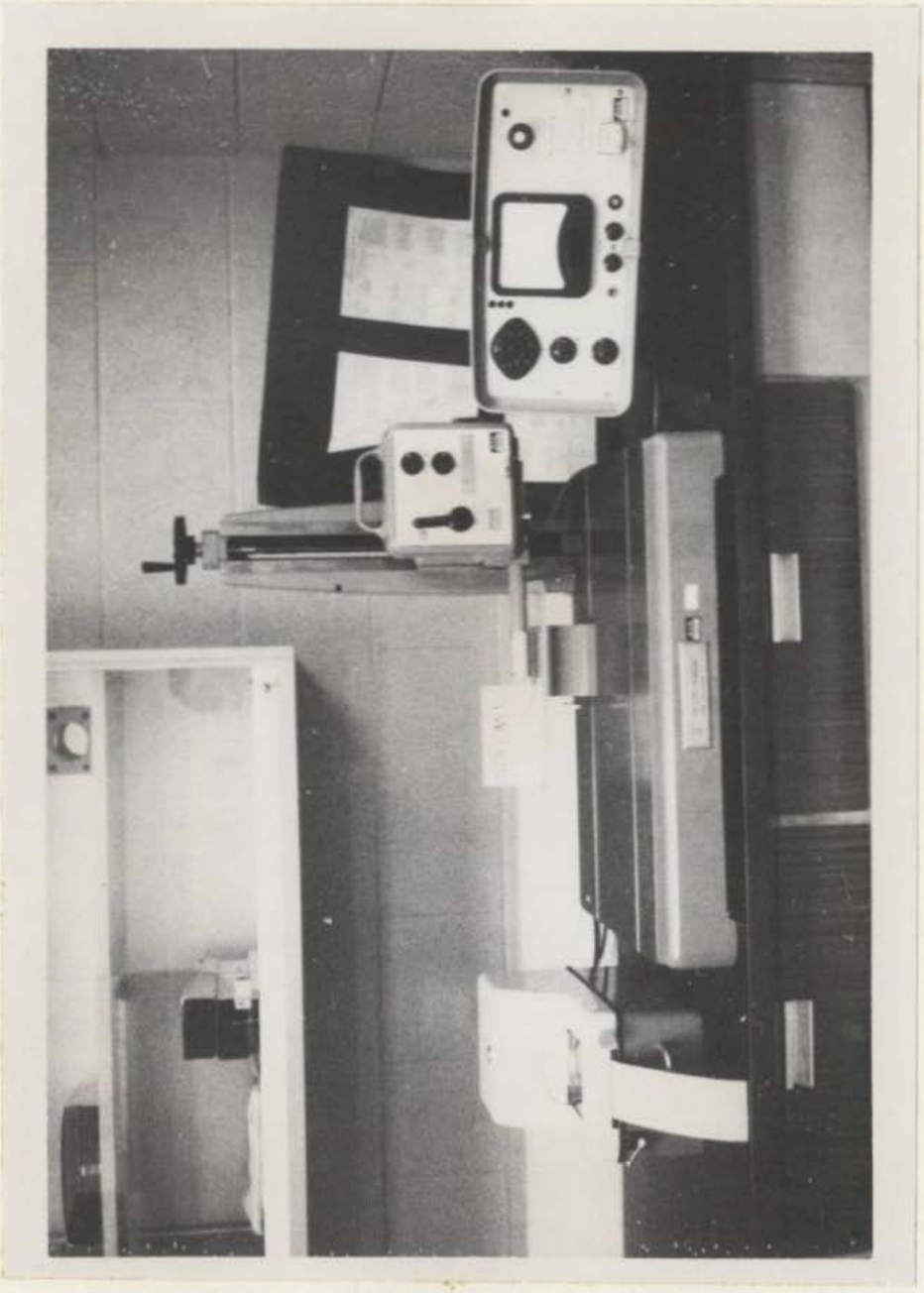


FIG 6b. TAYLOR HOBSON No. 4 TALYSURF MACHINE

TABLE 3a. SURFACE ROUGHNESS OF DIFFERENT CONE MATERIALS

Material / Tested Shape	Stainless Steel CLA -- microns	Polished Aluminium CLA -- microns	Sanded Aluminium CLA -- microns
Plate 6 cms x 6 cms	20	30	50
Cone $\alpha = 15^{o}$	22.5	37.5	52.5
Cone $\alpha = 30^{o}$	22.5	32.5	55
Cone $\alpha = 90^{o}$	22.5	40	60

TABLE 3b. DIRECT SHEAR TEST RESULTS FOR DETERMINATION OF ROUGHNESS - SILICA 70 SAND

Density Index (I_D)	Soil to Soil Friction Angle (ϕ)	Stainless Steel to Soil Friction		Polished Aluminium to Soil Friction		Sanded Aluminium to Soil Friction	
		(δ)	(δ/ϕ)	(δ)	(δ/ϕ)	(δ)	(δ/ϕ)
0.71	41.5^o	18.75^o	0.45	21^o	0.50	27^o	0.65
0.45	39.5^o	17.85^o	0.45	19^o	0.48	25.75^o	0.65
0.26	36^o	15.12^o	0.42	18.7^o	0.52	22.30^o	0.62
(δ/ϕ) average		0.44		0.50		0.64	

to maintain a constant density at all depths for loose sand.

Colour markings were made in a wooden box (0.914 m x 0.685 m x 0.914 m) at 25 cms intervals and sand was carefully placed up to the required height. Compaction was done with the help of an electrically operated vibrator. As soon as the top layer of sand reached the 25 cms marking, a further quantity of sand was placed and vibrated in the same manner until the desired volume was obtained. This was achieved by controlling the time of vibration for each layer. After compaction was completed up to the topmost layer, total weight of sand was determined. Thus, knowing the volume, the final unit weight was calculated. Raining technique was used for construction of loose targets. Sand was poured in while maintaining a constant height of drop from the existing target surface. As soon as the desired height of the sample was obtained, the box was weighed carefully. Thus the final unit weight was calculated. Three different densities of sand target prepared:

1. Dense sand (S1 type): 16.18 KN/m^3
2. Medium dense sand (S2 type): 15.05 KN/m^3
3. Loose sand (S3 type): 14.09 KN/m^3

For saturated samples, the same procedure was adopted as previously described for dry samples. After the target was constructed, water was added in the form of light spray. The container that held the soil was not perfectly water tight resulting in some drainage of water from the sample. Saturated samples tested in this investigation are not fully saturated in the strict sense.

3.6.2. Modelling Clay

Before preparation of the target material, Standard Proctor compaction tests were done to obtain the relationship between dry unit weight and water content for this type of soil. The results are shown in Fig. 7.

The material was thoroughly pulverized and dried. A predetermined quantity of water was added to the soil and placed in a large concrete mixing machine (Fig. 8). When the mixture was homogeneous then it was taken out from the machine. The volume of a cylindrical container (0.9144 m x 0.4572 m) was accurately calculated. The soil mixture was placed inside the container and compacted with a Modified AASHTO hand hammer. The desired bulk density was obtained using precalculated number of blows per layer of soil.

Representative samples were taken at random and at different depths during the target preparation to calculate the exact water content and bulk density of the target material. Cylindrical steel tubes were used to collect samples for calculating the unit weight of soil and also to perform triaxial shear tests. Vane shear tests were also conducted before and after each set of experiments at different depths. Two different types of clay samples were used as follows:

(i) Medium stiff clay (C1 type)

Dry density = 14.51 KN/m^3

Water content = 29.61%

(ii) Soft clay (C2 type)

Dry density = 13.50 KN/m^3

Water content = 34.15%

3.6.3. Target Properties

In addition to target preparation, several tests were conducted to determine the physical properties of soil. These include specific gravity, grain size distribution, Atterberg limits (clay) and maximum and minimum void ratio (sand). These tests were performed immediately after preparation of the target.

Classification data for silica-70 sand are:

Mean diameter	= 0.115 mm
Coefficient of uniformity	= 1.95
Specific gravity of grains	= 2.60
Maximum void ratio	= 0.95
Minimum void ratio	= 0.42

The gradation curve for this soil is shown in Fig. 9a and is classified as medium to fine sand size.

The grain size distribution of modelling clay is shown in Fig. 9b. It has the following properties:

L.L	= 37%
P.L	= 21%
Plasticity Index	= 16%
Specific gravity	= 2.80

A complete set of properties of the targets are tabulated in Tables 4a, 4b and 4c.

3.6.4. Shear Tests

The shear strength of silica-70 sand was determined using triaxial compression tests and direct shear tests, while for

modelling clay, the strength properties were determined using triaxial compression tests and vane shear tests. Triaxial tests were conducted with confining pressures 103.4 KPa (15 psi), 137.9 KPa (20 psi) and 206.8 KPa (30 psi). The results are shown in Figs. 10a, 10b, 10c, 10d and 10e.

A series of direct shear tests were conducted on silica-70 sand to determine the values of the angle of shear resistance (ϕ) and relative roughness of different cone material (δ/ϕ). The tests were conducted in a constant rate of strain shear box WF 25000 (Fig. 11). The value of angle shear resistance (ϕ) as obtained from direct shear tests are compared with triaxial test results in Figs. 12a and 12b.

A similar method was adopted to determine adhesion (c_a) between modelling clay and steel. The results are shown in Table 4c.

Comparison of vane shear test results with that obtained from triaxial tests for modelling clay is shown in Table 4b. The final value of cohesion (c) was taken as the average of the two test results.

3.6.4.1. Penetrometer to Soil Friction Angle

To determine the friction angle between the penetrometer material and soil, tests were conducted in the WF 25000 shear box. The upper half was filled with silica-70 sand at a desired initial density and the lower half of the shear box is replaced by a solid plate of the penetrometer material. The results are shown in Table 3b. The three different penetrometer cone materials tested are:

(Text continued page 55)

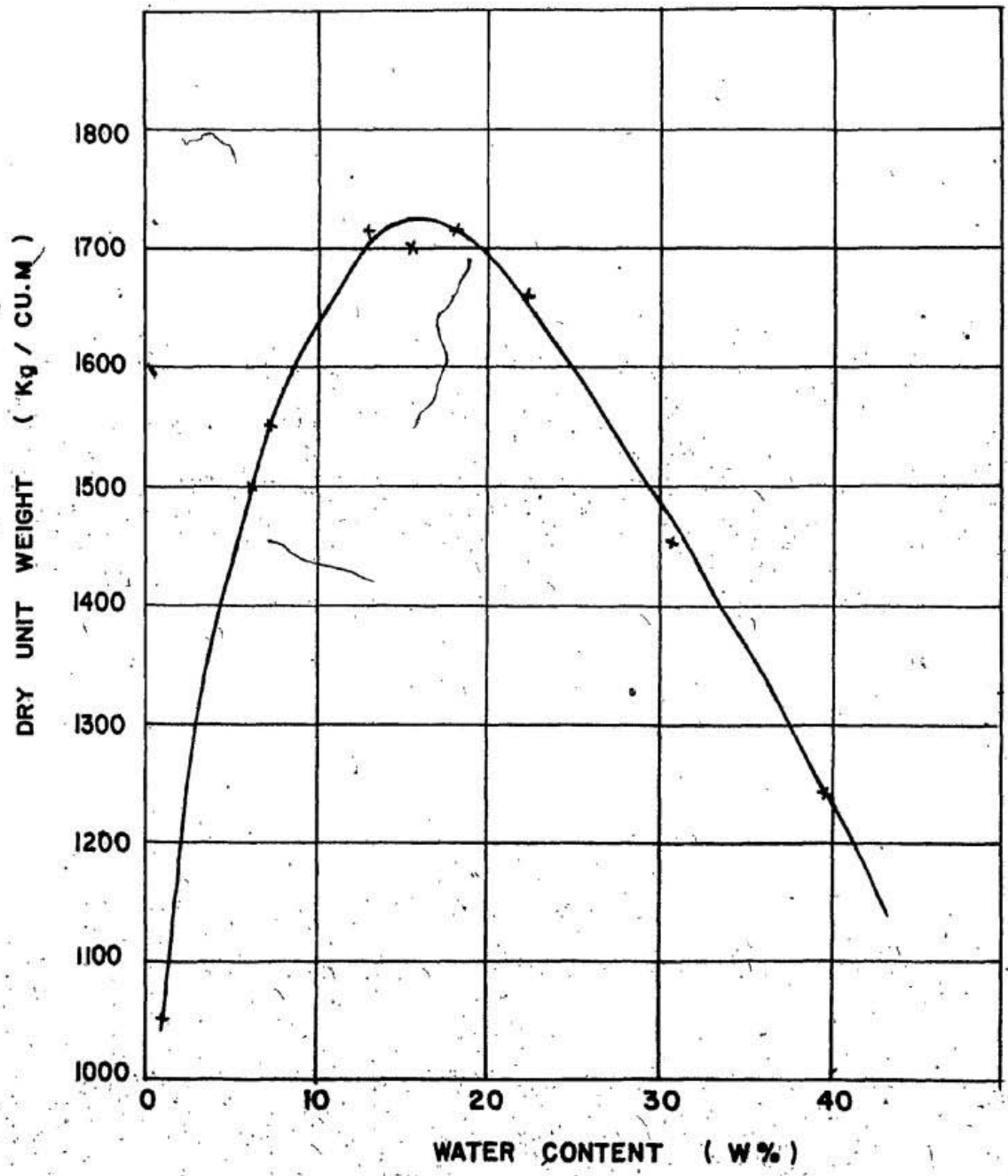


FIG 7. STANDARD PROCTOR COMPACTION TEST FOR MODELLING CLAY

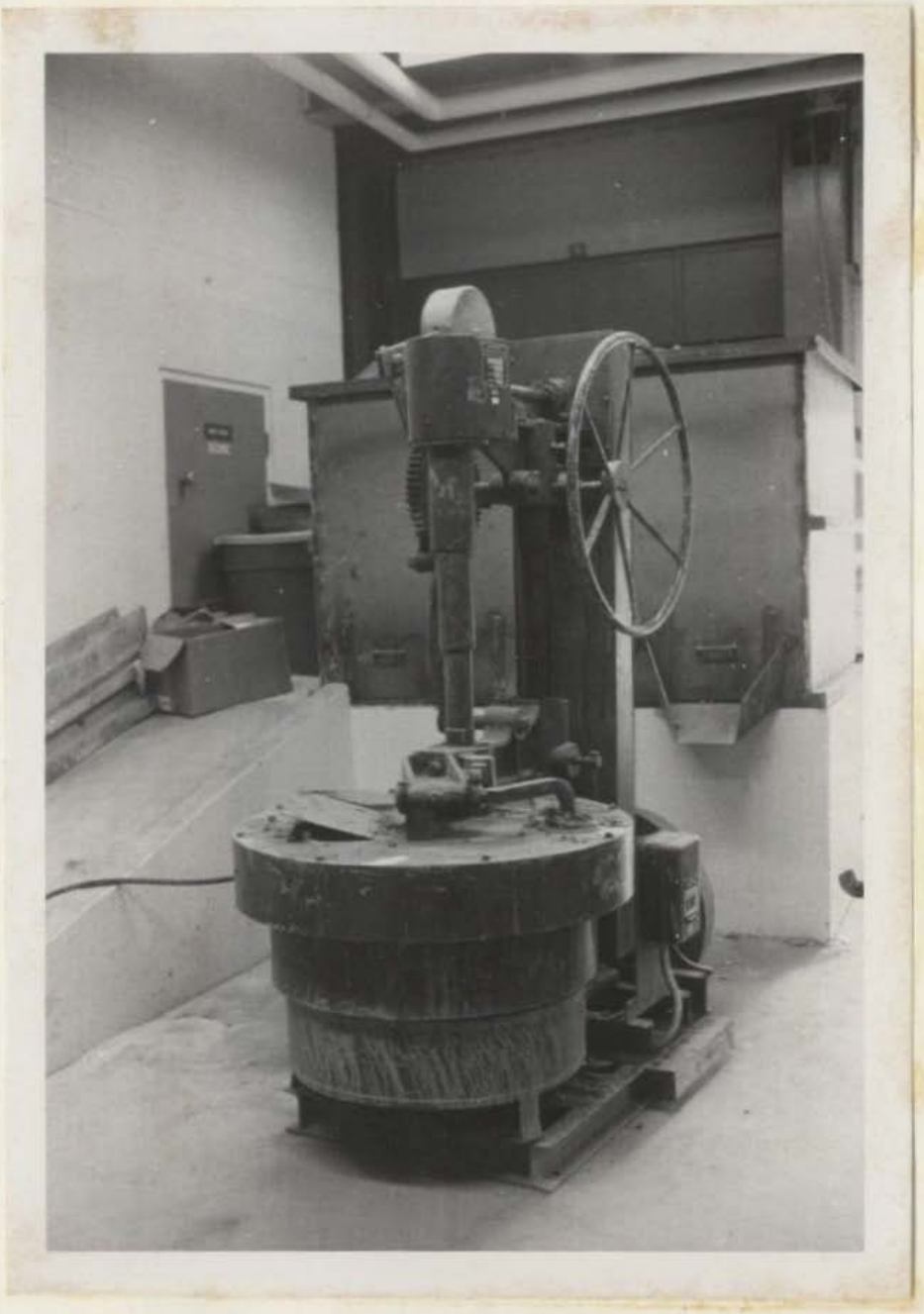


FIG 8. EQUIPMENT FOR MIXING CLAY SAMPLES

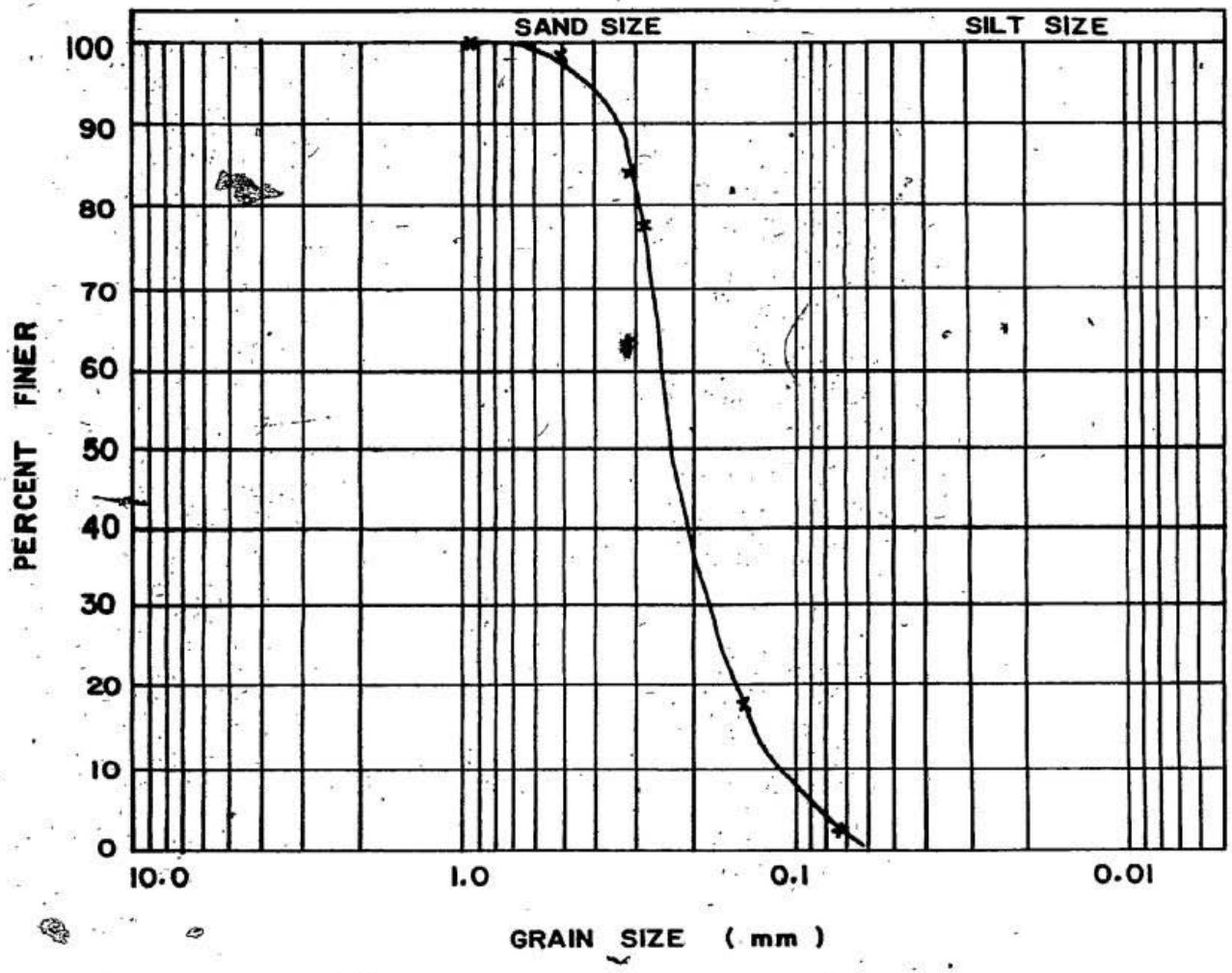


FIG 9a. GRAIN SIZE DISTRIBUTION FOR SILICA-70 SAND

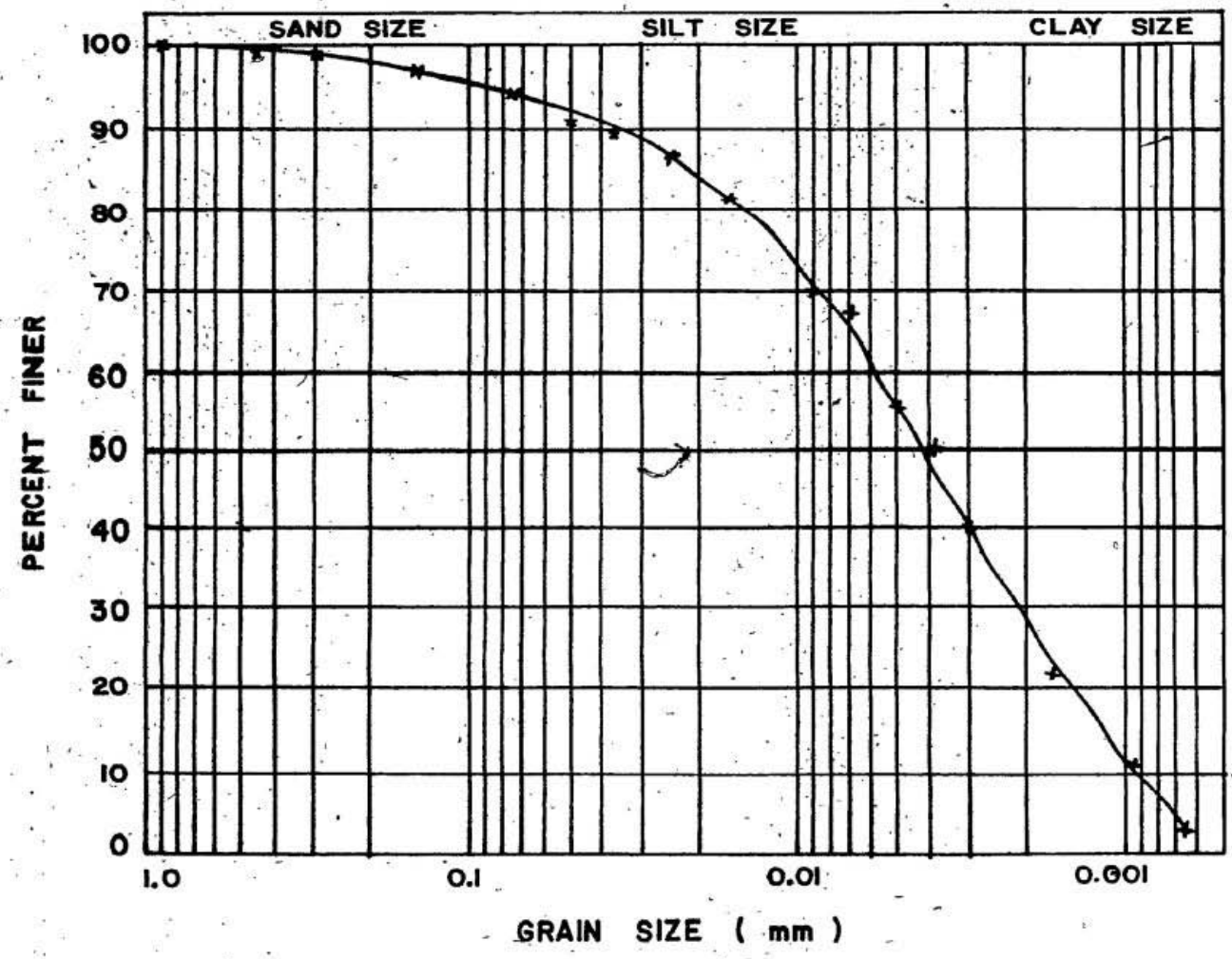


FIG 9b. GRAIN SIZE DISTRIBUTION FOR MODELLING CLAY

TABLE 4a. PROPERTIES OF SAND TARGETS

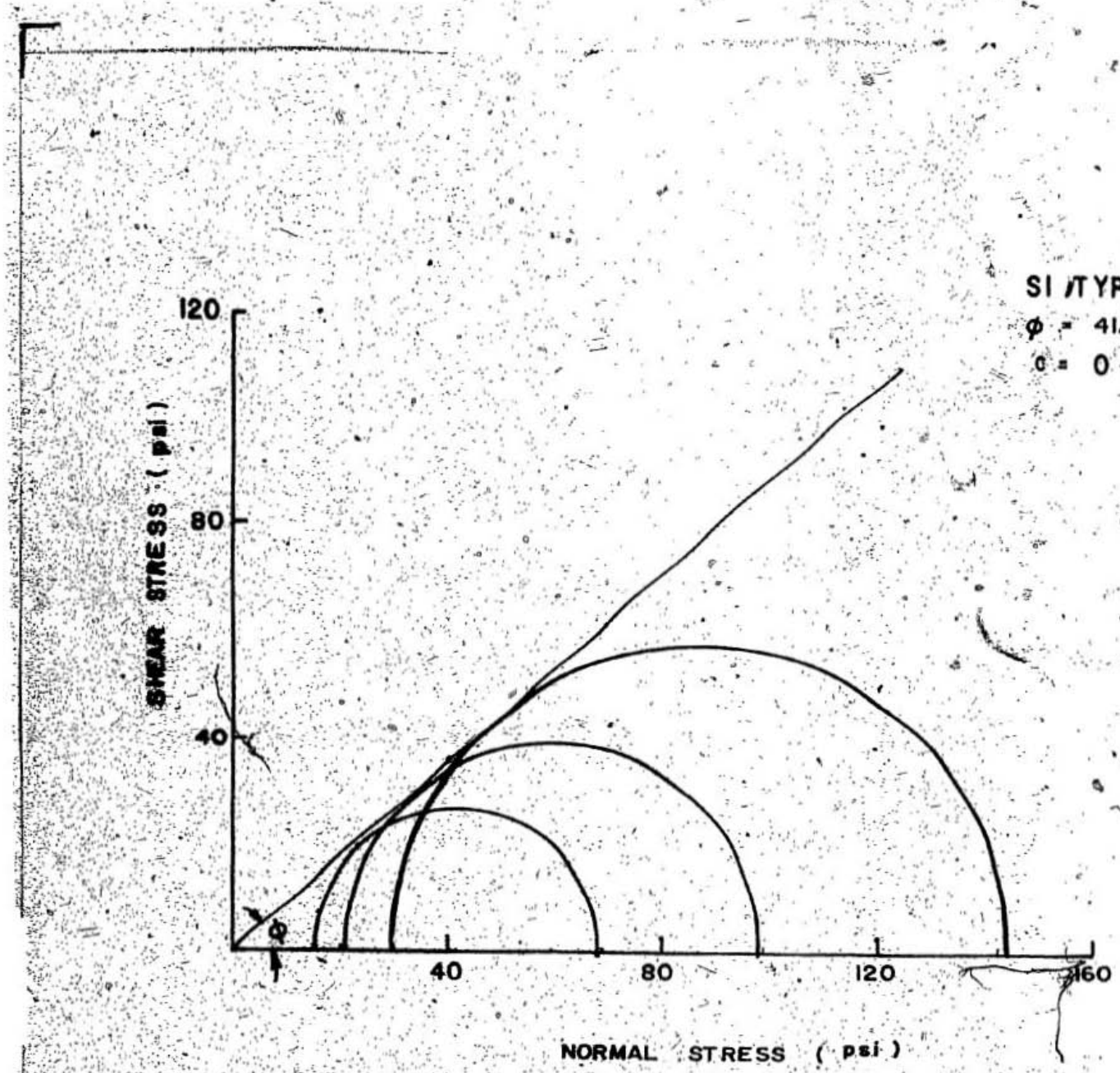
Soil Type	Dry Unit Weight (γ_d) KN/m^3	Angle of Shear Resistance (ϕ)		Cohesive Strength (c) KPa	Void Ratio (e)	Density Index (I_D)	Specific Gravity (G)
		Triaxial	Direct Shear				
S1	16.18	41.5^o	41^o	0	0.58	0.71	2.60
S2	15.05	39.5^o	39.15^o	0	0.70	0.45	2.60
S3	14.09	36^o	35.52^o	0	0.81	0.26	2.60

TABLE 4b. PROPERTIES OF CLAY TARGETS

Soil Type	Dry Unit Weight (γ_d) KN/m^3	Water Content (w) %	Cohesion (c) KPa			Angle of Shear Resistance(ϕ)	Liquid Limit %	Plastic Limit %	Plasticity Index %	Specific Gravity (G)
			Triaxial	Vane Shear	Average					
C1	14.51	29.61	35.60	36.50	36.05	4^o	37%	21%	16%	2.80
C2	13.50	34.15	16.20	15.85	16.02	3.5^o	37%	21%	16%	2.80

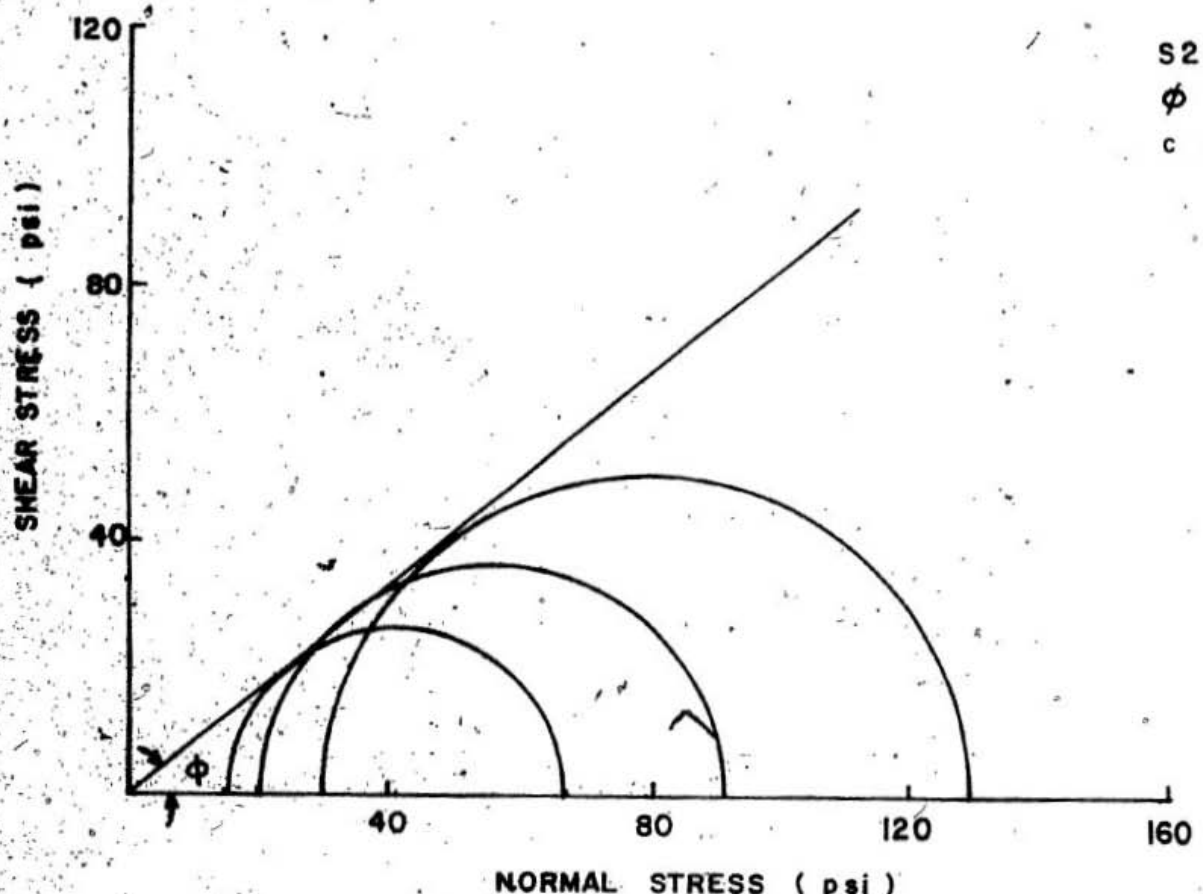
TABLE 4c. DIRECT SHEAR TEST RESULTS FOR DETERMINATION OF ADHESION (c_a)

Soil Type	Cohesion (c) KPa	Angle of Shear Resistance (ϕ)	Material	Normal Stress Kg/cm^2	Shear Stress at Failure Kg/cm^2	Adhesion (c_a) KPa	Av. Adhesion (c_a) KPa
C1	36.05	4°	Stainless Steel	2.347	0.300	29.4	28.88
				2.902	0.264	25.87	
				3.458	0.320	31.36	
C2	16.02	3.5°	Stainless Steel	2.347	0.140	13.72	13.85
				2.902	0.140	13.72	
				3.458	0.144	14.11	



1 psi = 6.895 KN/sq.m

FIG 10a. TRIAXIAL TEST TESULTS FOR SILICA- 70 SAND (SI TYPE SOIL)



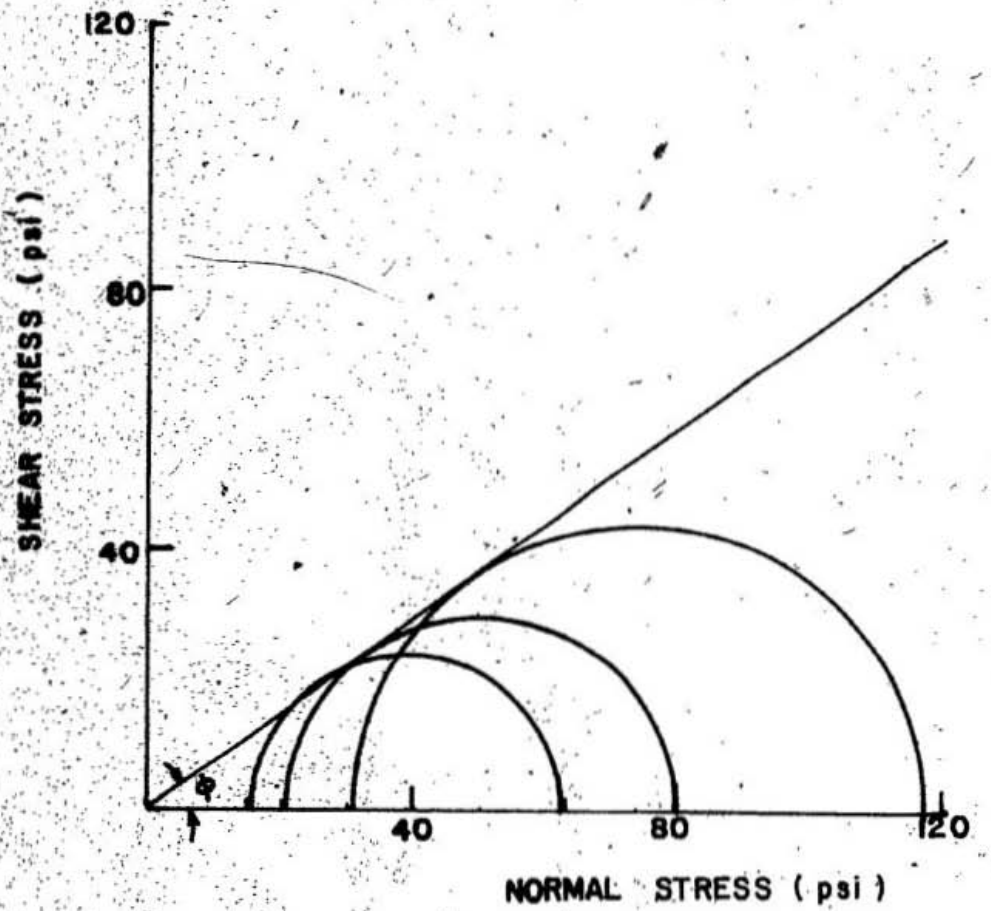
S2 TYPE SOIL

ϕ = 39.5°

c = 0

1 psi = 6.895 KN/ sq.m

FIG 10b. TRIAXIAL TEST RESULTS FOR SILICA- 70 SAND (S2 TYPE SOIL)



S3 TYPE SOIL

ϕ = 36°

c = 0

1 psi = 6.895 KN/sq.m

FIG. 10c. TRIAXIAL TEST RESULTS FOR SILICA- 70 SAND (S3 TYPE SOIL)

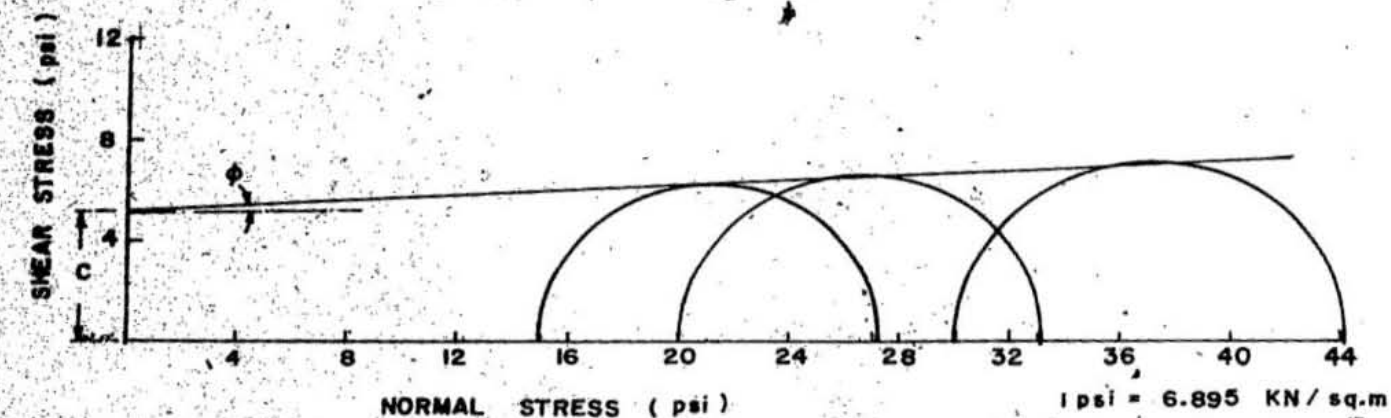


FIG 10d. TRIAXIAL TEST RESULTS FOR MODELLING CLAY .

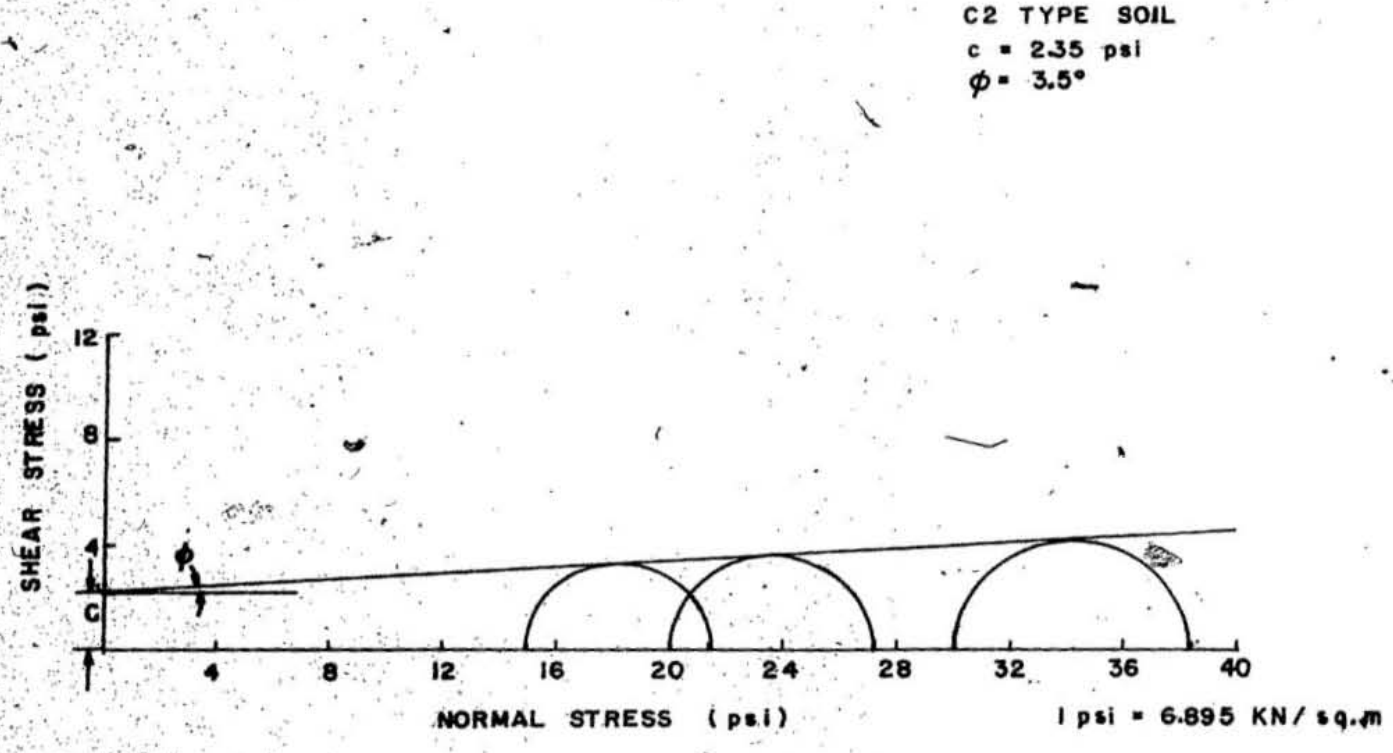


FIG 10e. TRIAXIAL TEST RESULTS FOR MODELLING CLAY

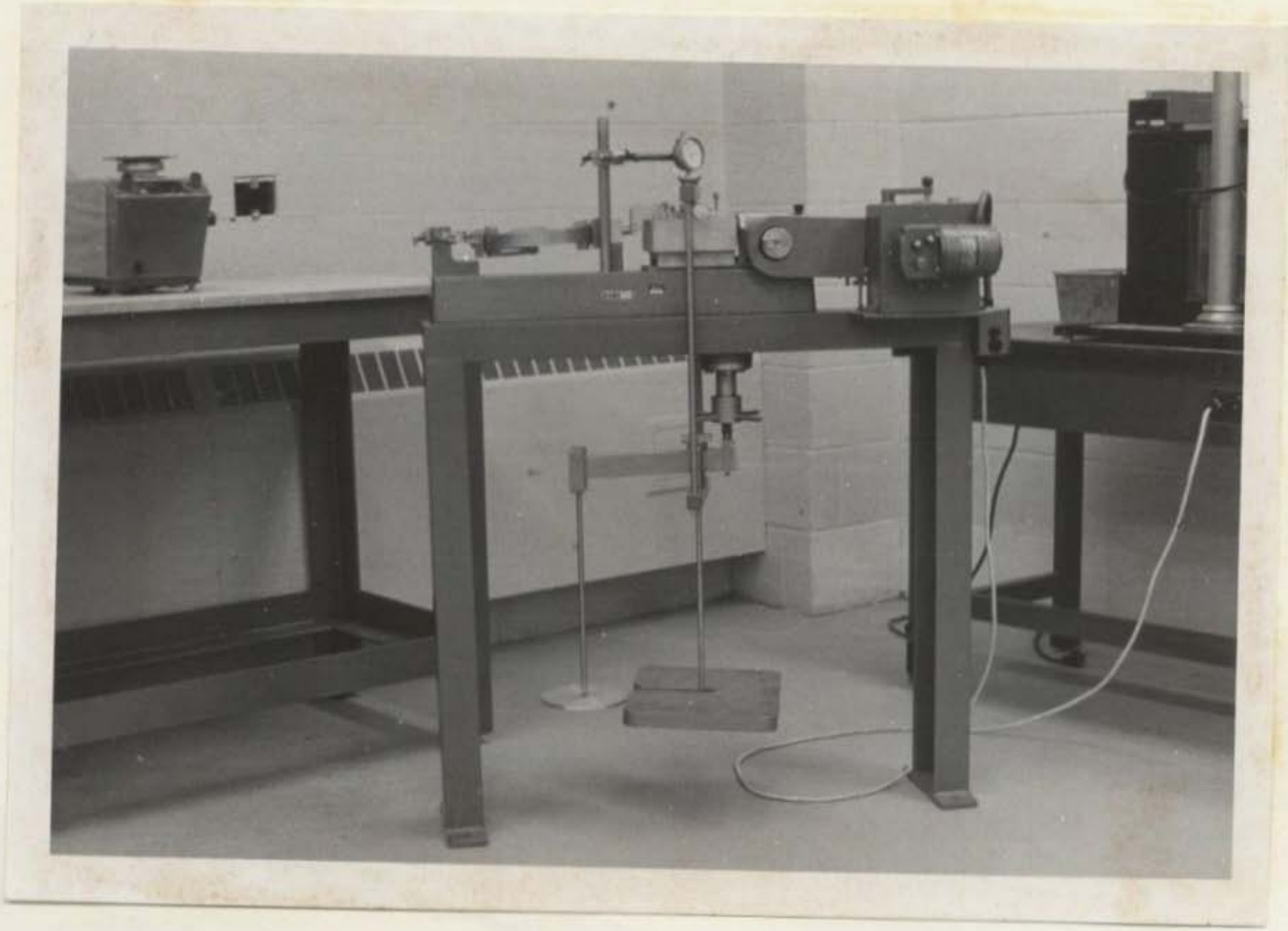


FIG 11. CONSTANT RATE OF STRAIN SHEAR BOX - WF 25000

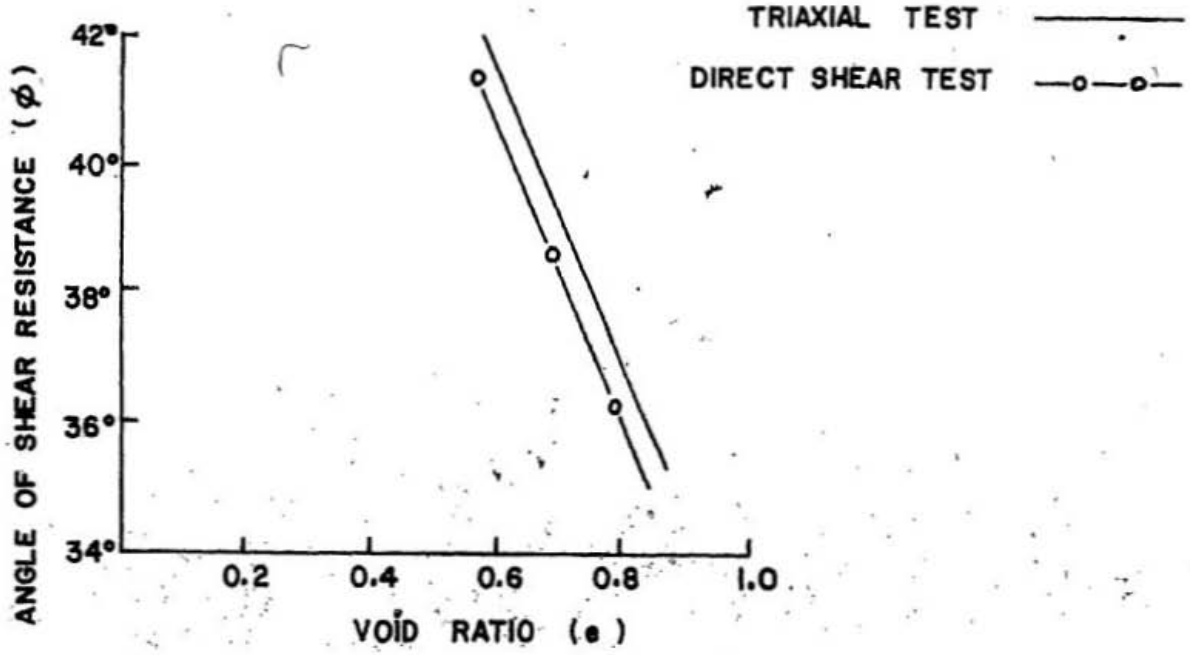


FIG 12a. VARIATION OF ϕ WITH e FOR SILICA 70 SAND AS DETERMINED BY DIRECT SHEAR AND TRIAXIAL TESTS

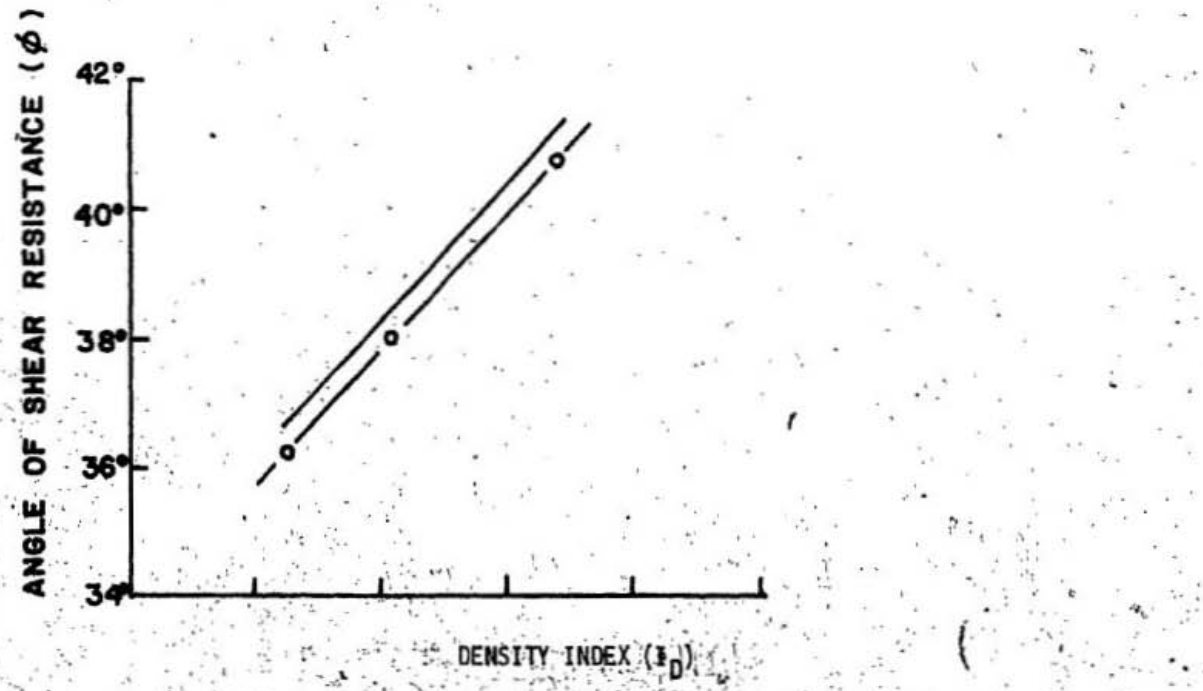


FIG 12b. VARIATION OF ϕ WITH I_D FOR SILICA 70 SAND AS DETERMINED BY DIRECT SHEAR AND TRIAXIAL TESTS

1. Stainless Steel
2. Polished Aluminium
3. Sanded Aluminium

The values of direct shear test were corrected for the actual cone roughness. The correction factors were obtained from the results of "Talysurf" tests on both plates and cone as shown in Table 3a. Correction factors of 1.125, 1.2 and 1.166 were applied for stainless steel, polished aluminium and sanded aluminium, respectively. The corrected values of relative roughness (δ/ϕ) are:

Stainless Steel	$\delta/\phi = 0.5$
Polished Aluminium	$\delta/\phi = 0.6$
Sanded Aluminium	$\delta/\phi = 0.75$

In the next chapter, these values will be used in the calculations.

3.7. Summary

The methods of preparing the soil targets and the physical properties of the soils and the penetrometers are given in this chapter. Results of conventional laboratory tests have been presented and these results will be used for comparison and correlation with the penetrometer tests.

CHAPTER IV

ANALYSIS OF RESULTS AND DISCUSSION

4.1. General

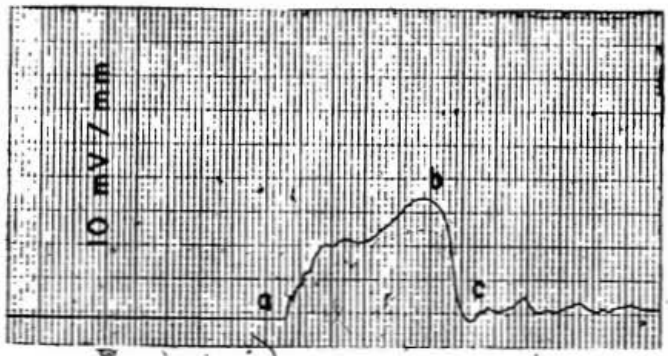
Free fall penetration tests as described in the previous chapter were conducted and the output from the penetrometer was recorded on a 3-channel chart recorder and also an instrumentation tape recorder. Typical raw data from the chart recorder is shown in Fig. 13. The record obtained is a voltage output, from the accelerometer, the cone load cell and the sleeve load cell, as a function of real time. Representative raw data for different types of soil is given in Appendix B.

(a) Acceleration/deceleration record

As soon as the penetrometer is released, it is under a constant acceleration 'g' due to gravity till it strikes the soil target. This corresponds to the initial horizontal straight line of the deceleration record. Upon impact, the penetrometer decelerates, the magnitude of which increases with the depth of penetration, as shown in the range ab of the record. At b, the deceleration is a maximum and it tapers off in the range bc.

At c, there is an acceleration pulse at the end of penetration event. At this time the penetrometer has passed through maximum penetration and is experiencing a very small upward movement. The soil resistance would thus be negative. Scott and Pearce (1975)

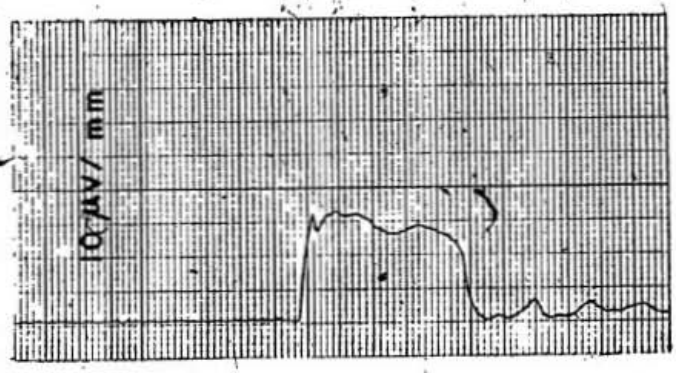
(Text continued page 58)



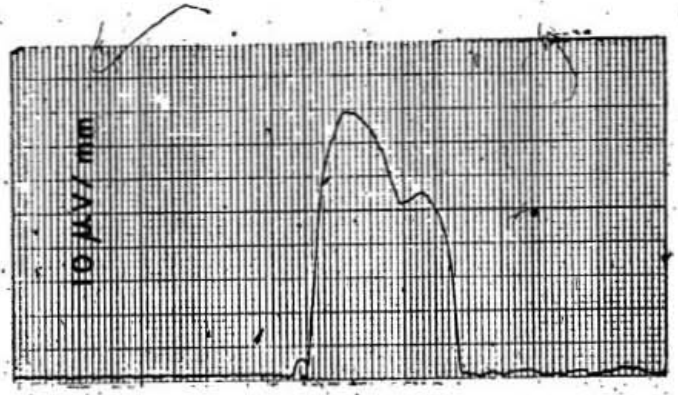
C2 TYPE SOIL
PENETROMETER
3.56 cms DIA.
CONE 30°
STAINLESS STEEL

TIME (5 milli sec/ mm)

DECELERATION



CONE RESISTANCE



SLEEVE RESISTANCE

FIG 13, TYPICAL OUTPUT FROM A FREE FALL PENETRATION TEST

studied this phenomenon in some detail and attributed it to a rebound phenomenon with a kinetic energy of about one-tenth the initial impact energy. However, this part of the penetration event has very little effect on the total depth of penetration and is not considered in further detail in this analysis. Beyond c, the accelerometer reaches a stable level gradually.

(b) Cone thrust record

Similar to the deceleration curve, cone resistance rises sharply soon after impact with the soil, and is steady up to the point corresponding to the maximum deceleration and then decreases rapidly at the end of the event. It may be noted that after the penetrometer comes to a stop, it still records a cone resistance equivalent to the weight of the penetrometer.

(c) Friction sleeve record

In Fig. 13, it is seen that there is a steady increase in friction sleeve resistance conforming to the pattern shown by the other two readings. Measurement of sleeve friction is significant only in the analysis of cohesive soils and this will be discussed in greater detail subsequently.

4.2. Computation of Penetration Depth

From the accelerometer output, time histories of velocity and displacement could be calculated using the method of double integration

$$V(t) = \int_0^t a(t)\, dt + V_o \quad \ldots\ldots\ldots\ldots\ldots\ldots \quad (36)$$

$$Z(t) = \int_0^t \{ \int_0^t a(t)dt + V_o \}\, dt + Z_o \quad \ldots\ldots\ldots\ldots \quad (37)$$

where $V(t)$ = Velocity at time t

$a(t)$ = Acceleration at time t

V_o = Impact velocity

$Z(t)$ = Displacement at time t

Z_o = Displacement at t = 0

The decleration function for the free fall tests is not a simple function and a mathematical solution is thus not easily possible. Solutions can be obtained using numerical method. From the output of the accelerometer, one can establish the zero reference line from the end of penetration event. A check on the accelerometer record can be made by verifying the output during free fall, with respect to the base line and see if it represents "lg" according to the calibration of the accelerometer.

Acceleration values were scaled from the chart record at 5 milli-second intervals and the whole curve was assumed to be a series of trapezoidal increments, in this short interval. If $a_0, a_1, a_2 \ldots a_n$ are the acceleration values at times $t_0, t_1, t_2 \ldots t_n$, velocity V_n at time t_n can be written as

$$V_n = \sum_{i=1}^{n} \{ \frac{a_i + a_{i-1}}{2} \}(t_i - t_{i-1}) + V_o \quad \ldots\ldots\ldots \quad (38)$$

Initial impact velocity, V_o, could be calculated either by knowing the height of free fall or from the acceleration trace up to the instant of impact. The depth of penetration can be written as:

$$Z_n = \sum_{i=1}^{n} \{\frac{V_i + V_{i-1}}{2}\}(t_i - t_{i-1}) + Z_o \quad \ldots\ldots\ldots\ldots (39)$$

Velocity and displacement histories were computed from equations (38) and (39) for the penetration tests. The values of penetration depths as computed above were compared with the depths of penetration actually measured. The agreement was good for all the tests (Tables 5a and 5b).

The deceleration, cone resistance and sleeve friction records were then re-plotted as a function of the depth.

As already described in Chapter III, three series of tests, S1, S2 and S3 were conducted in dry sand representing dense, medium and loose target, and three sets of tests were conducted in wet sand with the same dry densities. Two series of tests, C1 and C2, were conducted in clay representing medium stiff and soft clay targets. Curves similar to Fig. 13 were obtained for each test and these were re-plotted as a function of depth after computing the depth of penetration. Results obtained are discussed further below.

4.3. Velocity Variation with Depth

The actual velocity of penetration was calculated and plotted as a function of the depth for the experiments conducted. Using the theory of Murff and Coyle (1973) as given in equation (34), a computer program was developed (Appendix C) to calculate predicted velocity

of penetration at different depths.

A comparison of the two results is shown in Figs. 14a, 14b, 14c and 14d, for the three series of tests in dry sand.

On the basis of a comparison of predicted and experimental velocity profiles, it is concluded that the maximum penetration depends on the projectile cone shape and size, relative density of the target material, impact velocity, projectile diameter and projectile weight.

4.4. Free Fall Penetration Tests on Silica-70 Sand

The different theories discussed in Chapter II were used and theoretical values of penetration resistance and velocity were computed at different depths. The experimental values are compared and discussed below.

4.4.1. Cone Resistance using the Soil Properties

According to Wang's (1971) theory, the penetrometer resistance Q_u for sand is given by

$$Q_u = C_1 x \quad \ldots\ldots\ldots\ldots \text{(eqn. 29)}$$

The value of C_1 itself can be evaluated from equation (28) which relates the impact velocity and maximum penetration depth to the various other parameters. By using this approach, theoretical cone resistance was calculated at different depths and shown in Fig. 15a. Comparison of these values with the measured cone resistance shows that experimental values are marginally higher than the theoretical results.

4.4.1.1. Theoretical Cone Resistance from Deceleration Record

Cone resistance can also be obtained from the value of deceleration at different depths of penetration using the equation of Orrje and Broms (1970):

$$\sigma_m = \frac{mg}{A} - \frac{m}{A}\ddot{Z} \quad \ldots\ldots\ldots\ldots \text{(eqn. 32)}$$

The weight (W) of the penetrometer is known and using this and the deceleration record, cone thrust was calculated at different depths. Theoretical curves were plotted as shown in Figs. 15b and 15c and compared with the profiles of cone resistance actually measured with load cells. It can be seen that there is a good agreement between theoretical prediction and measured values.

Although the theoretical computations of Orrje and Broms (1970) show a better correlation, the set of data required for the two theoretical approaches discussed are entirely different. It is therefore not appropriate to evaluate the merits of one theory over the other.

4.4.1.2. Cone Resistance using Meyerhof's Bearing Capacity Theory

In all the experiments, the actual value of the angle of shear resistance was determined from direct and triaxial shear tests. Using Meyerhof's theory, Mitchell et al. (1978) interpolated and gave the values of N_q as a function of ϕ for a standard penetrometer. From these values theoretical cone resistance (q_c) was calculated using the bearing capacity formula (equation 6) for cohesionless soil. These are shown as a function of depth in Fig. 15d and compared with.

(Text continued page 74)

TABLE 5a. COMPARISON OF PREDICTED AND MEASURED PENETRATION DEPTH

Soil Type	Projectile Diameter cms	Nose length/ Diameter	Mass of Projectile Kg	Impact Velocity m/sec	Density Index (I_D)	Maximum Penetration by Numerical Method cms	Predicted Penetration by Murff and Coyle (1973) cms	Measured Penetration cms
S1	3.56	0.866	10	7.75	0.71	28.89	28.23	30.00
S1	3.56	1.165	10	7.75	0.71	25.63	29.16	28.75
S1	3.56	1.866	10	7.75	0.71	31.56	31.62	31.25
S2	3.56	0.866	10	7.75	0.45	34.08	37.61	33.00
S2	3.56	1.165	10	7.75	0.45	30.50	38.63	33.00
S2	3.56	1.866	10	7.75	0.45	37.27	41.26	38.50
S3	3.56	0.866	10	7.75	0.26	62.47	61.96	60.00
S3	3.56	1.165	10	7.75	0.26	53.88	63.12	55.25
S3	3.56	1.866	10	7.75	0.26	62.61	66.02	65.00

TABLE 5b. COMPARISON OF PREDICTED AND MEASURED PENETRATION DEPTH

Soil Type	Projectile Diameter cms	Nose length/ Diameter	Mass of Projectile Kg	Impact Velocity m/sec	Density Index (I_D)	Maximum Penetration by Numerical Method cms	Predicted Penetration by Murff and Coyle (1973) cms	Measured Penetration cms
S1	7.62	0.866	14	7.75	0.71	17.71	15.91	17.50
S1	7.62	1.148	14	7.75	0.71	16.99	16.90	17.00
S1	7.62	1.866	14	7.75	0.71	26.49	20.08	22.50
S2	7.62	0.866	14	7.75	0.45	24.20	22.59	25.00
S2	7.62	1.148	14	7.75	0.45	22.63	23.81	22.50
S2	7.62	1.866	14	7.75	0.45	30.51	27.57	30.00
S3	7.62	0.866	14	7.75	0.26	57.87	43.33	60.00
S3	7.62	1.148	14	7.75	0.26	51.14	45.00	55.00
S3	7.62	1.866	14	7.75	0.26	59.92	49.84	60.00

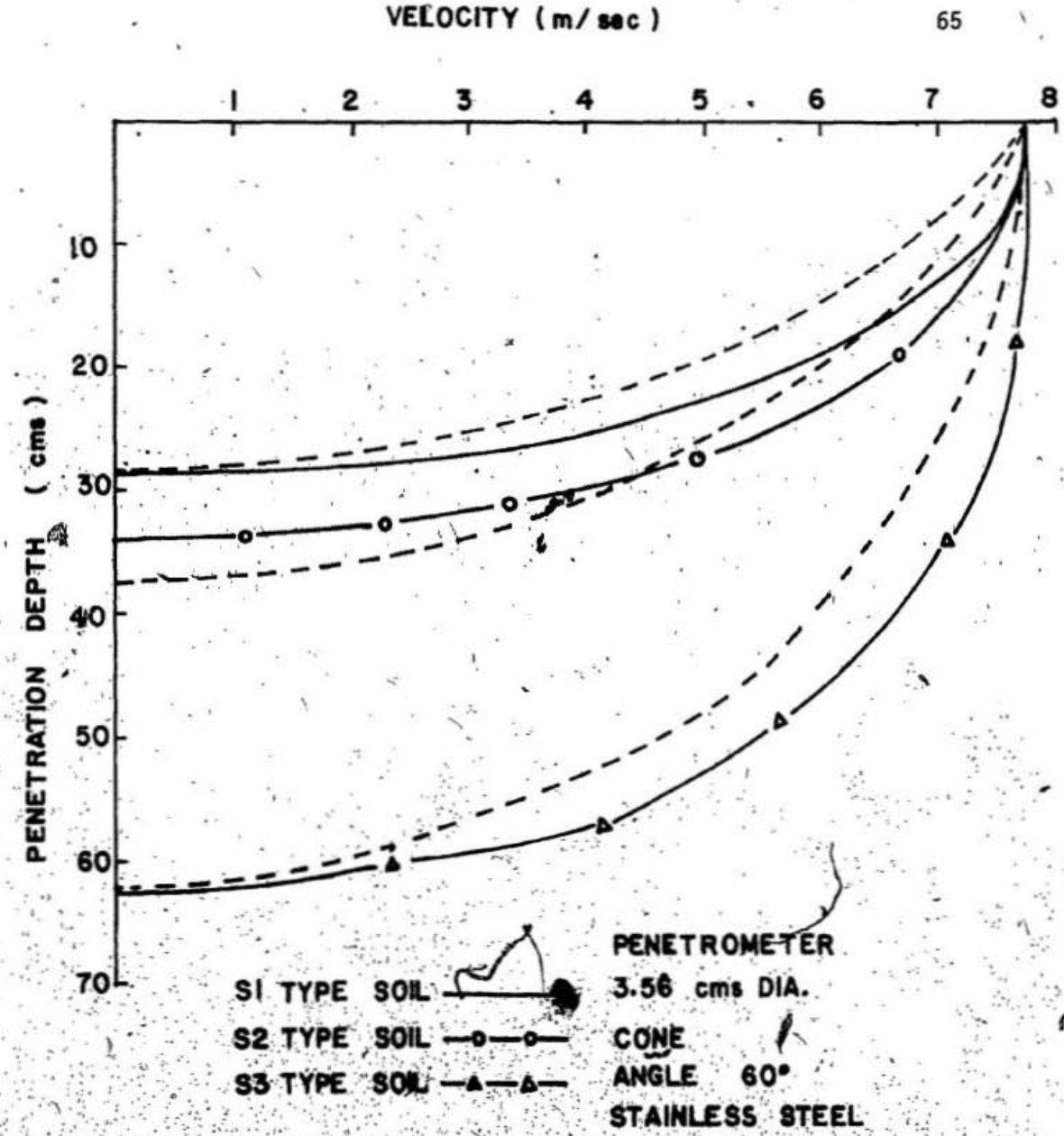


FIG 14b. COMPARISON OF PREDICTED AND EXPERIMENTAL VELOCITY OF PENETRATION FOR 3.56 cms DIA PENETROMETER (S1, S2 & S3 TYPES OF SOIL)

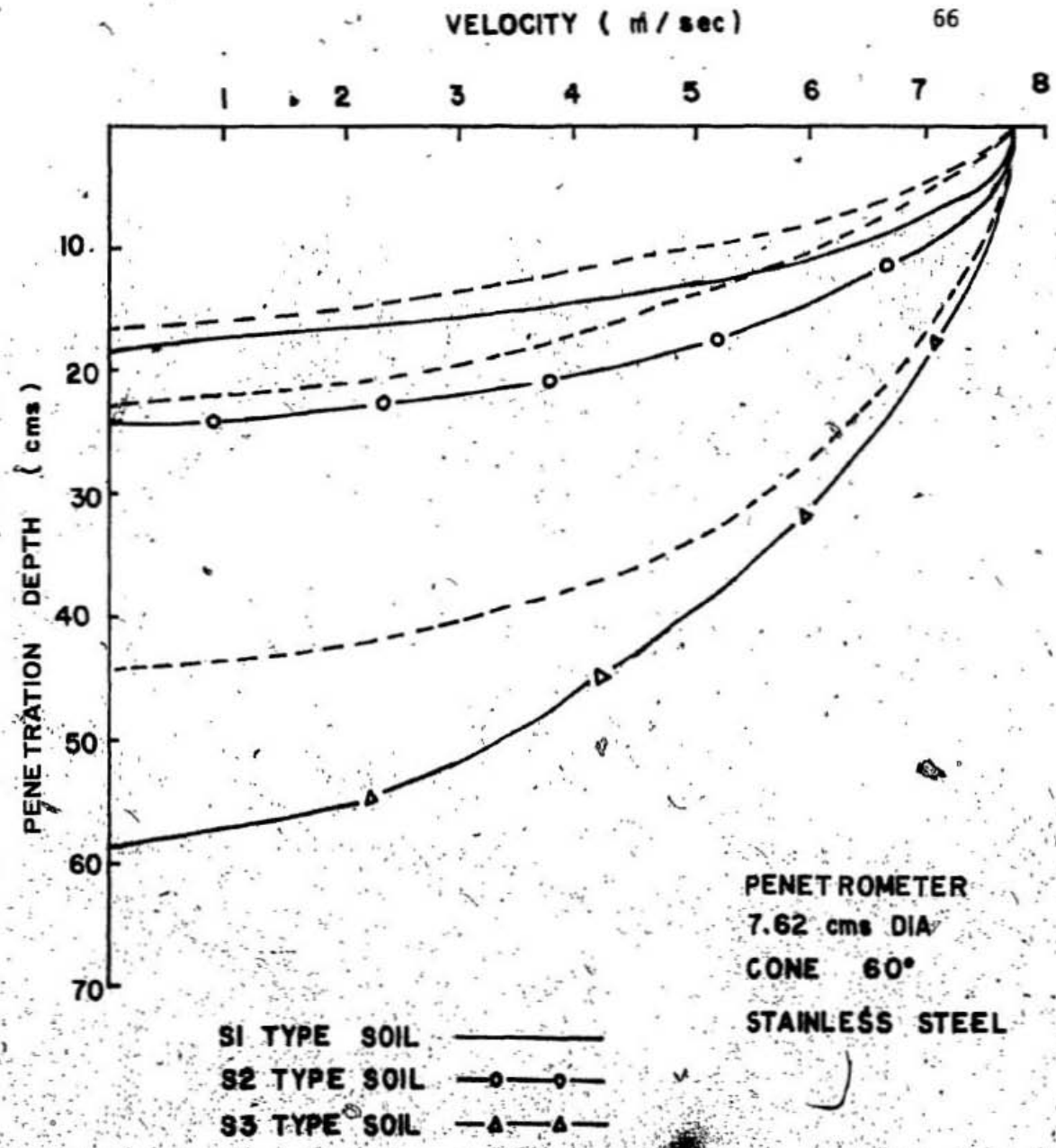


FIG 14b. COMPARISON OF PREDICTED AND EXPERIMENTAL VELOCITY OF PENETRATION FOR 7.62 cms DIA PENETROMETER (S1, S2 & S3 TYPES OF SOIL)

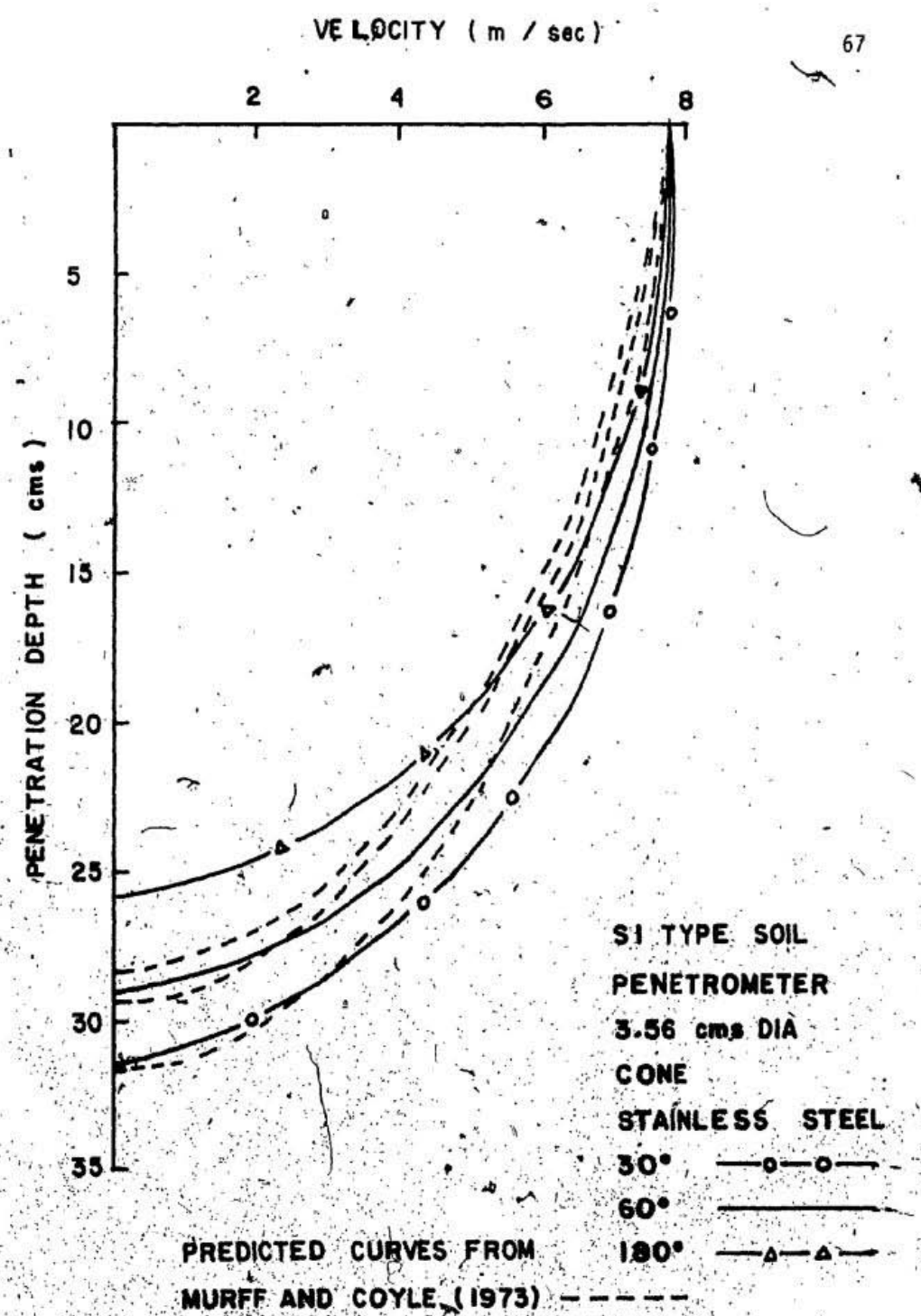


FIG 14c. COMPARISON OF PREDICTED AND EXPERIMENTAL VELOCITY OF PENETRATION FOR 3.56 cms DIA PENETROMETER (α = 15°, 30° & 90°)

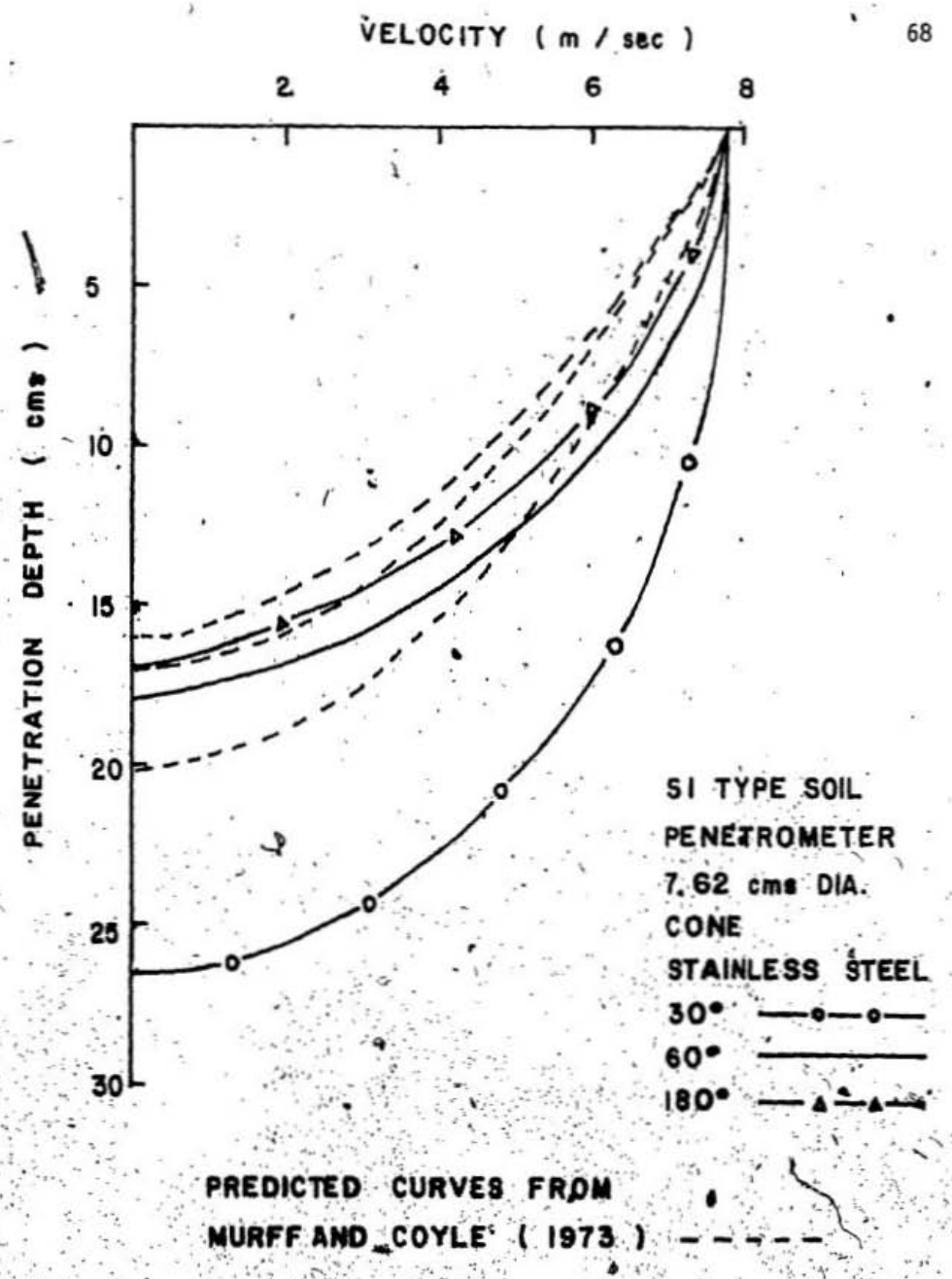


FIG 14d. COMPARISON OF PREDICTED AND EXPERIMENTAL VELOCITY OF PENETRATION FOR 7.62 cms DIA PENETROMETER (α = 15°, 30° & 90°)

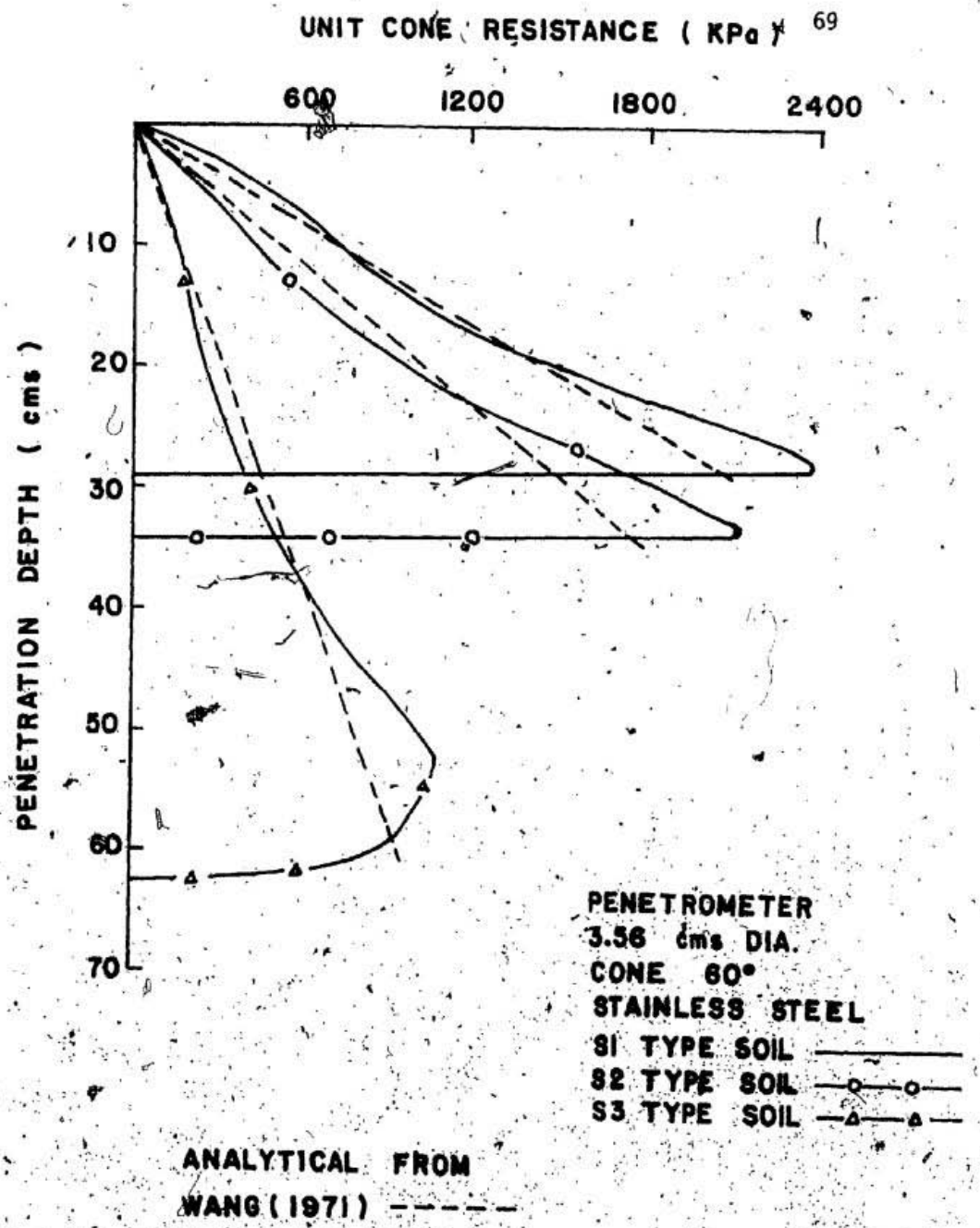


FIG 15a. COMPARISON OF ANALYTICAL AND MEASURED UNIT CONE RESISTANCE FOR 3.56 cm DIA PENETROMETER (WANG, 1971)

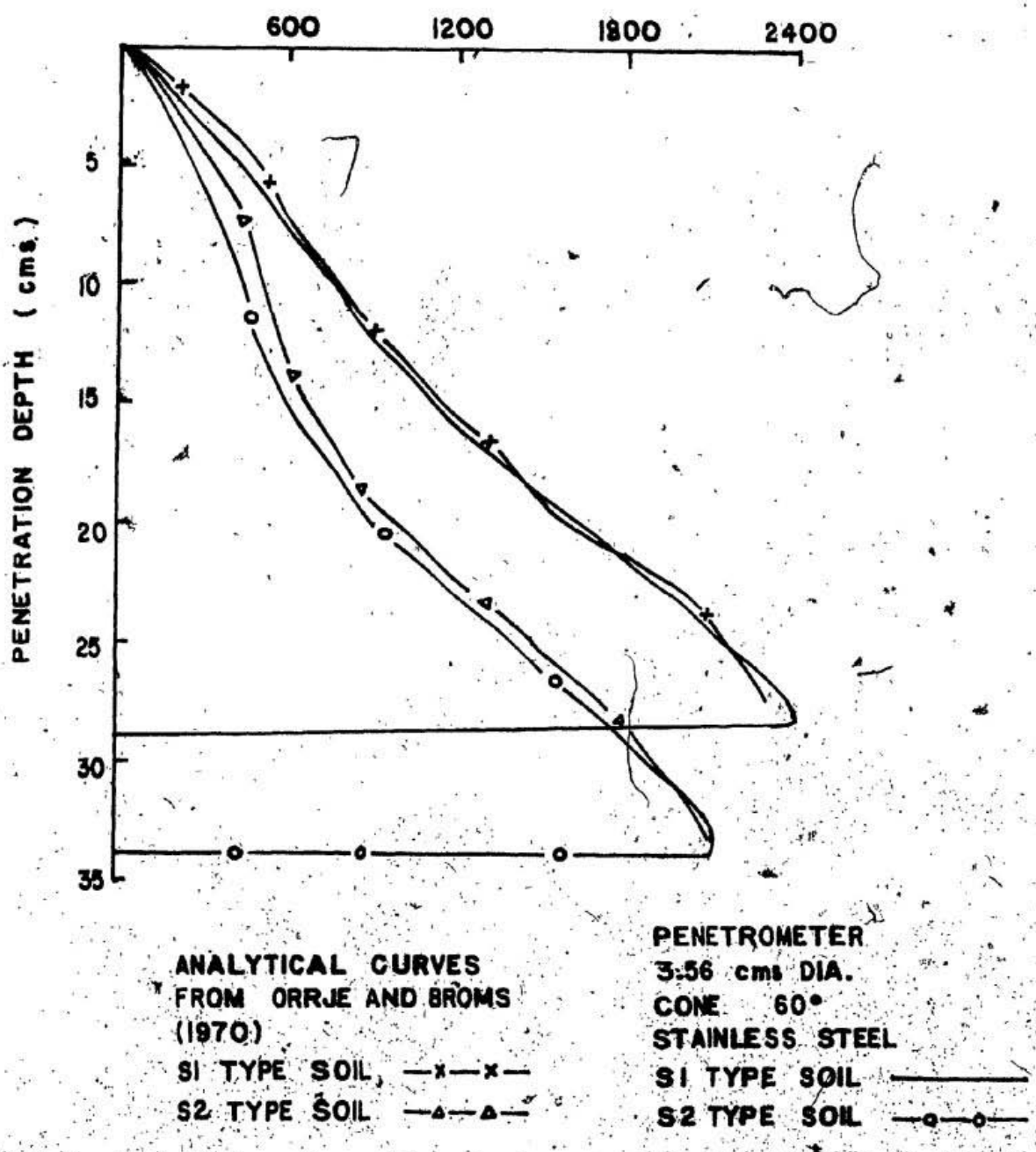


FIG 15b. COMPARISON OF ANALYTICAL AND MEASURED UNIT CONE RESISTANCE FOR 3.56 cms DIA PENETROMETER (ORRJE & BROMS, 1970)

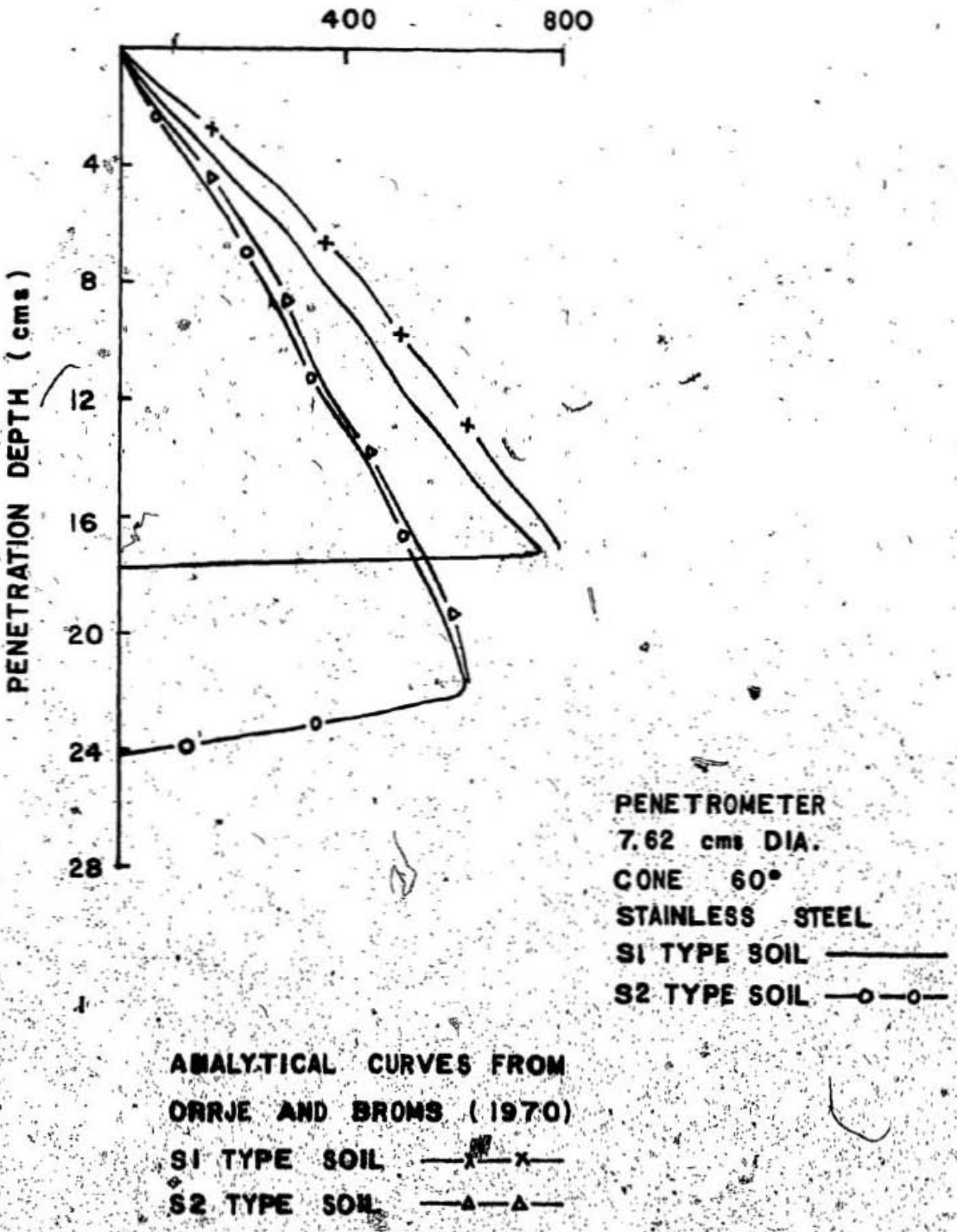


FIG 15c. COMPARISON OF ANALYTICAL AND MEASURED UNIT CONE RESISTANCE FOR 7.62 cms DIA PENETROMETER (ORRJE & BROMS 1970)

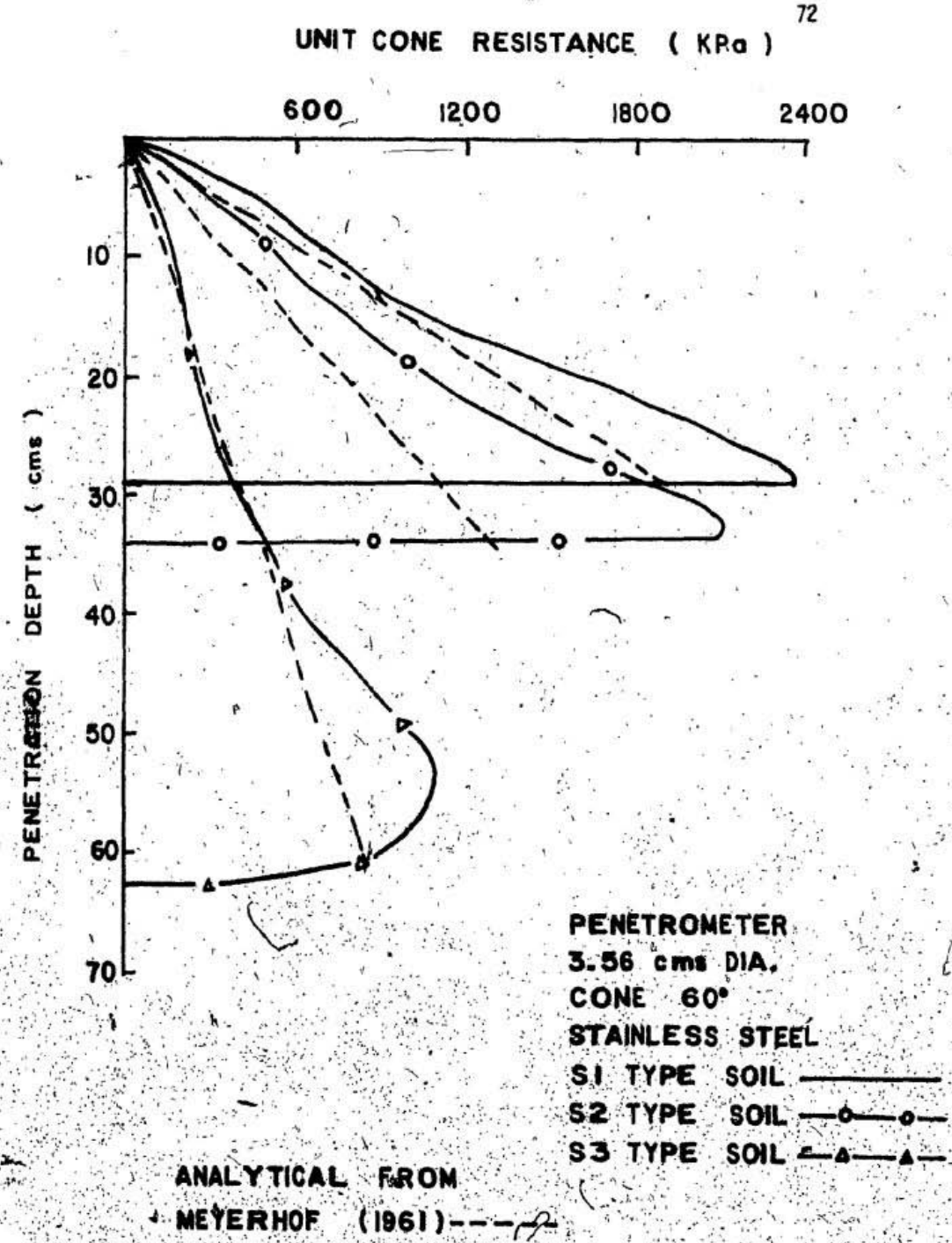


FIG 15d. COMPARISON OF ANALYTICAL AND MEASURED UNIT CONE RESISTANCE FOR 3.56 cms DIA PENETROMETER (MEYERHOF, 1961)

TABLE 6. COMPARISON OF ANGLE OF SHEAR RESISTANCE (ϕ)

(1) Soil Type	(2) Diameter of the Penetrometer cms	(3) Nq value from Wang (1971)	(4) ϕ value from Wang (1971)	(5) Nq value from Meyerhof (1961)	(6) ϕ value from Meyerhof (1961)	(7) ϕ value from triaxial test	(8) Remarks
S1	3.56	422	43^0	511.5	43.5^0	41.5^0	A good agreement is observed in ϕ values between analytical and measured from triaxial tests. The values in cols. (4) & (6) are higher than col. (7). This is attributed to the rate of loading (Whitman, 1957; Orrje and Broms, 1970). Although strain-rate is negligible in sand, there will be difference between quasi-static and dynamic tests.
S2	3.56	325	42^0	412	42.75^0	39.5^0	
S3	3.56	106	37.5^0	120	37.75^0	36^0	

the cone resistance as measured in the free fall tests. From the measured values of the cone resistance and using Wang's (1971) and Meyerhof's (1961) theories, the theoretical value of the angle of soil shear resistance ϕ was computed and compared with the triaxial test results in Table 6.

It was already pointed out in paragraph 4.3 that the velocity profile is influenced by different variables of the penetrometer and the soil. It is common knowledge that in the case of static penetration test, the shape of the penetrometer, the roughness of cone material, the diameter of penetrometer and the type of soil material influence the static cone resistance. In order to evaluate the effect of these variables on the free fall penetration test, tests were conducted with (i) cone angles of 30^0, 60^0 and 180^0; (ii) cone materials of stainless steel, polished aluminium and sanded aluminium; (iii) penetrometers of diameter 3.56 cms and 7.62 cms; and (iv) dense (S1 type), medium dense (S2 type) and loose (S3 type) targets. The influence of these variables are discussed below.

4.4.2. Effect of Penetrometer Diameter and Mass

The effect of penetrometer size and its weight were grouped as a variable W/A and to study the effect of this variable, tests were conducted with penetrometers of diameters 3.56 cms and 7.62 cms, weighing 10 Kg and 14 Kg, respectively.

It was observed that the 3.56 cms diameter penetrometer ($W/A = 1.0\ Kg/cm^2$) yielded more penetration than the 7.62 cms diameter penetrometer ($W/A = 0.30\ Kg/cm^2$). The results also indicate that an

increase in the penetrometer diameter produces a decrease in the total time of penetration and an increase in maximum deceleration. Cone thrust per unit area is much less for the larger diameter penetrometer than the smaller one. The results are shown in Figs. 16, 17 and 18. From Fig. 18 it is interesting to note that a 230% increase in W/A produces only about a 25% increase in total penetration at relative densities of 0.71 and 0.45, and about 10% at a relative density 0.26.

A relationship similar to Fig. 18 was reported by Murff and Coyle (1972). Young (1972) and Murff and Coyle (1972) also reported that the penetration depth is a function of W/A and impact velocity.

4.4.3. Effects of the Nose Shape

Cones with apex angles of 30^0, 60^0 and 180^0 were used in this investigation and the results are plotted in Figs. 19a, 19b, 20a, 20b and 20c. These results are similar to the findings of other investigators (Young, 1969; Murff and Coyle, 1972; Dayal, 1974). An increase in nose sharpness yields an increase in total depth of penetration.

From equation (34) it could be observed that maximum depth of penetration is proportional to the value of nose length/diameter (NL/D) of the penetrometer. As NL/D value for a 30^0 cone is higher than 60^0 and 180^0 cones, the penetration depth is maximum for a 30^0 cone. It is seen that the effect of the cone angle is similar in both the penetrometers. Meyerhof (1961) reported that for steel (semi-rough) penetrometers point resistance decreases as the cone angle of the tip decreases (sharper points).

(Text continued page 84)

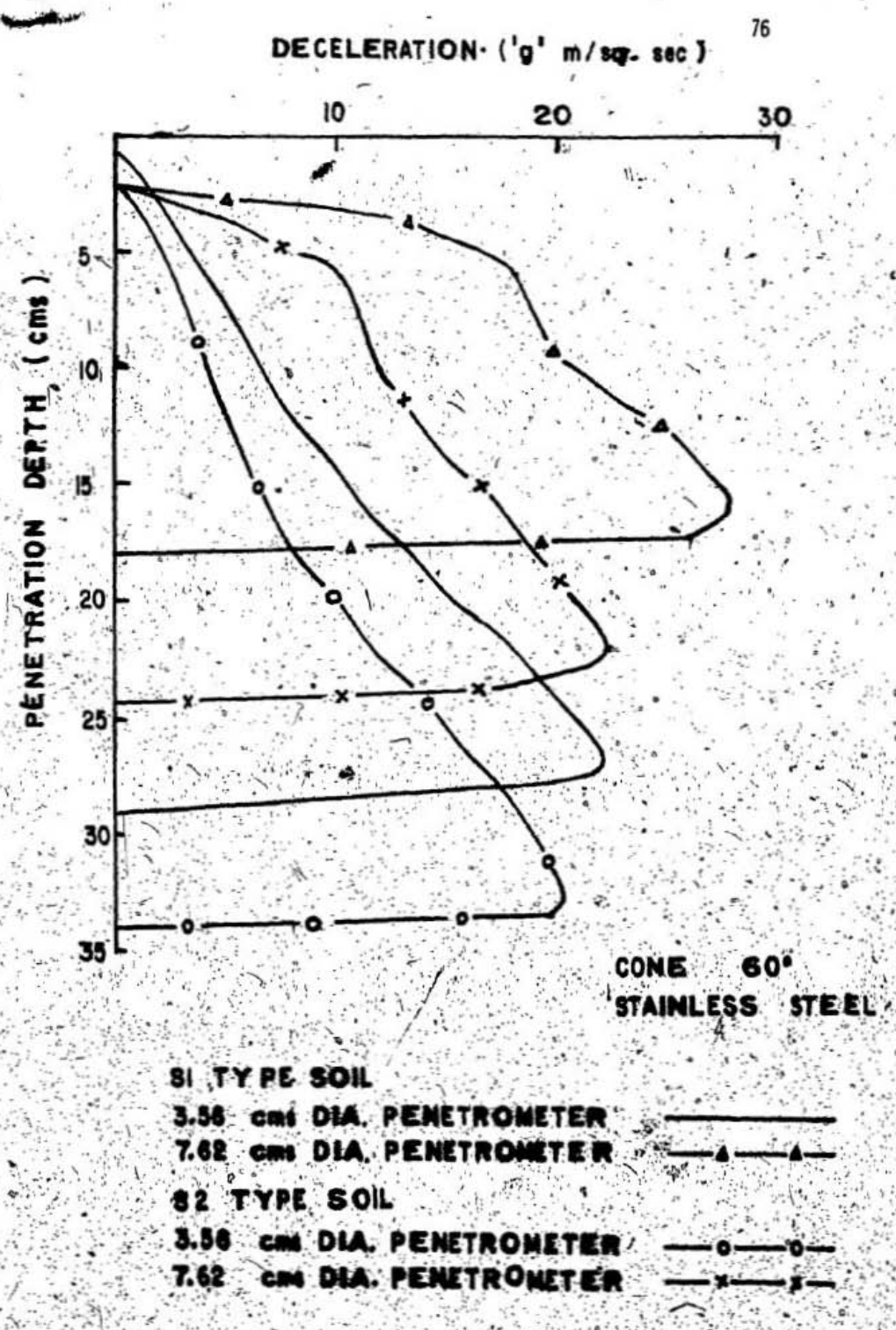


FIG 16. PLOT OF DECELERATION vs. PENETRATION DEPTH

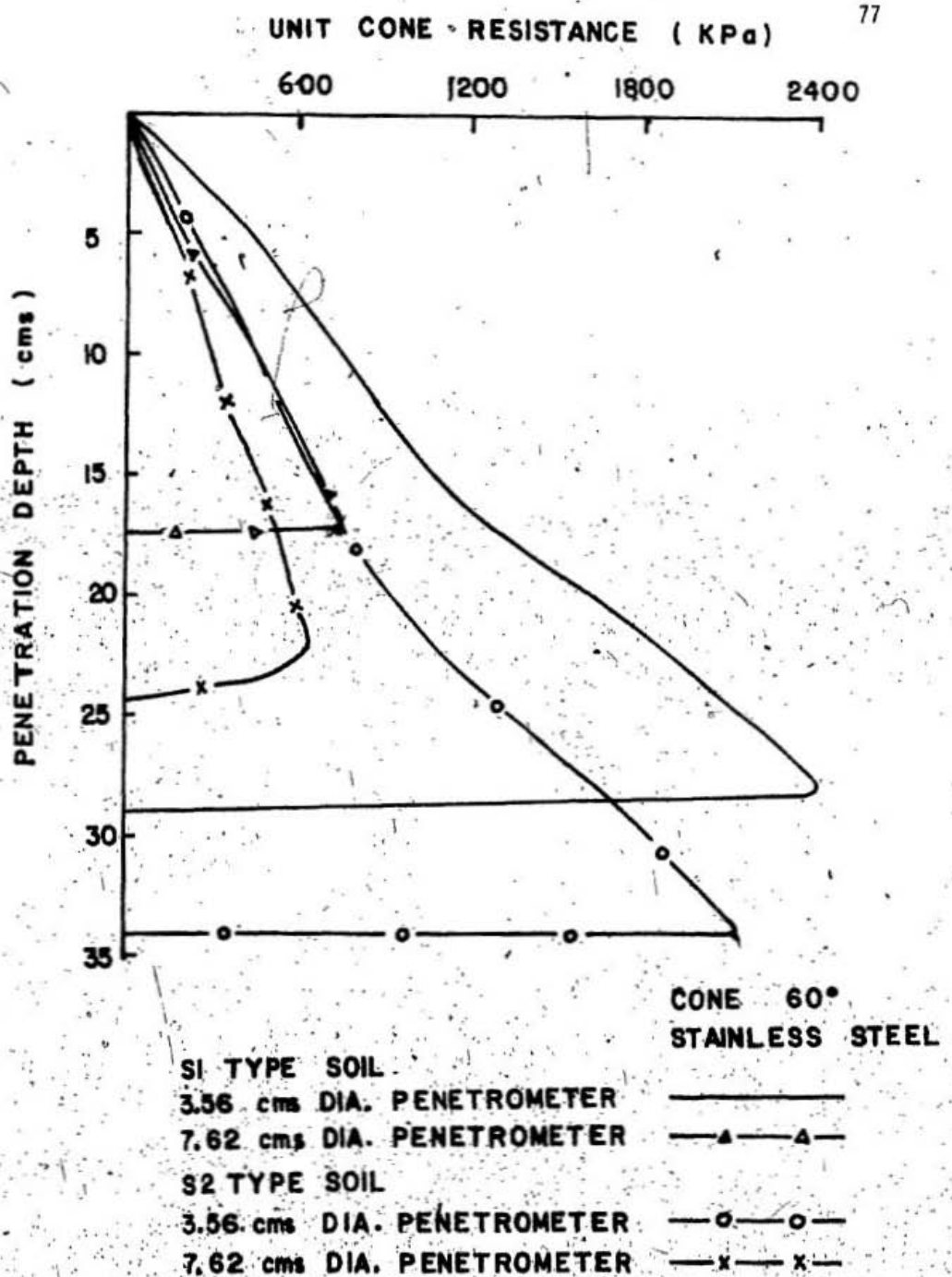


FIG 17. PLOT OF UNIT CONE RESISTANCE vs. PENETRATION DEPTH

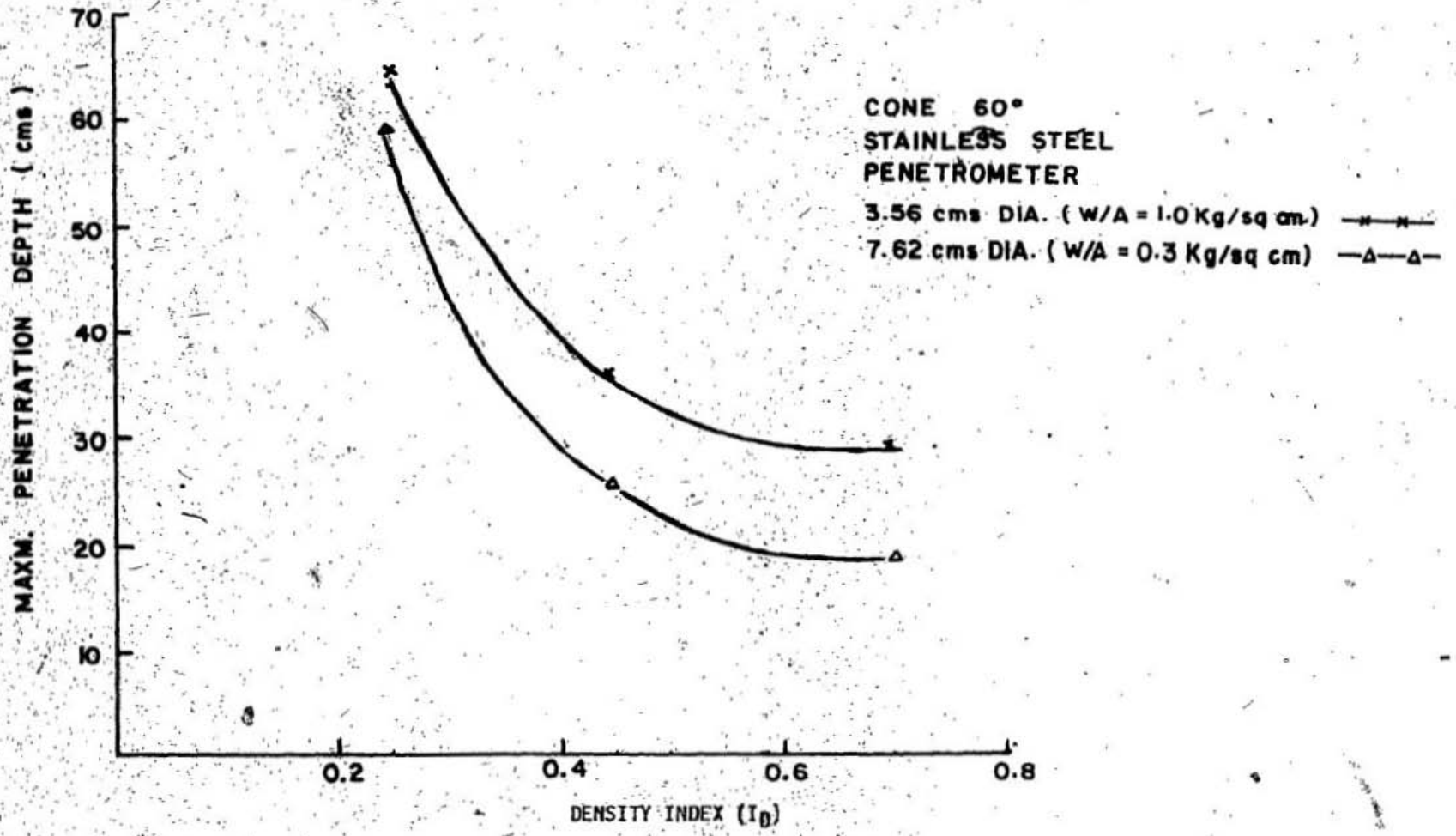


FIG 18. PLOT OF DENSITY INDEX vs. MAXIMUM PENETRATION DEPTH

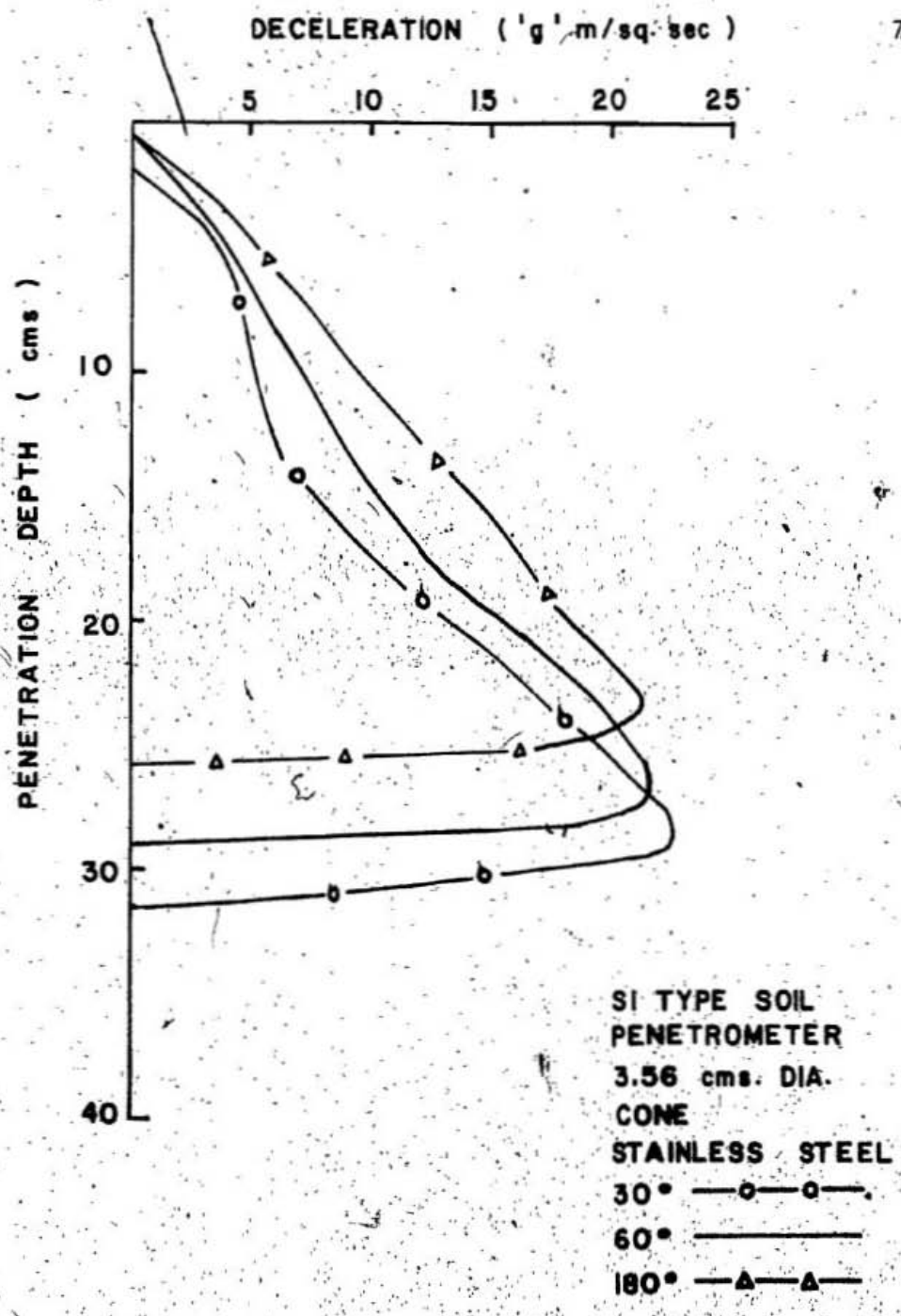


FIG 19a. PLOT OF DECELERATION vs. PENETRATION DEPTH

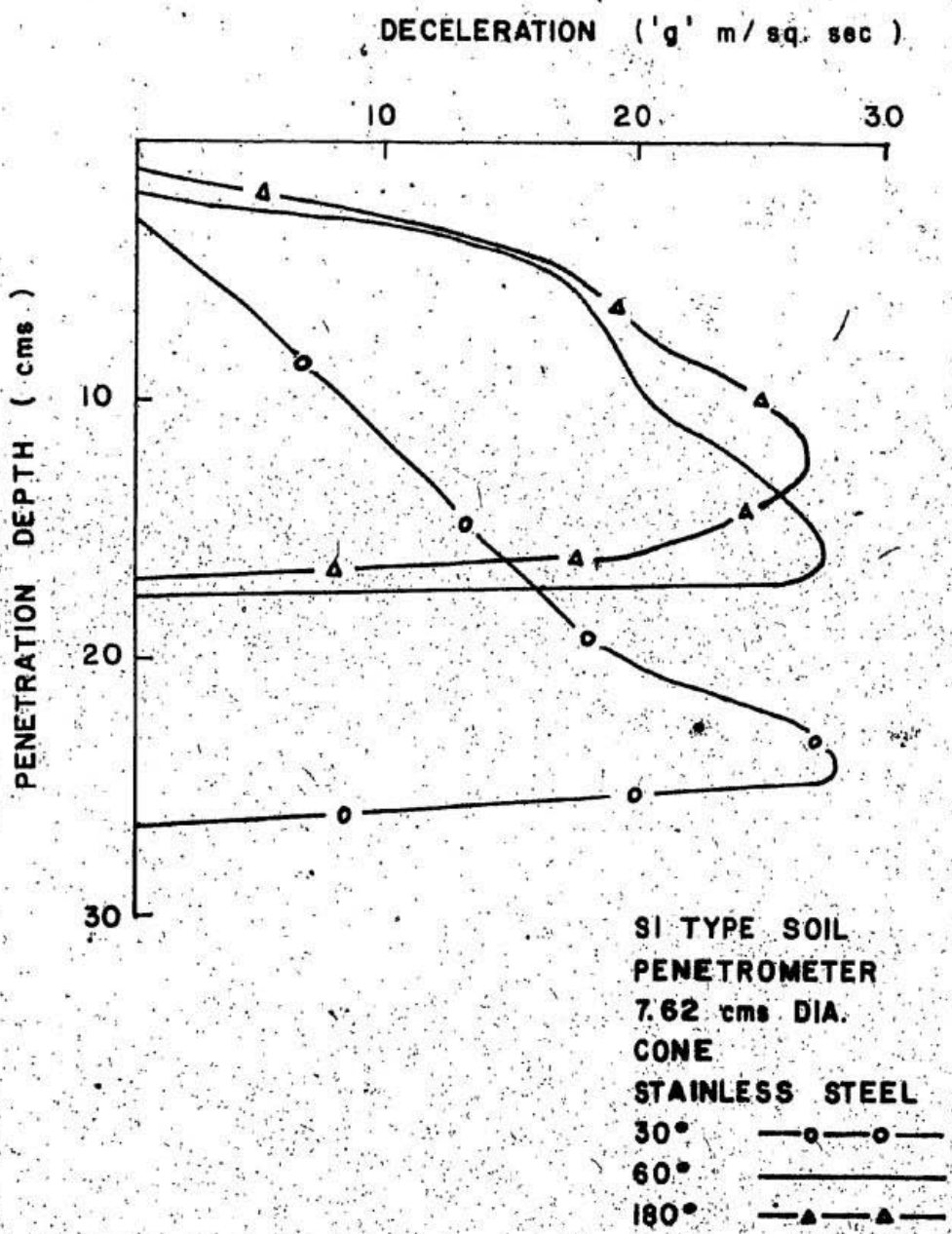


FIG 19b. PLOT OF DECELERATION vs. PENETRATION DEPTH

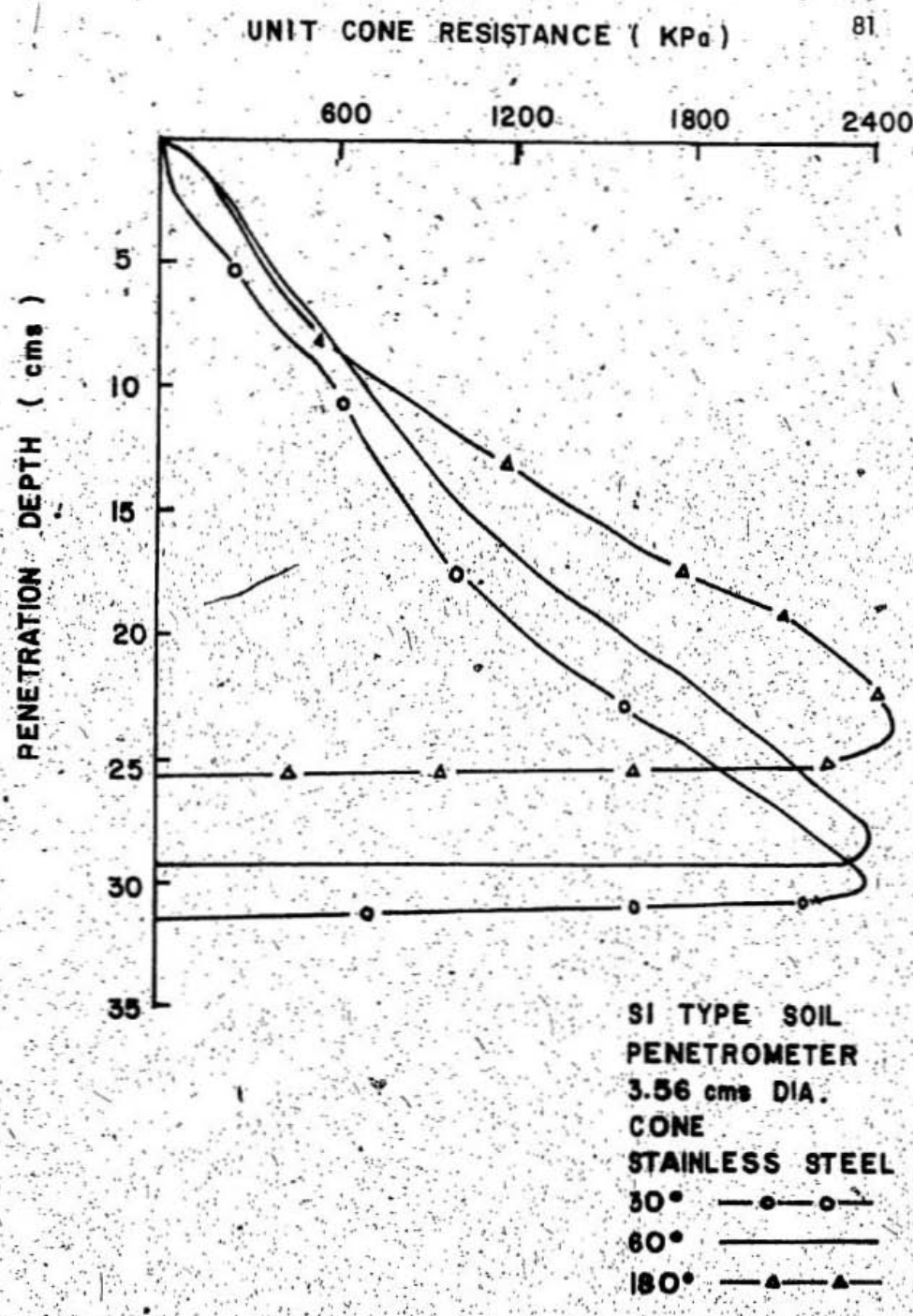


FIG 20a. PLOT OF UNIT CONE RESISTANCE vs. PENETRATION DEPTH FOR 3.56 cms DIA PENETROMETER (α = 15°, 30° & 90°)

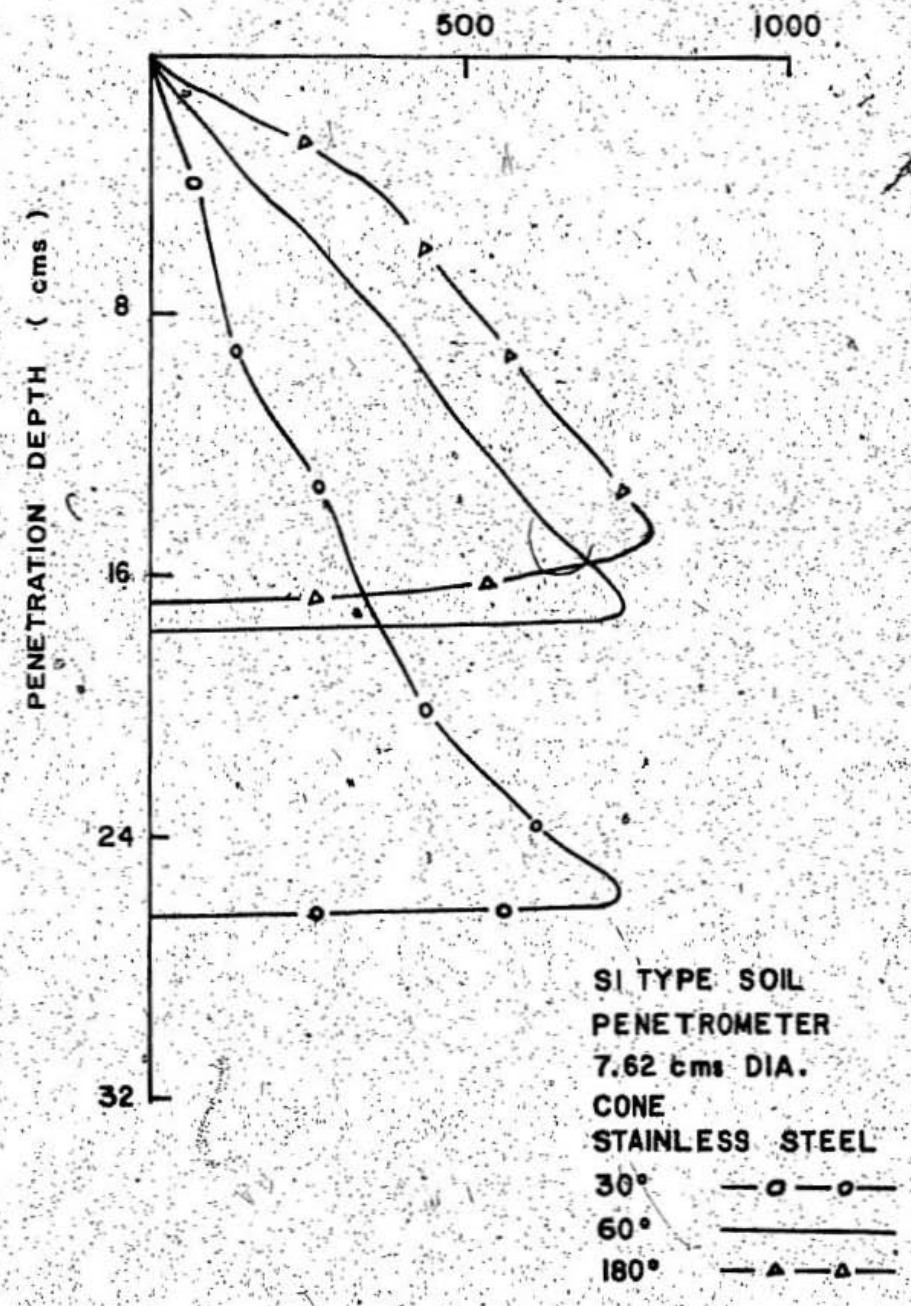
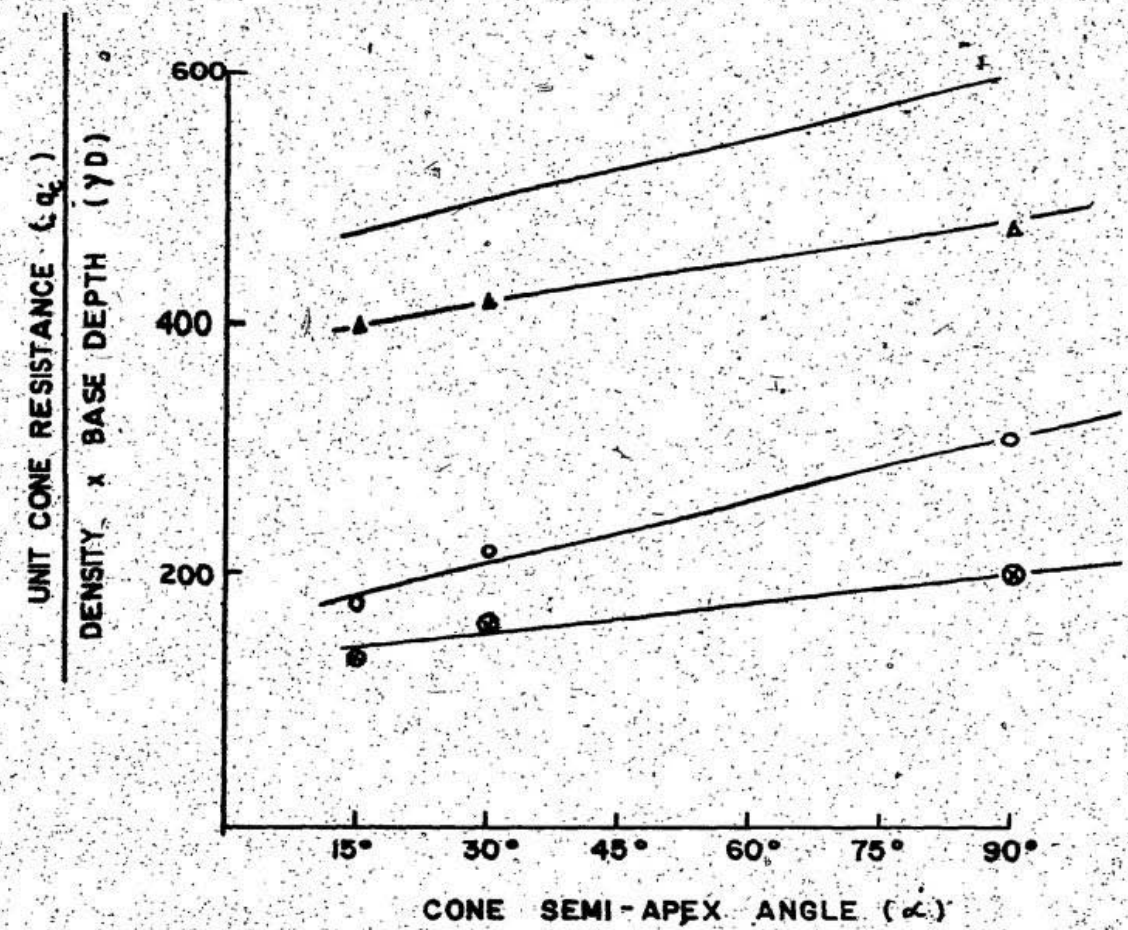


FIG 20b. PLOT OF UNIT CONE RESISTANCE vs. PENETRATION DEPTH FOR 7.62 cms DIA PENETROMETER (α = 15°, 30° & 90°)



CONE
STAINLESS STEEL

S1 TYPE SOIL

3.56 cms ϕ PENETROMETER ——

7.62 cms ϕ PENETROMETER —o—o—

S2 TYPE SOIL

3.56 cms ϕ PENETROMETER —△—△—

7.62 cms ϕ PENETROMETER —⊗—⊗—

FIG 20c. PLOT OF $q_c/\gamma D$ vs. CONE SEMI-APEX ANGLE

4.4.4. Effects of the Surface Roughness

Cone tips with stainless steel (δ/ϕ = 0.5), polished aluminium (δ/ϕ = 0.6) and sanded aluminium (δ/ϕ = 0.75) were used to observe the effect of roughness on penetration resistance. The angle of friction (δ) was determined from direct shear tests as described in Chapter III. Roughness was also quantitatively measured using Taylor-Hobson No. 4 Talysurf and corrections were made to the value of δ. It was observed that roughness of cone material has a significant influence on the penetration resistance and maximum depth of penetration. Increase in roughness produced an increase in peak deceleration and cone resistance and a decrease in penetration depth. The results are plotted in Figs. 21a and 21b.

Based on experimental test results, Karafiath (1973) reported that an increase in base friction increases the penetration resistance. From Figs. 21a and 21b, it is seen that the penetration resistance increases with increasing roughness as seen from the results for steel cone and aluminium cones. However, in the tests with the 7.62 gms penetrometer, although the sanded aluminium cone shows a greater maximum penetration resistance, the difference between sanded aluminium and polished aluminium cones is not so well defined.

It is also observed from Figs. 21c and 21d that $q_c/\gamma D$ increases linearly with roughness of cone material. A similar result was reported by Abdel-Gawad (1979) for quasi-static penetration tests.

4.4.5. Target Strength

Relative density of sand is the most important factor governing the penetration phenomenon. It is evident from Fig. 18 that the

maximum depth of penetration is effected significantly by changes in soil strength. Effect of the target strength on penetration event could be seen from Tables 7a, 7b and 7c. These results indicate that an increase in target strength yields an increase in peak deceleration, a decrease in total depth of penetration and an increase in cone resistance. Figs. 22a and 22b show a comparison of deceleration record for identical tests on dense, medium dense and loose sand. Cone resistance vs. penetration depth curves are shown in 23a and 23b. Fig. 24 shows the relationship between the angle of shear resistance (ϕ) and $q_c/\gamma D$. It is seen that the relationship is linear and the value of $q_c/\gamma D$ increases with increasing value of ϕ. It is also seen that the larger diameter penetrometer gives lower values than the standard size penetrometer. A similar result has been reported for quasi-static tests by Abdel-Gawad (1979).

4.4.6. Free Fall Tests on Wet Sand

In addition to test series S1, S2 and S3, an attempt was made to saturate the sand and conduct free fall tests on these targets. There were a number of experimental problems in obtaining completely saturated specimens. The sand itself was highly permeable and the container could not be made completely water tight at the joints. Although the results obtained in this series of tests are distinct, the test itself is to be considered deficient because of the above limitation. Results obtained for this test series are shown in Figs. 25a and 25b.

The peak deceleration is much higher in wet sand than the corresponding dry targets. Consequently, maximum penetration depth

(Text continued page 100)

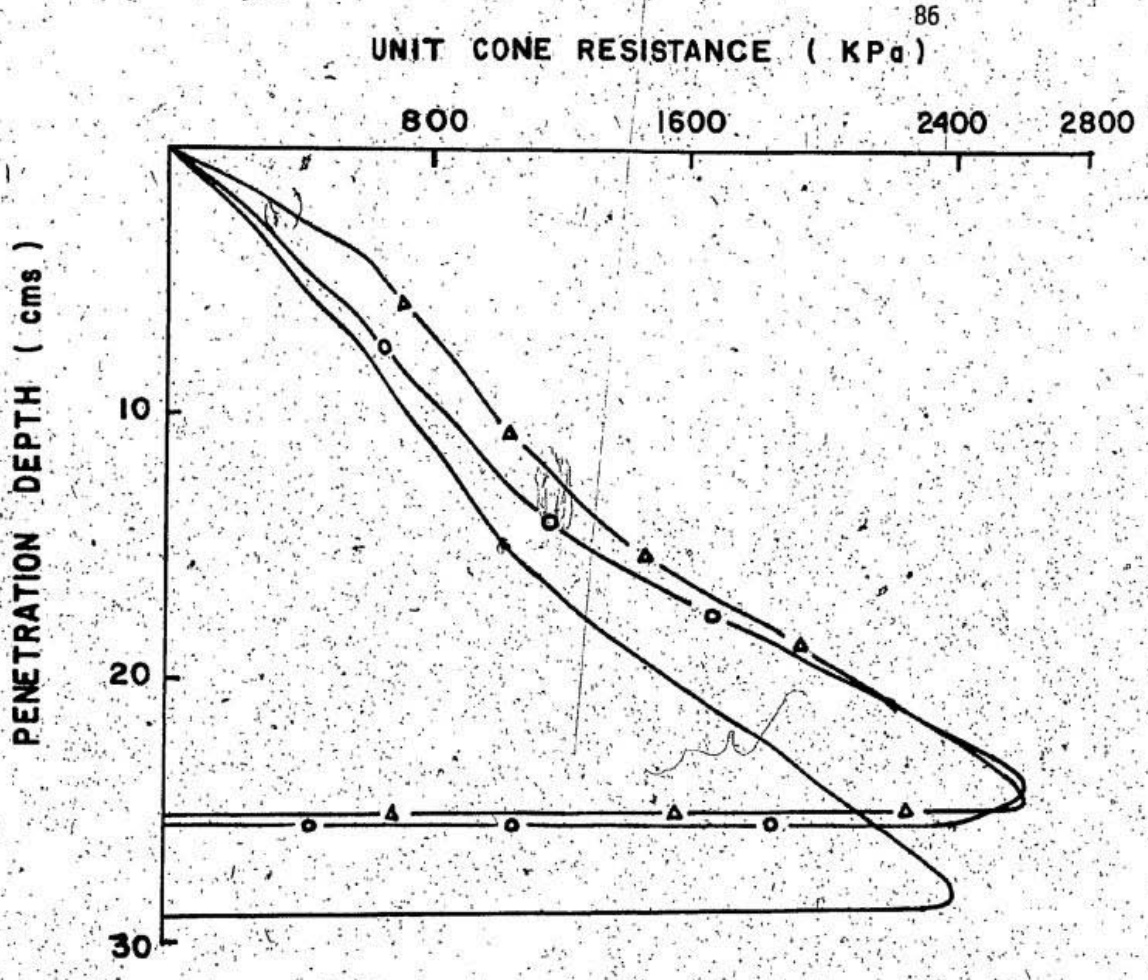


FIG 21a. PLOT OF UNIT CONE RESISTANCE vs. PENETRATION DEPTH FOR 3.56 cms DIA PENETROMETER (δ/ϕ = 0.5, 0.6 & 0.75)

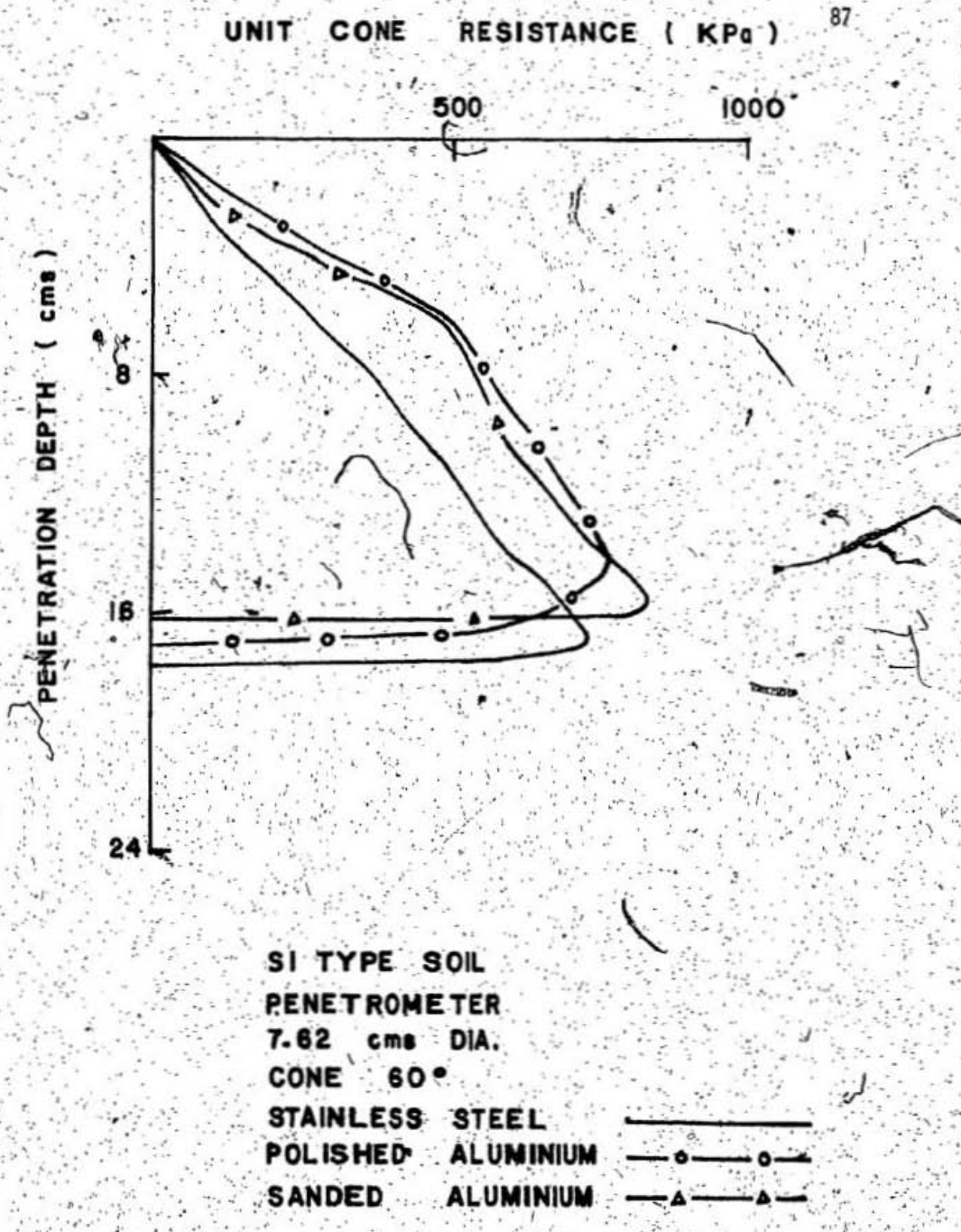


FIG 21b. PLOT OF UNIT CONE RESISTANCE vs. PENETRATION DEPTH FOR 7.62 cms DIA PENETROMETER (δ/ϕ = 0.5, 0.6 & 0.75)

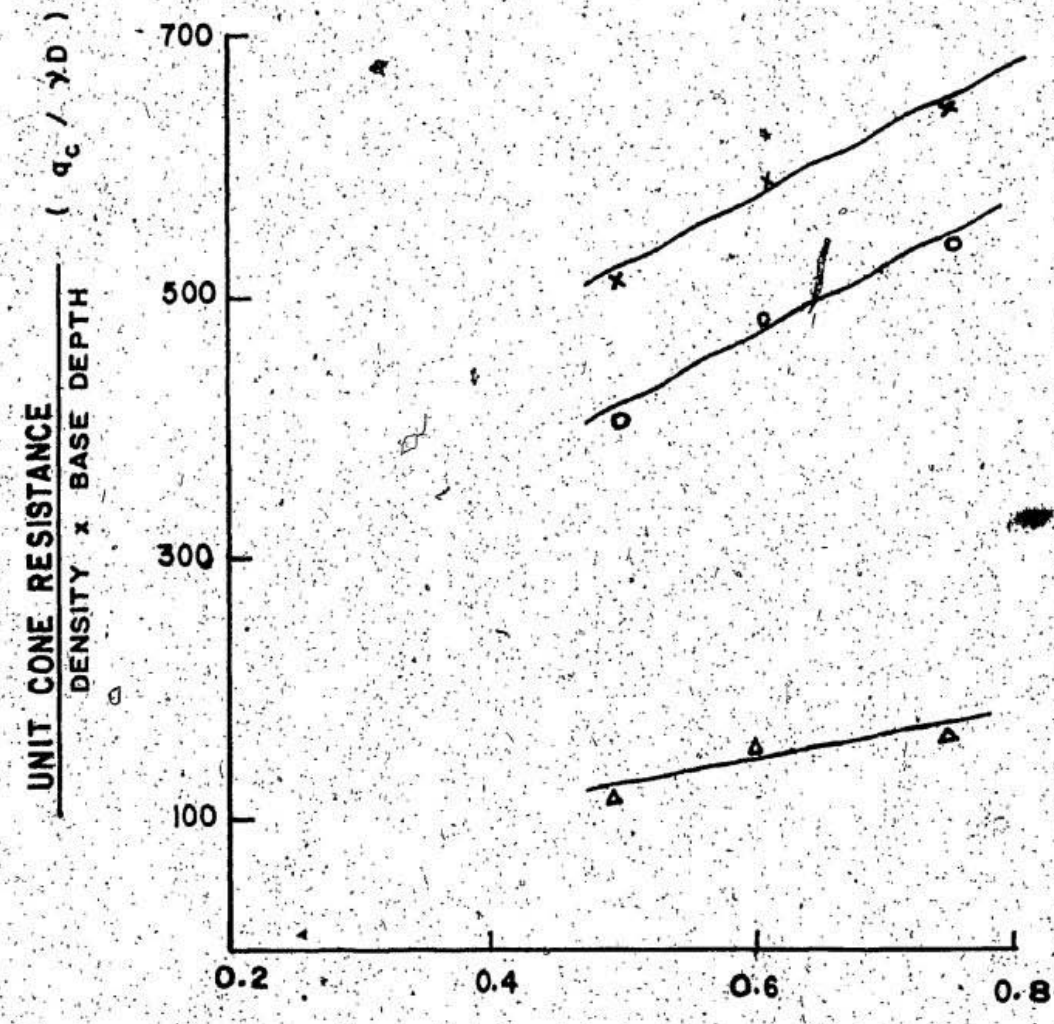


FIG 21c. PLOT OF $q_c/\gamma D$ vs. ROUGHNESS OF CONE MATERIAL FOR 3.56 cms DIA PENETROMETER (S1, S2 & S3 TYPES OF SOIL)

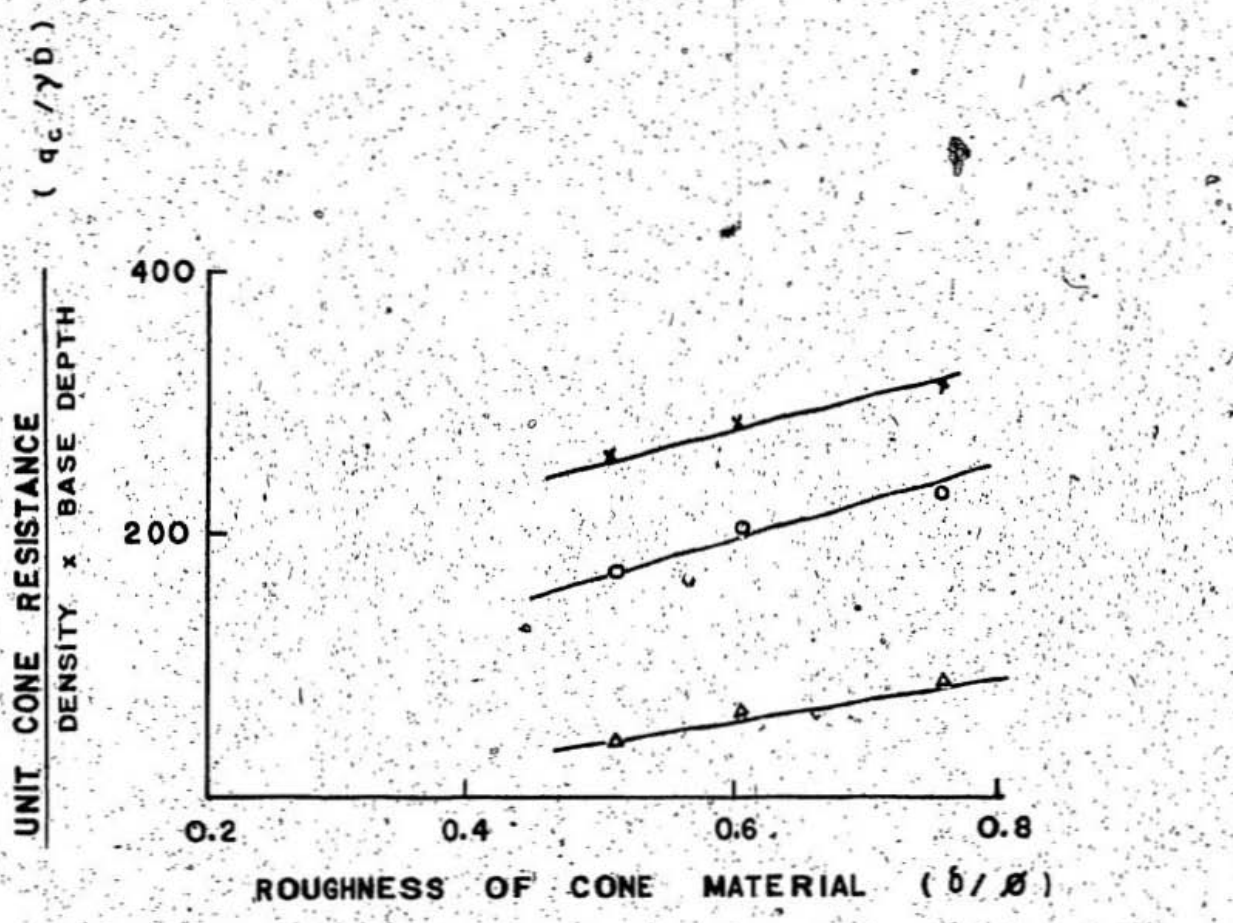


FIG 21d. PLOT OF $q_c/\gamma D$ vs. ROUGHNESS OF CONE MATERIAL FOR 7.62 cms DIA PENETROMETER (S1, S2 & S3 TYPES OF SOIL)

TABLE 7a. TEST RESULTS FOR DENSE SAND TARGETS

Soil Type	Diameter of the Penetrometer cms	Material of the Cone	Cone Angle	Maximum Cone Thrust KPa	Maximum Depth of Penetration (Computed) cms
S1	3.56 cms	Steel	30°	2391.4	31.56
S1	"	"	60°	2391.4	28.89
S1	"	"	180°	2469.6	25.63
S1	"	Aluminium	30°	2548.0	28.91
S1	"	"	60°	2626.4	25.62
S1	"	"	180°	2626.4	24.25
S1	"	Sanded Aluminium	30°	2626.4	27.40
S1	"	"	60°	2626.4	25.20
S1	"	"	180°	2704.8	23.52
S1	7.62 cms	Steel	30°	735.17	26.49
S1	"	"	60°	735.17	17.71
S1	"	"	180°	777.59	16.99
S1	"	Aluminium	30°	791.72	25.66
S1	"	"	60°	777.59	16.94
S1	"	"	180°	848.14	15.88
S1	"	Sanded Aluminium	30°	820.00	23.74
S1	"	"	60°	834.14	16.34
S1	"	"	180°	890.69	15.50

TABLE 7b. TEST RESULTS FOR MEDIUM DENSE SAND TARGET

Soil Type	Diameter of the Penetrometer cms	Material of the cone	Cone Angle	Maximum Cone Thrust KPa	Maximum Depth of Penetration (Computed) cms
S2	3.56	Steel	30^0	2195.2	37.27
S2	"	"	60^0	2116.8	34.08
S2	"	"	180^0	2273.6	30.50
S2	"	Aluminium	30^0	2352.0	35.12
S2	"	"	60^0	2273.6	31.49
S2	"	"	180^0	2469.6	28.03
S2	"	Sanded Aluminium	30^0	2548.0	33.26
S2	"	"	60^0	2391.0	31.23
S2	"	"	180^0	2665.6	27.67
S2	7.62 cms	Steel	30^0	622.07	30.51
S2	"	"	60^0	622.07	24.20
S2	"	"	180^0	650.34	22.63
S2	"	Aluminium	30^0	636.21	28.84
S2	"	"	60^0	678.62	21.71
S2	"	"	180^0	706.90	19.66
S2	"	Sanded Aluminium	30^0	678.62	27.91
S2	"	"	60^0	721.04	21.04
S2	"	"	180^0	763.44	19.21

TABLE 7c. TEST RESULTS FOR LOOSE SAND TARGET

Soil Type	Diameter of the Penetrometer cms	Material of the Cone	Cone Angle	Maximum Cone Thrust KPa	Maximum Depth of Penetration (Computed) cms
S3	3.56 cms	Steel	30^{o}	1078.0	62.61
S3	"	"	60^{o}	1058.4	62.47
S3	"	"	180^{o}	1274.0	53.88
S3	"	Aluminium	30^{o}	1215.2	60.90
S3	"	"	60^{o}	1332.8	60.80
S3	"	"	180^{o}	1372.0	51.70
S3	"	Sanded Aluminium	30^{o}	1372.0	61.50
S3	"	"	60^{o}	1372.0	56.84
S3	"	"	180^{o}	1391.6	49.41
S3	7.62 cms	Steel	30^{o}	303.96	59.92
S3	"	"	60^{o}	339.32	57.87
S3	"	"	180^{o}	353.45	51.14
S3	"	Aluminium	30^{o}	452.40	54.94
S3	"	"	60^{o}	452.40	52.06
S3	"	"	180^{o}	480.60	44.36
S3	"	Sanded Aluminium	30^{o}	480.69	44.90
S3	"	"	60^{o}	508.96	43.36
S3	"	"	180^{o}	508.96	42.70

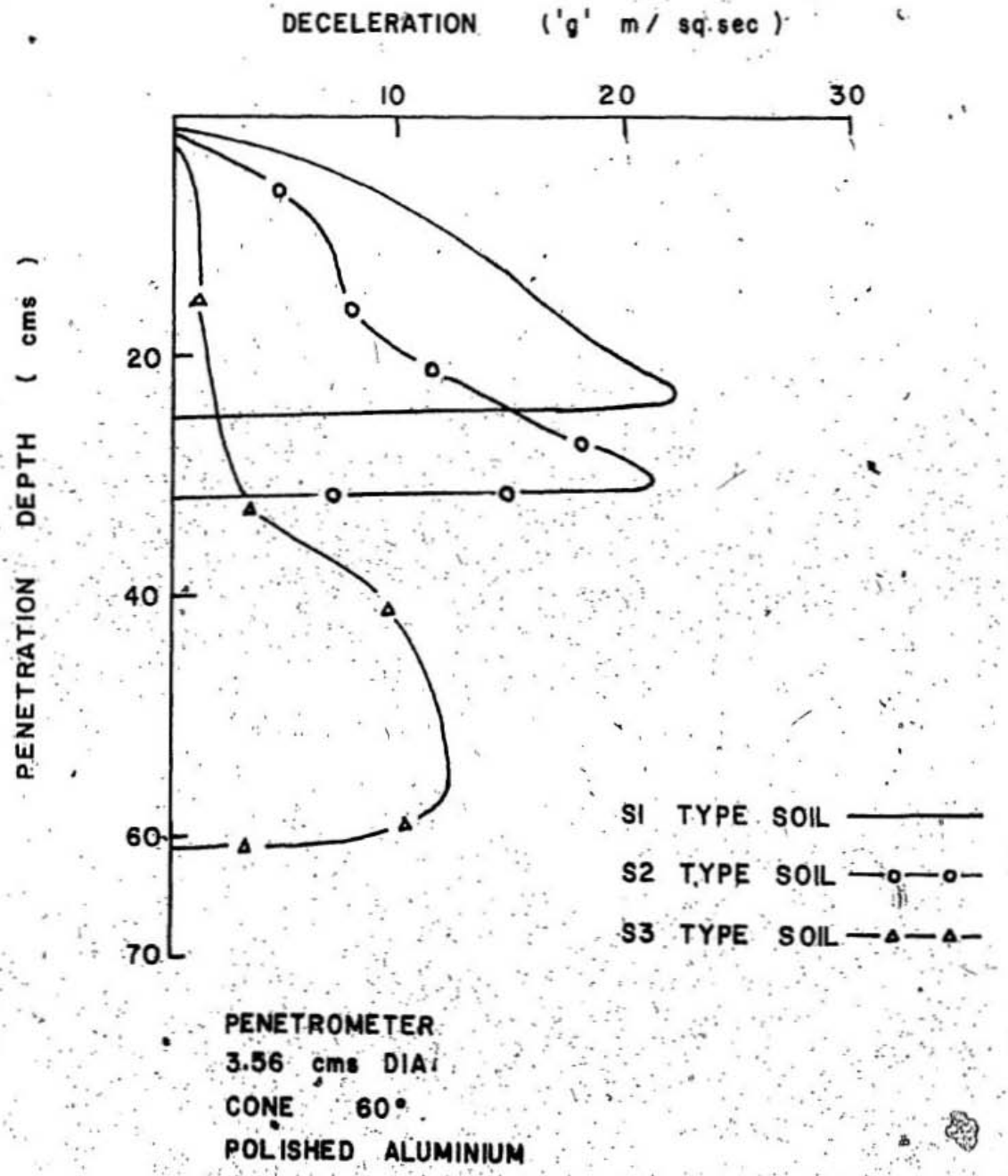


FIG 22a. PLOT OF DECELERATION vs. PENETRATION DEPTH FOR 3.56 cms DIA PENETROMETER

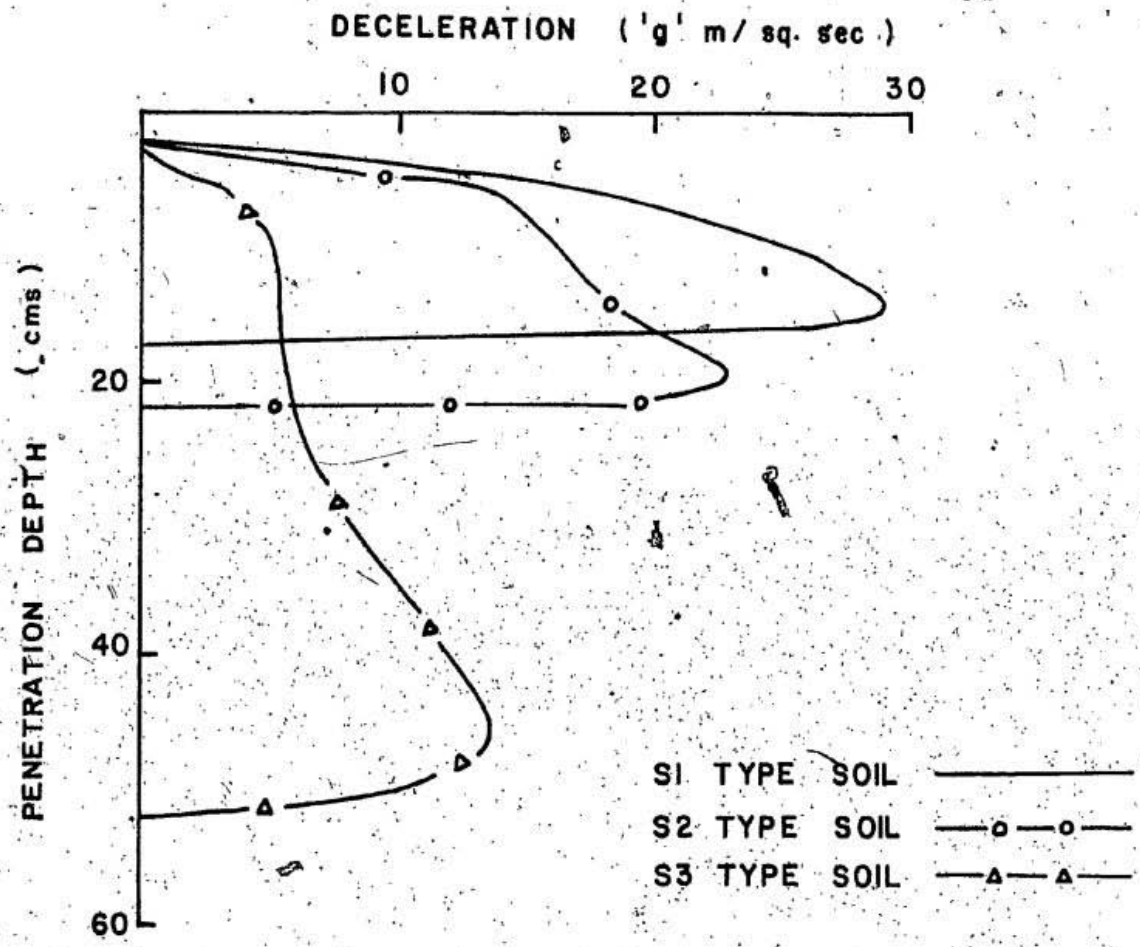


FIG 22b. PLOT OF DECELERATION vs. PENETRATION DEPTH FOR 7.62 cms DIA PENETROMETER

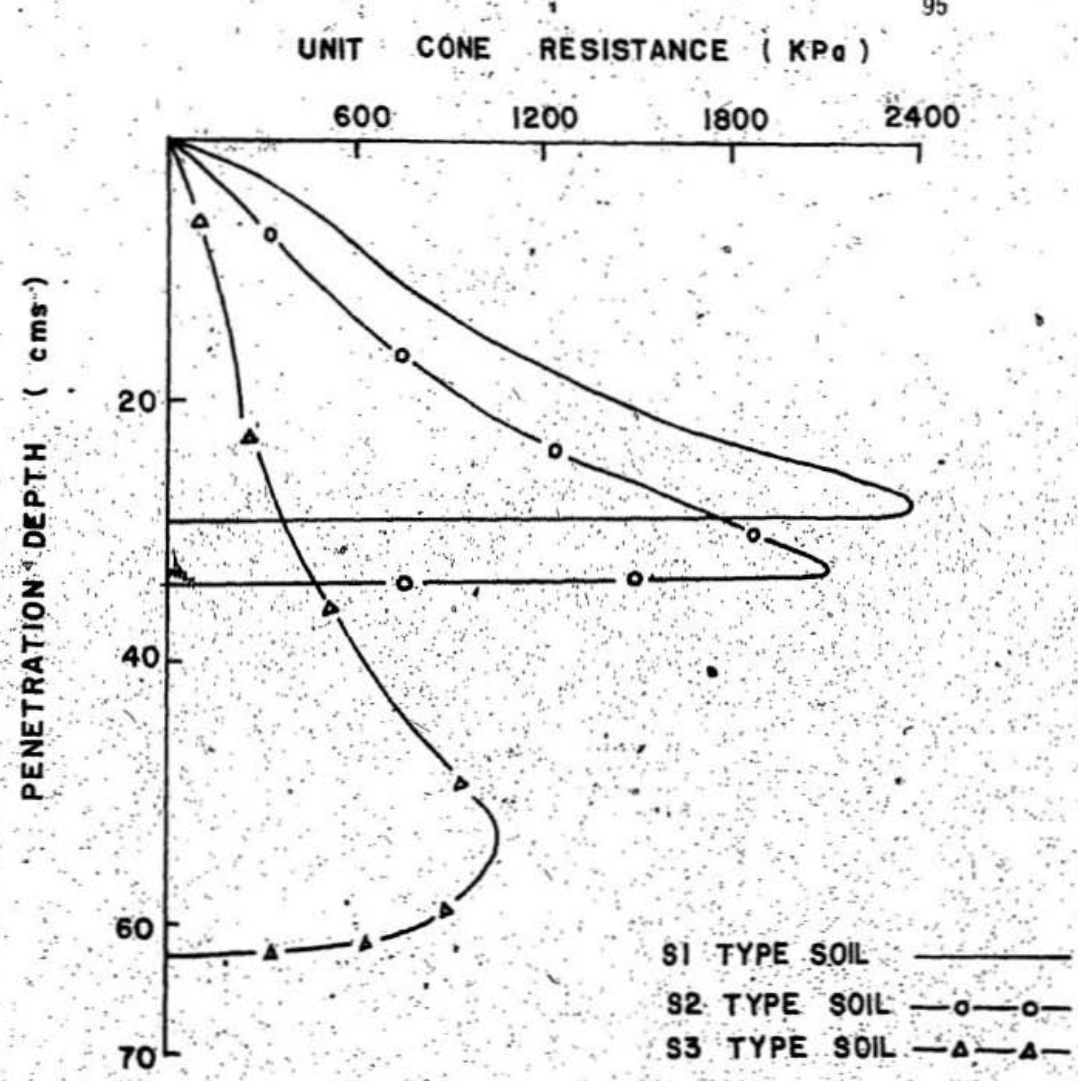


FIG 23a. PLOT OF UNIT CONE RESISTANCE vs. PENETRATION DEPTH FOR 3.56 cms DIA PENETROMETER

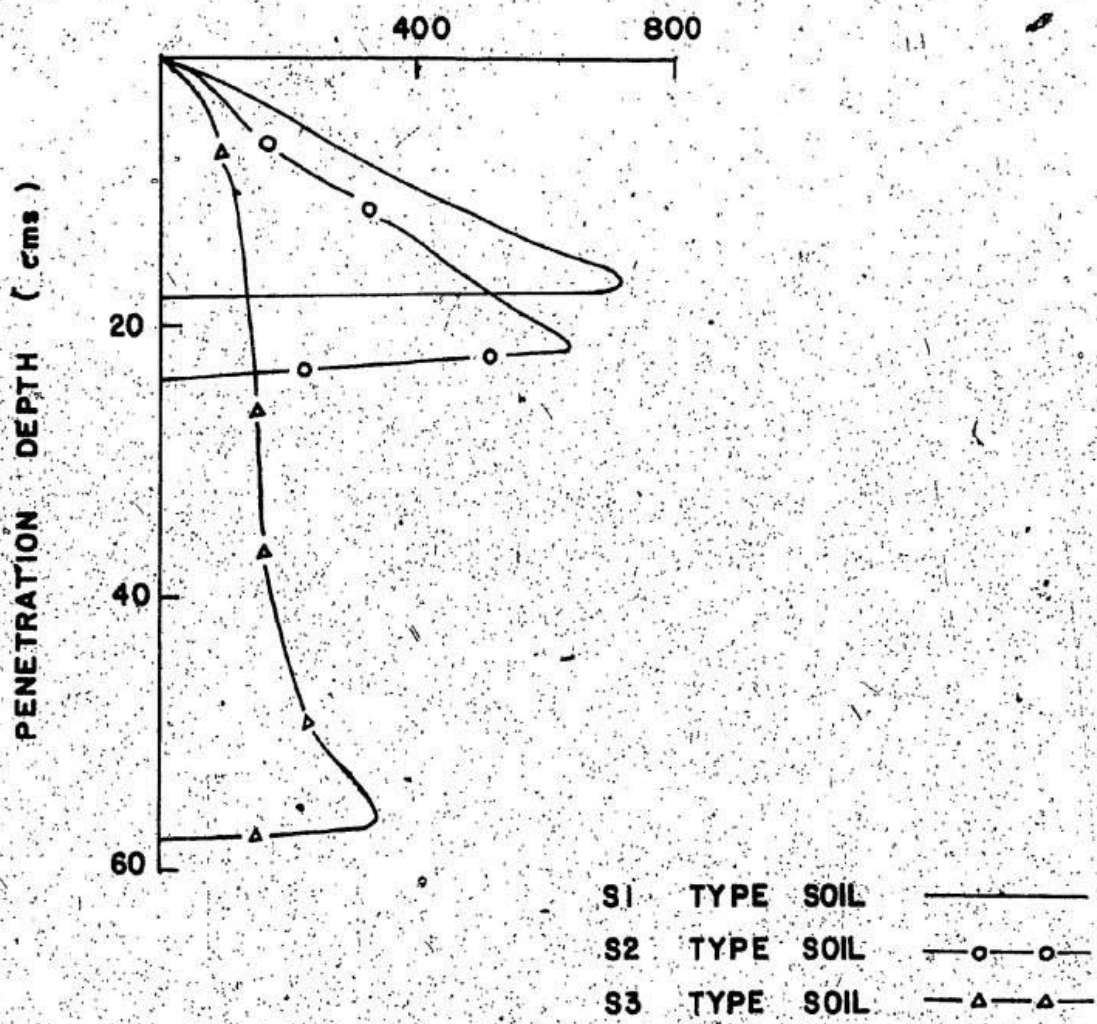


FIG 23b. PLOT OF UNIT CONE RESISTANCE vs. PENETRATION DEPTH FOR 7.62 cms DIA PENETROMETER

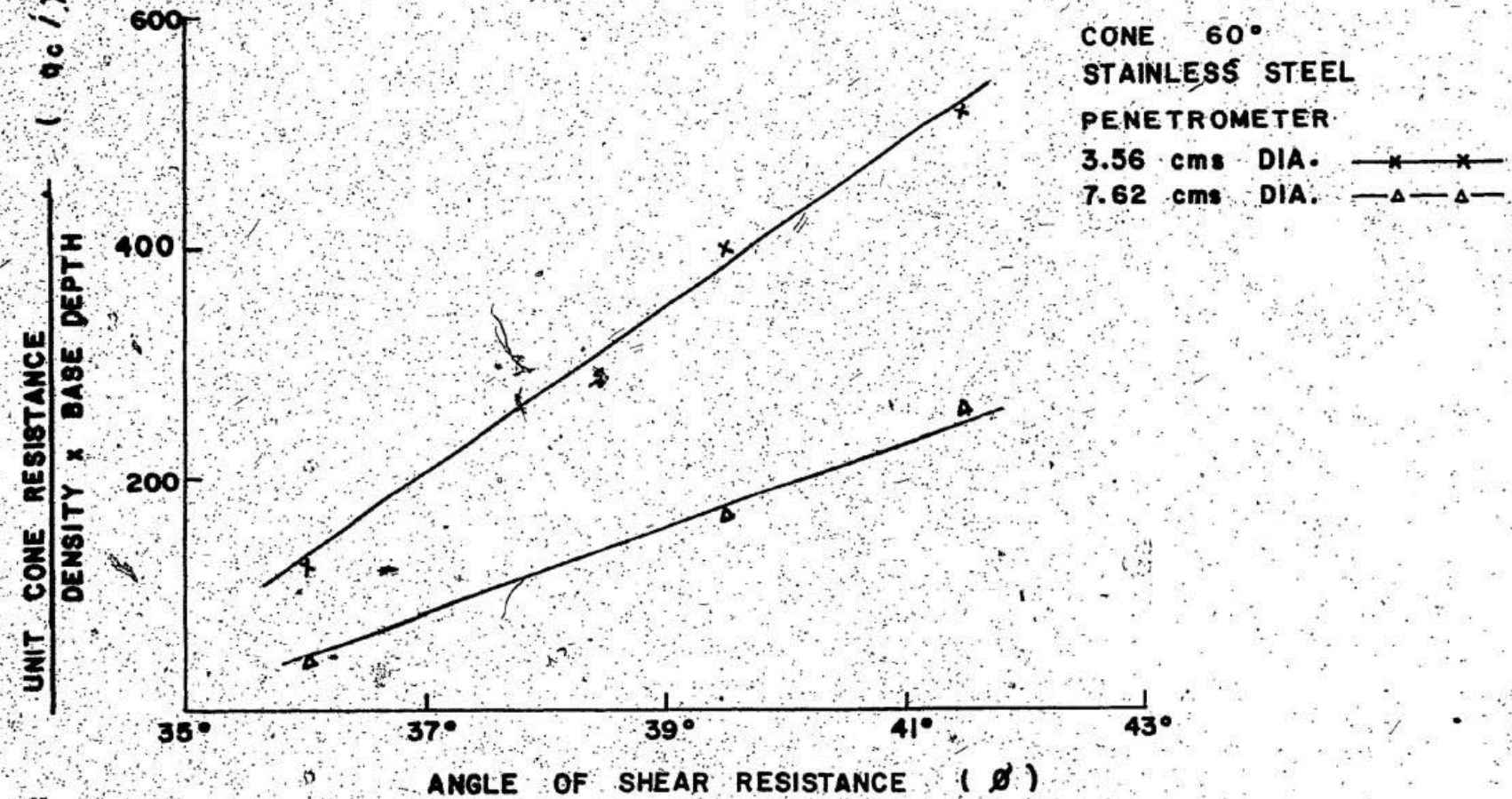


FIG 24. PLOT OF $q_c / \gamma D$ vs. ANGLE OF SHEAR RESISTANCE

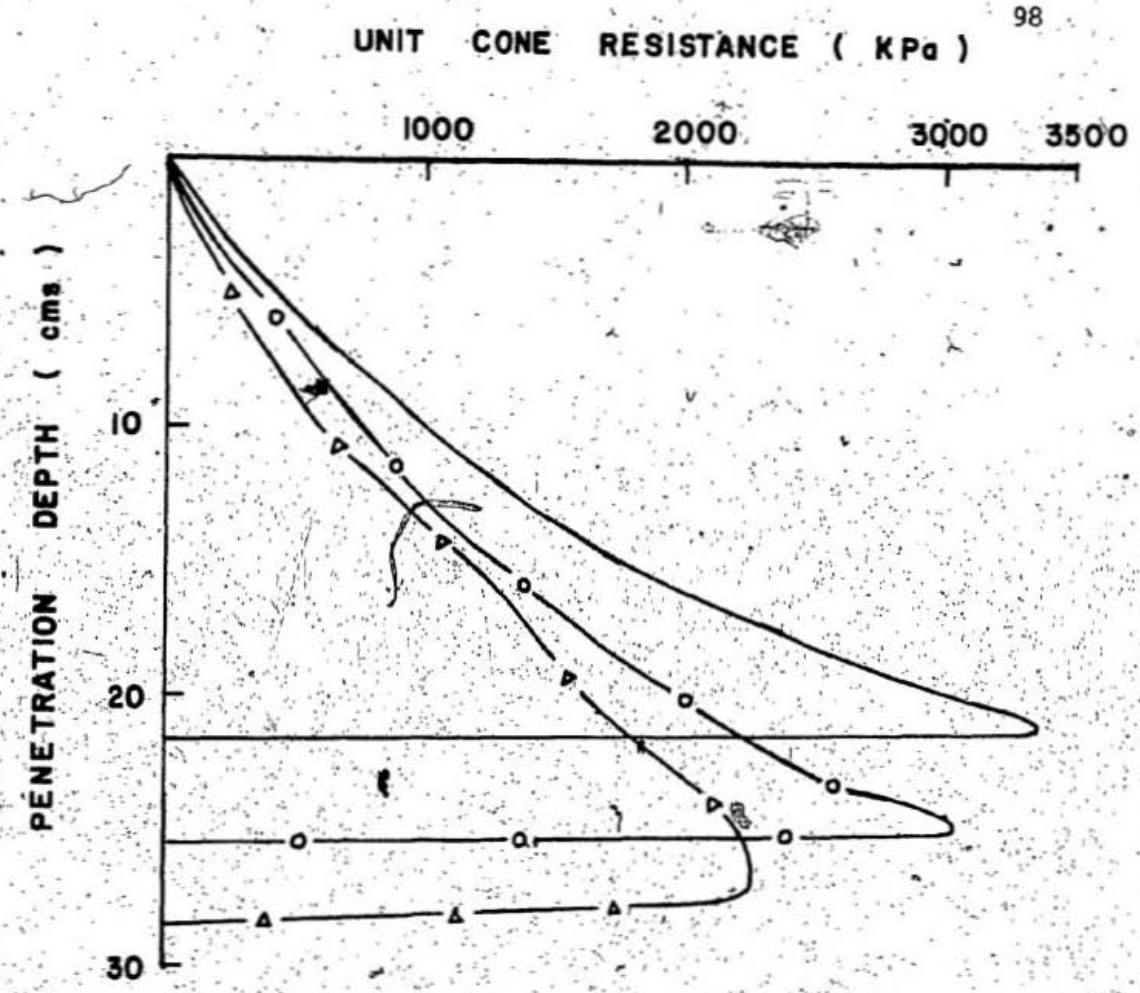


FIG 25a. PLOT OF UNIT CONE RESISTANCE vs. PENETRATION DEPTH FOR 3.56 cms DIA PENETROMETER (WET SAND TARGET)

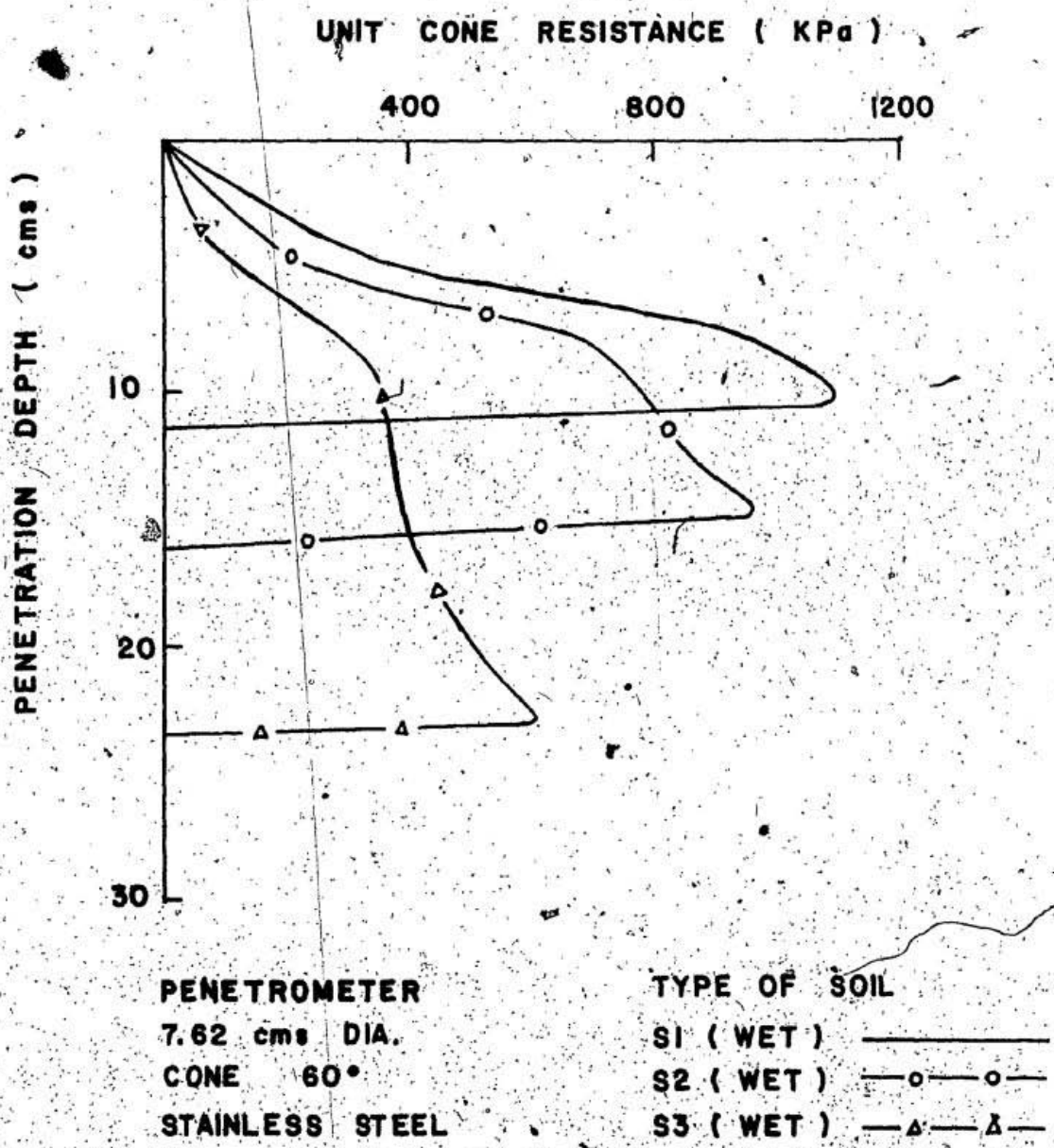


FIG 25b. PLOT OF UNIT CONE RESISTANCE vs. PENETRATION DEPTH FOR 7.62 cms DIA PENETROMETER (WET SAND TARGET)

is less. From Figs. 23a and 25a, a comparison of the cone resistance for dry sand and wet sand shows that the resistance in wet dense sand is higher by at least 40% and 90-100% for loose sand.

A similar phenomenon has been reported by Schmertmann (1974) in static penetration tests. It has been suggested that the permeability of the soil results in an acclerated flow of the pore water ahead of the penetrometer and induces a negative poor pressure in the soil. This causes an apparent increase in the soil resistance. Drozd (1965) has made similar observations in dynamic penetration tests in which a dynamic penetrometer was used. The increased resistance was labelled by Drozd (1965) as an untrue cohesion.

In those tests (Drozd, 1965) piezometric observations were made and it was found that the effect was most pronounced in saturated loose sand. A similar phenomenon can be noticed comparing Fig. 23a with Fig. 25a and Fig. 23b with Fig. 25b, where the change in penetration resistance is more pronounced in loose sand.

4.5. Summary of Test Results--Silica-70 Sand

Test results on cohesionless soil (sand) could be summarized as below:

1. Penetration depth and maximum cone resistance are dependent on the mass per unit area (W/A) of the penetrometer. Penetration depth can be increased by increasing the value of W/A. The other factors which also affects the depth of penetration are nose shape, roughness of the cone, relative density of sand and diameter of the penetrometer.

2. Deceleration profile obtained from free fall penetration could be directly used to obtain soil resistance at different depths of penetration. Soil resistance calculated by this method showed a good agreement with the measured values of cone resistance by load cells.

3. Free fall penetration test results can be used to estimate the angle of shear resistance (ϕ) with good accuracy.

4. Among the three different cone shapes used in this investigation, soil resistance was maximum for 180^{o} cone and penetration depth was maximum for 30^{o} cone. An increase in cone sharpness yielded an increase in maximum penetration and decrease in cone resistance.

5. Soil density (i.e., Density Index) has significant influence on the penetration mechanism. It is evident from Figs. 18 and 23a that a change in Density Index from loose to medium dense state would produce an abrupt increase in cone resistance and also decrease in penetration depth.

6. Due to the effect of negative pore water pressure, cone resistance and peak deceleration is much higher for wet sand than the corresponding dry targets. This is an important consideration and should be accounted for in the interpretation of results from field tests.

4.6. Free Fall Penetration Tests on Modelling Clay

Test results for the two types of cohesive soil targets are discussed below. The properties of this clay has been discussed in Chapter III. As the angle of shear resistance is very small (3.5^{o}-4^{o}),

the soil is considered as purely cohesive for the purpose of analysis.

Tests were performed with penetrometers of the two sizes and cones with semi-apex angles of 15^{o}, 30^{o} and 90^{o} were used. Cone roughness is not an influencing factor in cohesive soils (Durgunoglu and Mitchell, 1973) and hence only the stainless steel cones were used in all the tests. Results showing penetration depth vs. deceleration, cone and sleeve friction resistance are plotted in Figs. 26a, 26b, 26c, 27a, 27b, 27c and 27d.

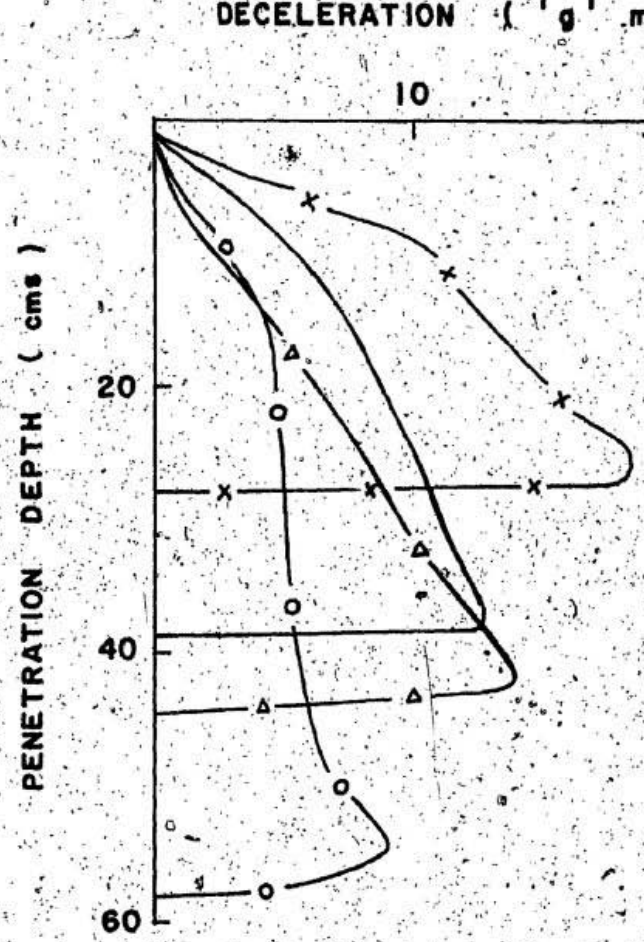
The different parameters which influence the penetration mechanism are examined below as was done for the sand targets. The characteristic feature in the case of cohesive soil targets is the sleeve friction resistance, which is a significant quantity. This was small and negligible for sand. As observed in sand targets, soil resistance for a penetrometer with 180^{o} cone is maximum in cohesive targets also. But sleeve resistance is the least among three types of cones used in this investigation.

4.6.1. Sleeve Friction and Soil Adhesion

The sleeve friction or side friction in cohesive soils is generally attributed to adhesive resistance between the soil and the penetrometer. Adhesion (c_a) between stainless steel and clay was determined from direct shear tests and the results are shown in Table 8. Similarly, the sleeve friction measured in the free fall penetration tests were expressed as unit sleeve resistance and shown in Table 8.

It is found that the value of unit sleeve resistance compares favourably with the adhesion (c_a) values.

(Text continued page 112)



CONE 60°
STAINLESS STEEL
C1 TYPE SOIL
3.56 cms. DIA. PENETROMETER ——————
7.62 cms DIA. PENETROMETER —x—x—
C2 TYPE SOIL
3.56 cms. DIA. PENETROMETER —o—o—
7.62 cms. DIA. PENETROMETER —Δ—Δ—

FIG 26a. PLOT OF DECELERATION vs. PENETRATION DEPTH VARYING SOIL PROPERTIES AND PENETROMETER DIA

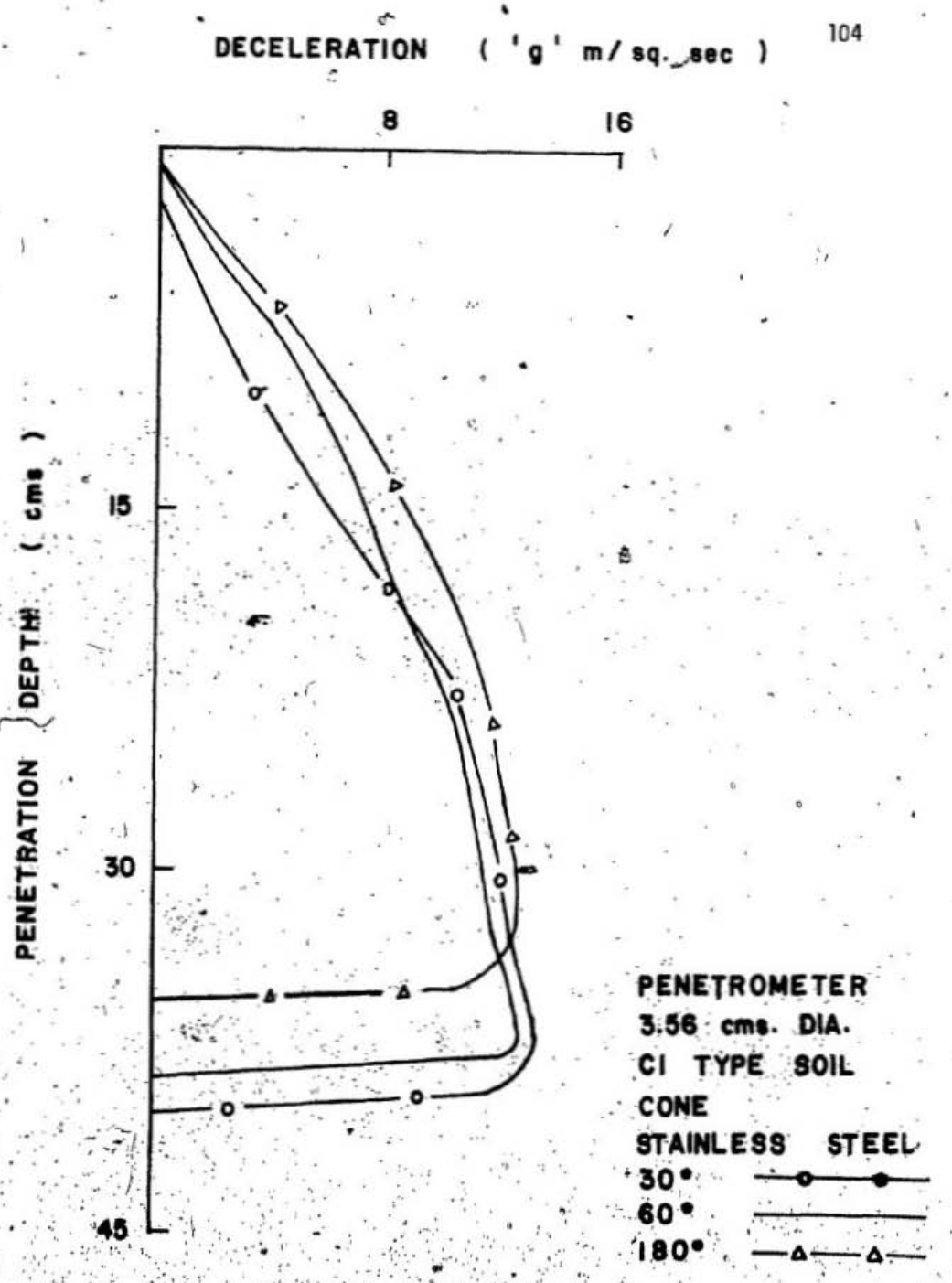


FIG 26b. PLOT OF DECELERATION vs. PENETRATION DEPTH FOR 3.56 cms. DIA PENETROMETER (α = 15°, 30° & 90°)

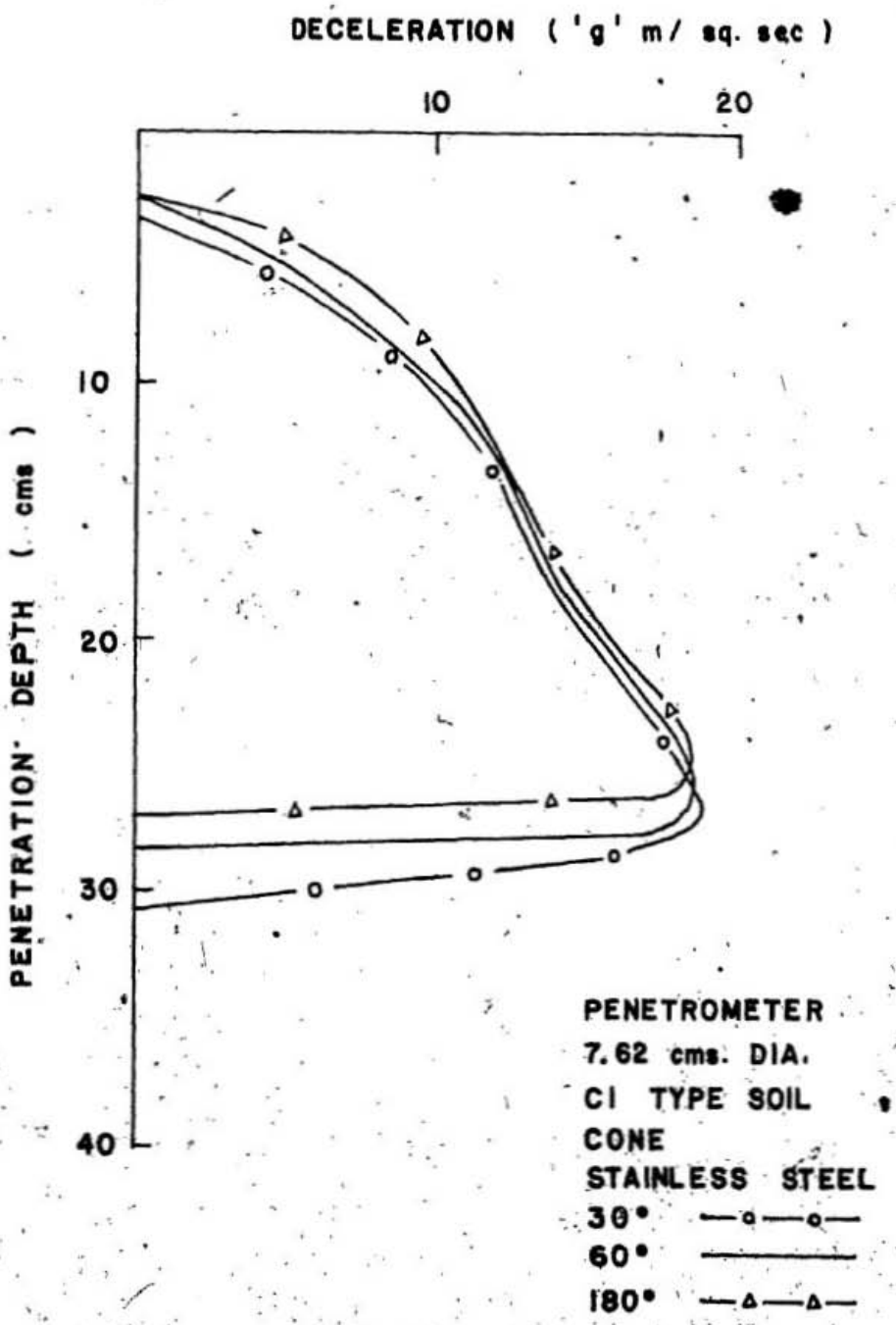


FIG 26c. PLOT OF DECELERATION vs. PENETRATION DEPTH FOR 7.62 cms DIA PENETROMETER (α = 15°, 30° & 90°)

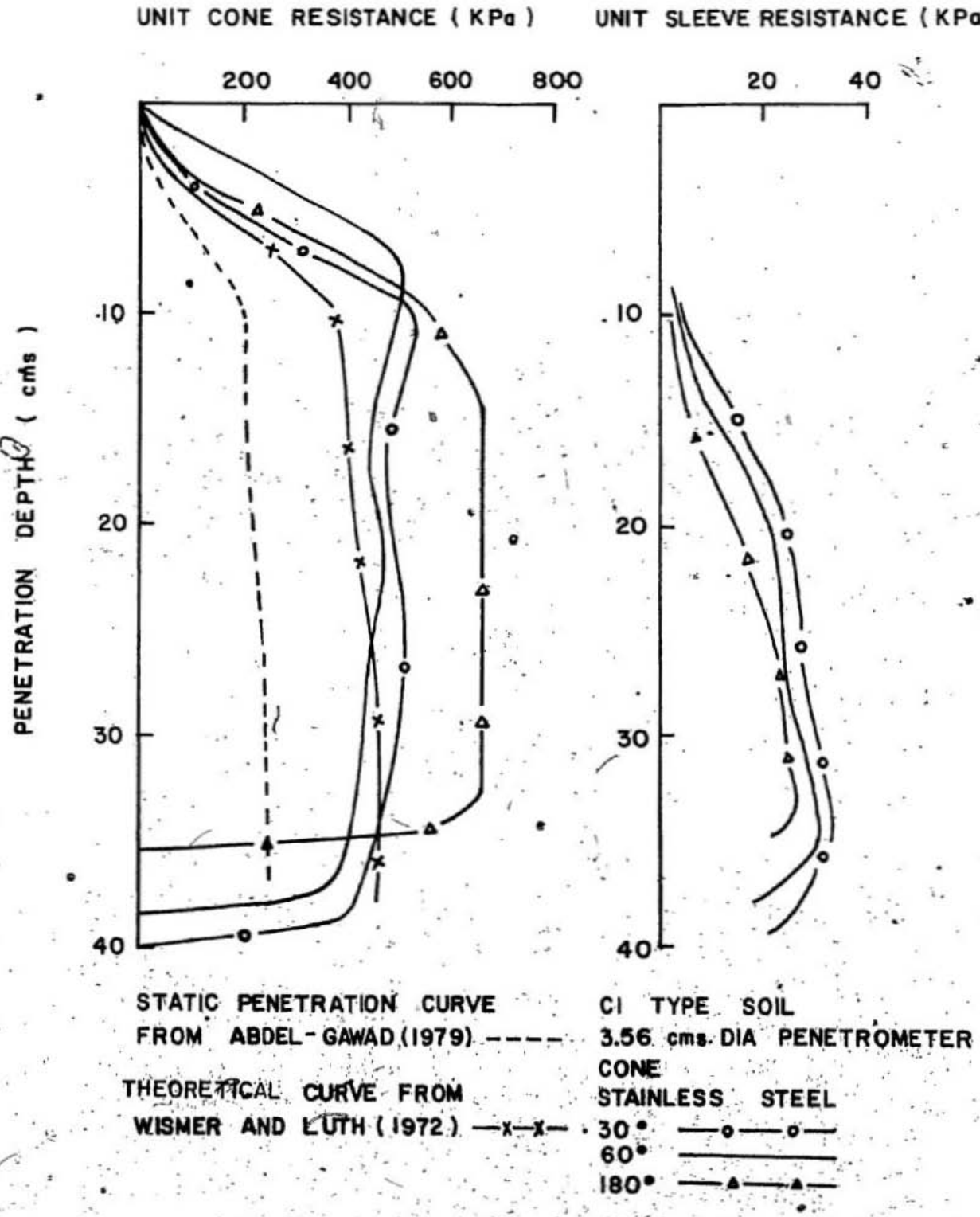


FIG 27a. COMPARISON OF ANALYTICAL AND MEASURED UNIT CONE RESISTANCE AND SLEEVE RESISTANCE FOR 3.56 cms DIA PENETROMETER

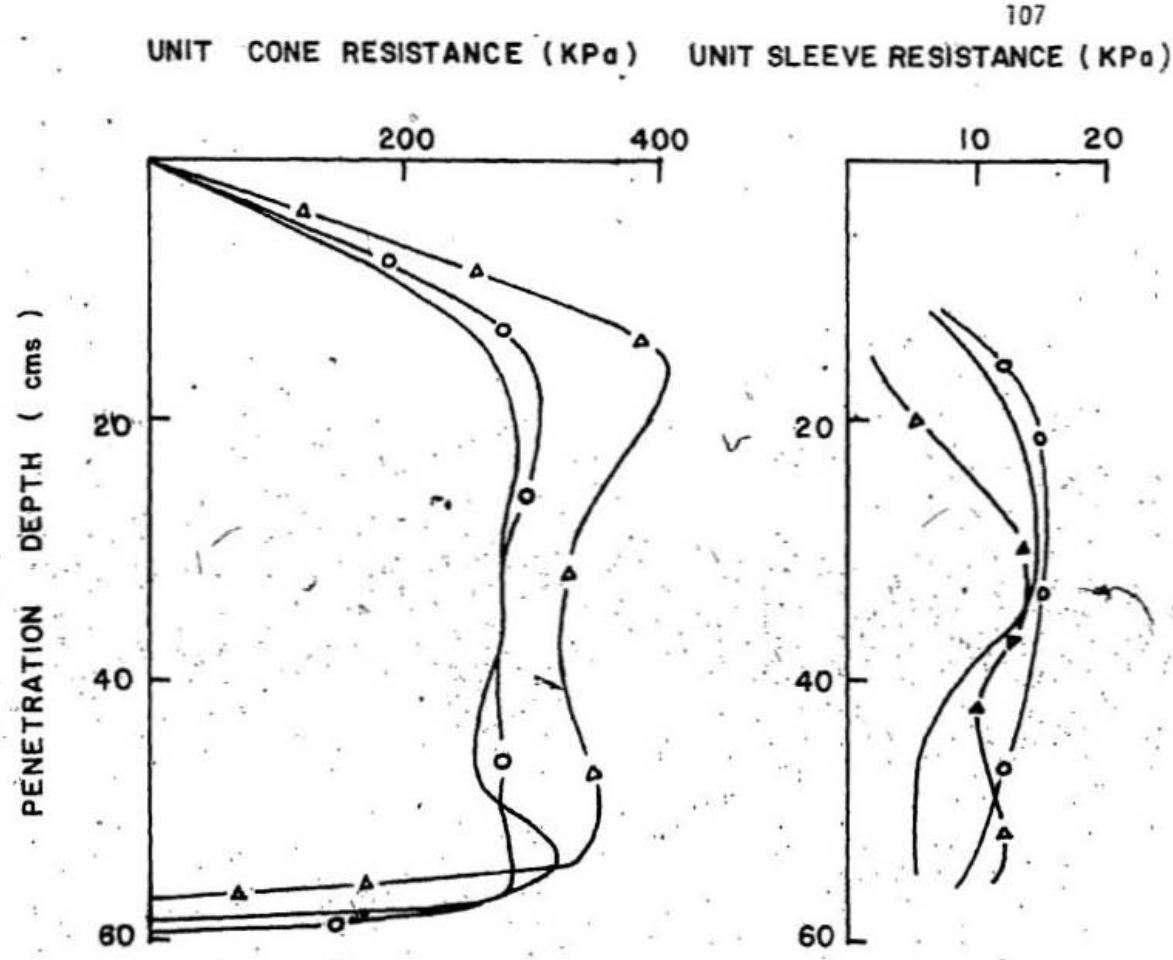
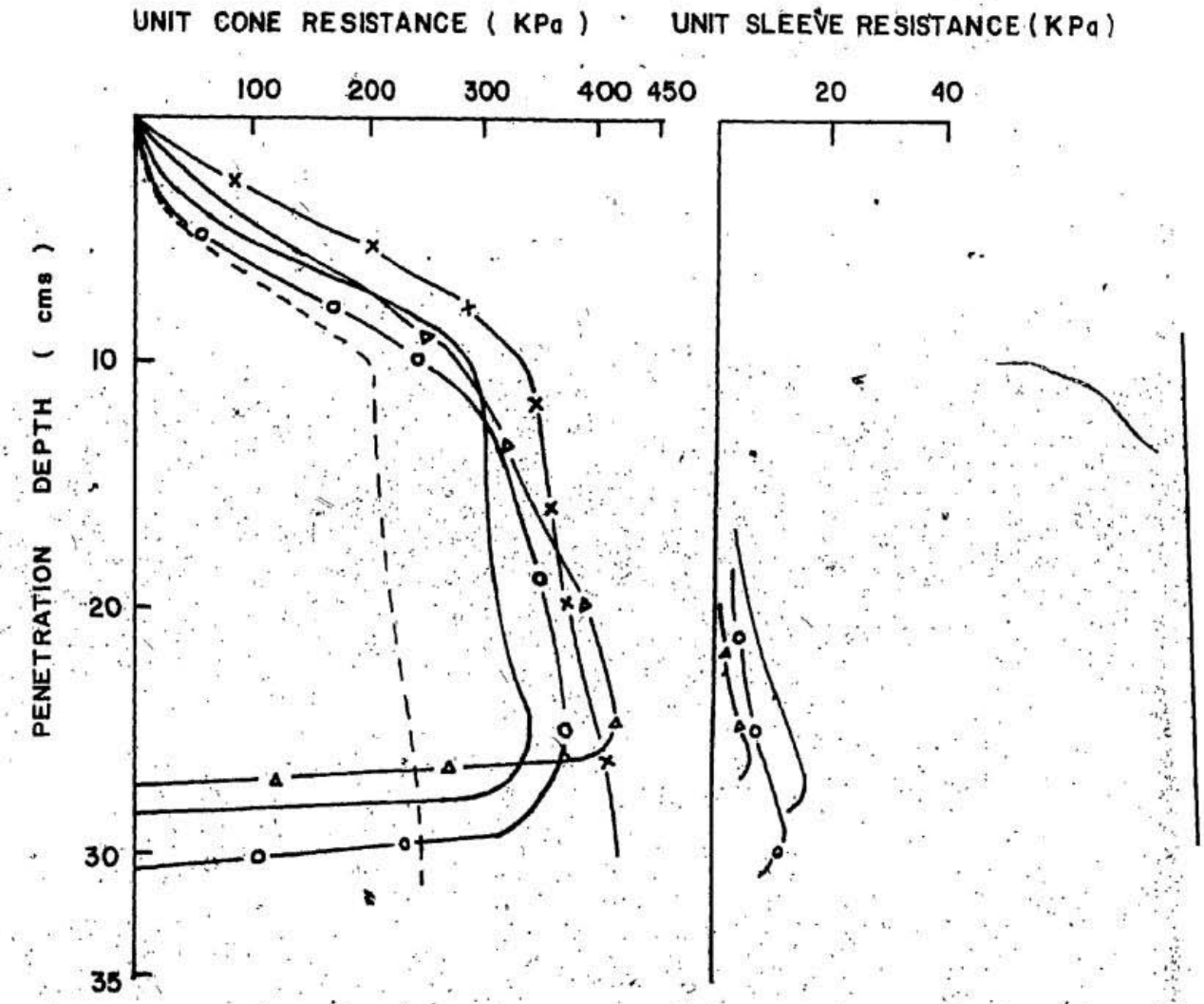


FIG 27b. PLOT OF UNIT CONE RESISTANCE AND UNIT SLEEVE RESISTANCE vs. PENETRATION DEPTH FOR 3.56 cms DIA PENETROMETER



STATIC PENETRATION CURVE
FROM ABDEL-GAWAD (1979) - - - -
3.56 cms DIA. PENETROMETER
VELOCITY = 1.76 cms / sec

THEORETICAL CURVE FROM
WISMER AND LUTH (1972) —x—x—

CI TYPE SOIL
7.62 cms. DIA. PENETROMETER
CONE
STAINLESS STEEL
30° —o—o—
60° ———
180° —Δ—Δ—

FIG 27c. COMPARISON OF ANALYTICAL AND MEASURED UNIT CONE RESISTANCE AND SLEEVE RESISTANCE FOR 7.62 cms DIA PENETROMETER

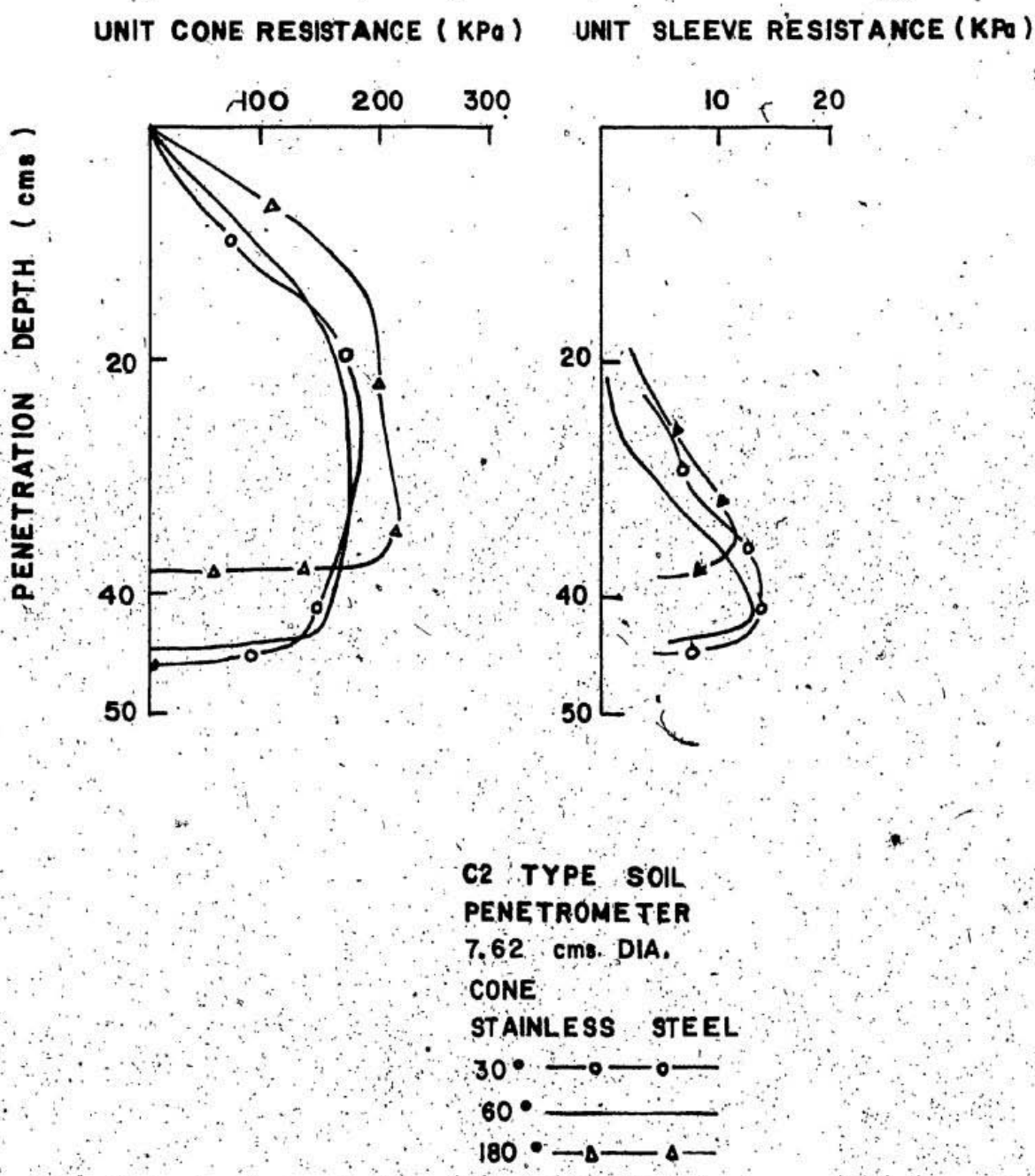


FIG 27d. PLOT OF UNIT CONE RESISTANCE AND UNIT SLEEVE RESISTANCE vs. PENETRATION DEPTH FOR 7.62 cms DIA PENETROMETER

TABLE 8. COMPARISON OF SLEEVE RESISTANCE AND ADHESION

Soil Type	Diameter of the Penetrometer cms	Cone Angle	Cone Material	Sleeve Resistance KPa	Adhesion (c_a) KPa
C1	3.56	30^o	Stainless Steel	33.51	
C1	3.56	60^o	Stainless Steel	31.75	28.88
C1	3.56	180^o	Stainless Steel	27.08	
C2	3.56	30^o	Stainless Steel	14.70	
C2	3.56	60^o	Stainless Steel	14.11	13.85
C2	3.56	180^o	Stainless Steel	12.93	

TABLE 9. CONE RESISTANCE FOR DIFFERENT NOSE SHAPES

Soil Type	Diameter of the Penetrometer cms	Cone Angle	Cone Resistance KPa	Ratio of Cone Resistance with respect to 60^{o} cone	
				Experimental	Meyerhof's Theoretical
C1	3.56	30^{o}	529.2	1.04	1.02
C1	3.56	60^{o}	509.6	1	1
C1	3.56	180^{o}	666.4	1.30	1.20
C2	3.56	30^{o}	303.6	0.92	1.02
C2	3.56	60^{o}	332.2	1	1
C2	3.56	180^{o}	431.2	1.29	1.20

4.6.2. Effect of Cone Shape

The cone resistance for tests with different cone shapes are shown in Table 9. The values obtained for a 60^{o} cone were taken as standard and the other two are expressed as a ratio of this standard value in the table. Meyerhof (1961) has expressed the bearing capacity factor (N_c) for different cone angles, and these values are also shown as ratios in the table with respect to the 60^{o} cone. Comparing the results, it is seen that the magnitude of cone pressure for the free fall condition is of a similar variation, when the cone angle is changed.

4.6.3. Effects of Water Content

Figs. 27a and 27b show plot of unit penetration resistance with respect to depth for modelling clay at the two water contents. The water content for C1 and C2 type soil are 29.61% and 34.15%, respectively. It may be seen that the penetration resistance decreases substantially with increasing water content. Similar results have been reported by Schmertmann (1974) and Melzer (1974) for quasi-static penetration test. The effect is attributed to an increase in the pore water pressure. Further, with decreasing degree of saturation, the frictional component of the soil bearing capacity becomes dominant. Tests with dry clay (Abdel-Gawad, 1979) have also clearly demonstrated this effect. Thus, a similar phenomenon is attributed to free fall penetration test also.

4.6.4. Effects of Strain-rate

Strain-rate effect is a well recognized phenomenon in cohesive soils (Whitman, 1957). This was discussed in detail in

Chapter II. Values of penetration resistance obtained by the free fall penetrometer can thus normally expected to be of a higher magnitude in comparison to quasi-static tests.

Wismer and Luth (1972) suggested a method of determining the equivalent quasi-static resistance of cohesive soils from dynamic test results. This was also distussed in Chapter II.

Equation (35), showing the strain-rate effects can be re-written as

$$\frac{q_{cd}}{q_c} = \left[\frac{\left(\frac{V_o}{d}\right)}{\left(\frac{V_s}{d_s}\right)}\right]^K \quad \ldots\ldots\ldots\ldots\ldots\ldots\ldots\ldots (40)$$

where q_{cd} = theoretical cone resistance for impact velocity V_o and diameter d

q_c = quasi-static cone resistance for a standard penetrometer with velocity V_s and diameter d_s

K = 0.100

If the penetrometer diameter is the same for both cases, then equation (40) reduces to

$$\frac{q_{cd}}{q_c} = \left[\frac{V_o}{V_s}\right]^K \quad \ldots\ldots\ldots\ldots\ldots\ldots\ldots\ldots (41)$$

or

$$q_{cd} = \left[\frac{V_o}{V_s}\right]^K q_c \quad \ldots\ldots\ldots\ldots\ldots\ldots\ldots\ldots (42)$$

Quasi-static penetration tests by Abdel-Gawad (1979) at a penetration rate 1.76 cm/sec in a soil similar to the Cl type of

soil shows a maximum unit cone resistance of 259.7 KPa. Those results are shown in Fig. 27a and 27c for the two types of penetrometer. Using equation (42), the cone resistance at a velocity of 7.75 m/sec can be written as

$$q_{cd} = 1.84\, q_c \quad \ldots\ldots\ldots\ldots \quad (43)$$

Thus, strain-rate effect can be said to cause an 84% increase in the soil resistance. Using equation (43) theoretical curves were drawn and shown in Fig. 27a and Fig. 27c. It can be seen that there is a good correlation between the resistance actually measured in a free fall penetration test and the theoretical curve obtained after correcting for strain-rate effects.

It may be relevant to point out here, that the values of sleeve friction measured and compared in Table 8 do not appear to show a significant effect due to strain-rate. This is an area that should be investigated further.

In dynamic tests, Murff and Coyle (1972) indicated that side-wall resistance is significant only under certain conditions. On the basis of experimental observations, Murff and Coyle (1973a) indicated that a critical velocity exists for all soils above which cavitation occurs. For impact velocities beyond the critical value, the resistance to penetration is experienced only by the nose of the projectile. Those critical velocities are in the order of 30 m/sec (100 ft/sec) and thus not exactly applicable to the free fall impact velocities of 7.75 m/sec obtained in this investigation. However, there is likely to be an effect of the velocity on the relative proportions of the cone and sleeve resistance. This is an area to

be pursued further.

For the soil type C2, no direct correlation was possible to determine the strain-rate effect, since quasi-static test results for this soil were not available. But, assuming the relationship obtained in equation (43), for a 60^{o} cone, an equivalent static cone resistance was obtained and was equated to

$$q_c = c\,N_c + \gamma D \quad \ldots\ldots\ldots \text{(eqn. 7)}$$

Using Meyerhof's (1976) values of N_c, c was calculated as 17.15 KPa. This compares very favourably with the actual cohesion (c) measured, which was 16.02 KPa.

4.7. Summary of Test Results--Modelling Clay

The major factor to be considered for free fall tests in clays is the effects of strain-rate. This effect not only influences the cone resistance but, depending on the velocity of penetration, it will influence the relative values of cone and sleeve resistance. While it is possible to quantify strain-rate effects and evaluate the soil shear strength, it is felt that this area requires further work.

CHAPTER V

CONCLUSIONS AND RECOMMENDATIONS

5.1. Summary and Conclusions

Free fall penetration tests were conducted with a standard 10.00 cm^2 "Fugro" type penetrometer and a 45.62 cm^2 penetrometer developed at Memorial University. For tests at sea, from structural design considerations, it is necessary to use the penetrometer of larger diameter. The laboratory experiments were designed to test both the penetrometers in the same soil target and obtain a correlation.

Tests were conducted in sand (dry and saturated) and clay (partially saturated) targets. Deceleration, cone thrust and sleeve friction were measured in each test and subsequently analyzed. Soil properties were determined by conventional laboratory tests. From the analysis of the free fall penetrometer tests, the following conclusions are drawn:

i. The cone resistance computed theoretically is in good agreement with experimental results.

ii. Penetration depth is a function of the impact velocity and also the ratio of W/A.

iii. An increase in cone sharpness increases the penetration depth. Similarly, an increase in cone roughness increases the penetration resistance.

iv. Soil density has a significant influence on the penetration mechanism.

v. Cone resistance increases in saturated sand due to negative pore pressure.

vi. Tests in clay show that the strain-rate influences the cone resistance values. However, the equivalent static values can be computed from the free fall tests using the equation of Wismer and Luth (1972).

vii. In clays, an increase in the degree of saturation decreases the cone resistance due to positive pore pressure effects.

viii. For the range of velocities tested, there was no change in the sleeve friction resistance in comparison with static tests.

5.2. Recommendations for Further Studies

Further experimental work is recommended to investigate the following effects:

i. Static and free fall penetration tests on the same soil target and correlation of results.

ii. Further investigation of the effects of W/A choosing two more values between the ranges tested in this investigation.

iii. Tests in saturated sand and clay targets with quantitative measurement of pore water pressure.

iv. Tests at different impact velocities and an evaluation of the strain-rate effect on sleeve friction.

v. Development of theoretical solutions using finite element techniques, with linear and non-linear soil response.

vi. More coordinated field and laboratory tests in order to objectively assess the soil properties from field tests.

REFERENCES

1. Abdel-Gawad, S.M., "Static Penetration Resistance of Soils," Dissertation to be submitted in partial fulfilment for M.Engg. degree, Memorial University of Newfoundland, St. John's, July, 1979.

2. Allen, W.A., Mayfield, E.B., and Morrison, H.L., "Dynamics of a Projectile Penetrating Sand," J. Applied Physics, Vol. 28, No. 3, 1957.

3. Artikoglu, N.O., "Determining Ultimate Bearing Capacity of Precast Reinforced Concrete Piles from Deep Sounding Tests in Alsancak Harbour," Proc. Fifth Int. Conf. Soil Mech. Found. Engg., Paris, Vol. 2, pp. 3-9, 1961.

4. Begemann, H.K.S., "The Friction Jacket Cone as an Aid in Determining the Soil Profile," Proc. Sixth. Int. Conf. Soil Mech. Found. Engg., Montreal, Vol. I, pp. 17-20, 1965.

5. Berre, T. and Bjerrum, L., "Shear Strength of Normally Consolidated Clays," Proc. Eighth Int. Conf. Soil Mech. Found. Engg., Moscow, Vol. I; Pt.I, pp. 39-49, 1973.

6. Bogdanovic, L., "The Use of Penetration Tests for Determining Bearing Capacity of Piles," Proc. Fifth Int. Conf. Soil Mech. Found. Engg., Paris, Vol. II, pp. 17-22, 1961.

7. Casagrande, A. and Wilson, S.D., "Effect of Rate Loading on the Strength of Clays and Shales at Constant Water Content," Geotechnique, Vol. II, pp. 251-263, 1951.

8. Chari, T.R., Smith, W.G., and Zielinski, A., "Use of Free Fall Penetrometer in Sea Floor Engineering," Conf. Rec., Ocean 78 IEEE-MTS Conf., 1978.

9. Chari, T.R., Abdel-Gawad, S.M., and Chaudhuri, S.N., "Geotechnical Survey of the Sea-floor with a Free Fall Penetrometer," Proc. Fifth Int. Conf. Port and Ocean Engg. under Arctic Conditions (POAC), Trondheim, Norway, August, 1979. (To be published).

10. CSA Standard B95-1962. Surface Texture (Roughness, Waviness and Lay). Canadian Standard Association, Ottawa, Canada.

11. Dayal, U., "Instrumented Impact Cone Penetrometer," Memorial University of Newfoundland, Canada, Ph.D. dissertation, 222 pp., 1974.

12. De Beer, E.E. and Martens, A., "Method of Computation of an Upper Limit for the Influence of the Heterogenity of Sand Layers on the Settlements of Bridges," Proc. Fourth Int. Conf. Soil Mech. Found. Engg., London, Vol. I, pp. 275-282, 1957.

13. De Ruiter, J., "Electrical Penetrometer for Site Investigations," J. Soil Mech. Found. Divn., Proc. ASCE, Vol. 90, no SM 2, pp. 457-473, Feb. 1971.

14. De Ruiter, J., "The Use of In-situ Testing for North Sea Soil Studies," Proc. Offshore Europe '75, Aberdeen, pp. 219.1-219.10, 1975.

15. Drozd, K., "The Influence of Variable Moisture Content in Sand on the results of Dynamic Penetration Test," Proc. Sixth Int. Conf. Soil Mech. Found. Engg., Montreal, Vol. 3, pp. 335-336, 1965.

16. Durgunoglu, Turan H. and Mitchell, James K., "Static Penetration Resistance of Soils," Space Sciences Laboratory, Univ. of California, Berkeley, 223 pp., 1973.

17. Durgunoglu, H.T. and Mitchell, J.K., "Static Penetration Resistance of Soils: I-Analysis, II-Evaluation of Theory and Implications for Practice," Proc. ASCE Specialty Conference on In-situ Measurement of Soil Properties, Vol. I, pp. 151-189, 1975.

18. Ferguson, G.H., McClelland, B., and Bell, W.D., "Seafloor Cone Penetrometer for Deep Penetration Measurements of Ocean Sediment Strength," Proc. 9th Offshore Technology Conf., OTC 2787, Vol. I, pp. 471-478, 1977.

19. Hitchings, G.A., Bradshaw, H., and Labiosa, T.D., "The Planning and Execution of Offshore Site Investigations for a North Sea Gravity Platform," Proc. 8th Offshore Technology Conf., OTC 2430, Vol. I, pp. 61-74, 1976.

20. Jones, J.M., "The Use of Impact Penetrometer in Remote Sensing Study of the Sea Bed Properties," 2nd CSCE Hydrotechnical Conference, Atlantic Region, Amherst, N.S., 1976.

21. Karafiath, Leslie L., "On the Effect of Base Friction on Bearing Capacity," J. Terramechanics, Vol. 9, No. 1, pp. 9-17, 1972.

22. Ladanyi, B. and Eden, W.J., "Use of Deep Penetration Test in Sensitive Clays," Proc. Seventh Int. Conf. Soil Mech. Found. Engg., Mexico, Session I, pp. 225-230, 1969.

23. Lambe, T.W., "Soil Testing for Engineers," John Wiley and Sons, New York, 1951.

24. Meigh, A.C. and Nixon, I.K., "Comparison of In-situ Tests for Granular Soils," Proc. Fifth Int. Conf. Soil Mech. Found. Engg., Paris, Vol. I, pp. 499-507, 1961.

25. Melzer, K.J., "Use of the WES Cone Penetrometer in Cohesive Soils," Proc. European Symposium on Penetration Testing, Stockholm, Vol. 2, Part 2, pp. 263-268, 1974.

26. Meyerhof, G.G., "Penetration Tests and Bearing Capacity of Cohesionless Soils," J. Soil Mech. Found. Divn., ASCE, Vol. 82, No. SM1, 1956.

27. Meyerhof, G.G., "The Ultimate Bearing Capacity of Wedge-Shaped Foundations," Proc. Fifth Int. Conf. Soil Mech. Found. Engg., Paris, Vol. 2, pp. 105-109, 1961.

28. Meyerhof, G.G., "Bearing Capacity and Settlement of Pile Foundations," J. Geotechnical Engg. Divn., Proc. ASCE, Vol. 102, No. GT 3, pp. 197-228, 1976.

29. Mitchell, J.K., and Durgunoglu, H.T., "In-situ Strength by Static Cone Penetration Test," Proc. Eighth Int. Conf. Soil Mech. Found. Engg., Moscow, Vol. 1.2, pp. 279-286, 1973.

30. Mitchell, J.K. and Lunne, Tom A., "Cone Resistance as Measure of Sand Strength," J. Geotechnical Engg. Divn., Proc. ASCE, Vol. 104, No. GT7, pp. 995-1012, July, 1978.

31. Murff, J.D. and Coyle, H.M., "A Laboratory Investigation of Low Velocity Penetration," Proc. Conf. Rapid Penetration of Terrestrial Materials, Texas A & M University, pp. 319-360, 1972.

32. Murff, J.D. and Coyle, H.M., "Prediction Method for Projectile Penetration," Tech. Notes, J. Soil Mech. Found. Divn., ASCE, No. SM 11, pp. 1033-1032, 1973.

33. Murff, J.D. and Coyle, H.M., "Low Velocity Penetration of Kaolin Clay," J. Soil Mech. Found. Divn., Proc. ASCE, No. SM5, pp. 375-389, May, 1973 (a).

34. O'Neill, H.M., "Direct Shear Test for Effective Strength Parameters," J. Soil Mech. Found. Divn., ASCE, Vol. 88, No. SM4, Proc. Paper 3232, 1962.

35. Orrze, O. and Broms, B., "Strength and Deformation Properties of Soils as Determined by a Free Falling Weight," Proc. Swedish Geotechnical Institute, No. 23, Stockholm, 1970.

36. Plantema, G., "Influence of Density on Sounding Results in Dry, Moist and Saturated Sands," Proc. Fourth Int. Conf. Soil Mech. Found. Engg., London, Vol. I, pp. 237-240, 1957.

37. Proceedings of European Symposium on Penetration Testing (ESOPT), Stockholm, Vol. 1, 2.1 and 2.2, 1974.

38. Richardson, J., Archie, M., and Whitman, R.V., "Effect of Strain-Rate upon Undrained Shear Resistance of a Saturated Remoulded Fat Clays," Geotechnique, Vol. XIII, pp. 310-324, 1963.

39. Roy, N., and Sarathi, P. "Strain Rate Behaviour of Compacted Silt," J. Geotechnical Engg. Divn., Proc. ASCE, pp. 347-360, 1976.

40. Sanglerat, G., "The Penetrometer and Soil Exploration," Elsevier Publishing Company, 1972.

41. Schmid, Werner E., "Penetration of Objects into the Ocean Bottom (The State-of-the-Art)", Naval Civil Engg. Laboratory Contract Report (Contract No. N62399-68-C-0044), Princeton, New Jersey, pp. 1-118, 1969.

42. Schmertmann, J.H., "Static Cone to Compute Static Settlement Over Sand," J. Soil Mech. Found. Divn., Proc. ASCE, Vol. 96, No. SM3, pp. 1011-1043, 1970.

43. Schmertmann, J.H., "Penetration Pore Pressure Effects on Quasi-static Cone Bearing, q_c," Proc. European Symposium on Penetration Testing, Stockholm, Vol. 2, Pt. 2, pp. 340-350, 1974.

44. Schmertmann, J., "The Measurement of In-situ Shear Strength," Proc. ASCE Specialty Conference on In-situ Measurements of Soil Properties, Vol. 2, pp. 57-138, 1975.

45. Schultze, E. and Melzer, K., "The Determination of the Density and the Modulus of Compressibility of Non-Cohesive Soils by Soundings," Proc. Sixth Int. Conf. Soil Mech. Found. Engg., Vol. I, pp. 354-358, 1965.

46. Scott, R.A. and Pearce, R.W., "Soil Compaction by Impact," Geotechnique, Vol. XXV, No. 1, pp. 19-30, 1975.

47. Terzaghi, K., "Theoretical Soil Mechanics," John Wiley & Sons, New York, 1943.

48. Thompson, L.J., Ferguson, G.H., Murff, J.D. and Cetiner, Ayhan, "The Effect of Soil Parameters on Earth Penetration," Technical Report to Sandia Laboratories, Texas A & M Research Foundation, College Station, Texas, July, 1969.

49. Turnage, G.W., "Influence of Viscous-Type and Inertial Forces on the Penetration Resistance of Saturated, Fine-Grained Soils," J. Terramechanics, Vol. 10, No. 2, pp. 63-76, 1973.

50. Turnage, G.W. and Freitag, D.R., "Effects of Cone Velocity and Size on Soil Penetration Resistance," Paper No. 69-670, Winter Meeting, American Society of Agricultural Engg., Chicago, 1969.

51. Van der Veen, C., "The Bearing Capacity of a Pile Predetermined by a Cone," Proc. Fourth. Int. Conf. Soil Mech. Found. Engg., London, pp. 72-75, 1957.

52. Vesic, A.S., Banks, D.D. and Woodard, J.M., "An Experimental Study of Dynamic Bearing Capacity of Footings on Sand," Proc. Sixth Int. Conf. Soil Mech. Found. Engg., Montreal, Vol. II, pp. 209-213, 1965.

53. Wang, L.W., "Low Velocity Projectile Penetration," J. Soil Mech. Found. Divn., ASCE, 97, No. SM12, pp. 1635-1653, 1971.

54. Whitman, R.V., "The Behaviour of Soils Under Transient Loadings," Proc. Fourth Int. Conf. Soil Mech. Found. Engg., London, Vol. I, pp. 207-210, 1957.

55. Whitman, R.V., "Some Considerations and Data Regarding the Shear Strength of Clays," Proc. Research Conf. Shear Strength of Cohesive Soils, Sponsored by the Soil Mech. Found. Divn., ASCE, Colorado, pp. 581-614, 1960.

56. Wismer, R.D. and Luth, H.J., "Rate Effects in Soil Cutting," J. Terramechanics, Vol. 8, No. 3, pp. 11-21, 1972.

57. Young, C.W., "Depth Prediction for Earth Penetration Projectiles," J. Soil Mech. Found. Divn., ASCE, Vol. 95, No. SM3, Proc. Paper 6558, pp. 803-817, 1969.

58. Young, C.W., "Empirical Equations for Predicting Penetration Performance in Layered Earth Materials for Complex Penetration Configurations," No. SC-DR-72 0523, Sandia Laboratories, Albuquerque, New Mexico, December, 1972.

59. Zuidberg, H.M., "The Seacalf, a Submersible Cone Penetrometer Rig," Marine Geotechnology, Vol. I, No. 1, pp. 15-32, 1975.

APPENDIX A

FIGURES SHOWING TALYSURF ROUGHNESS MEASUREMENTS

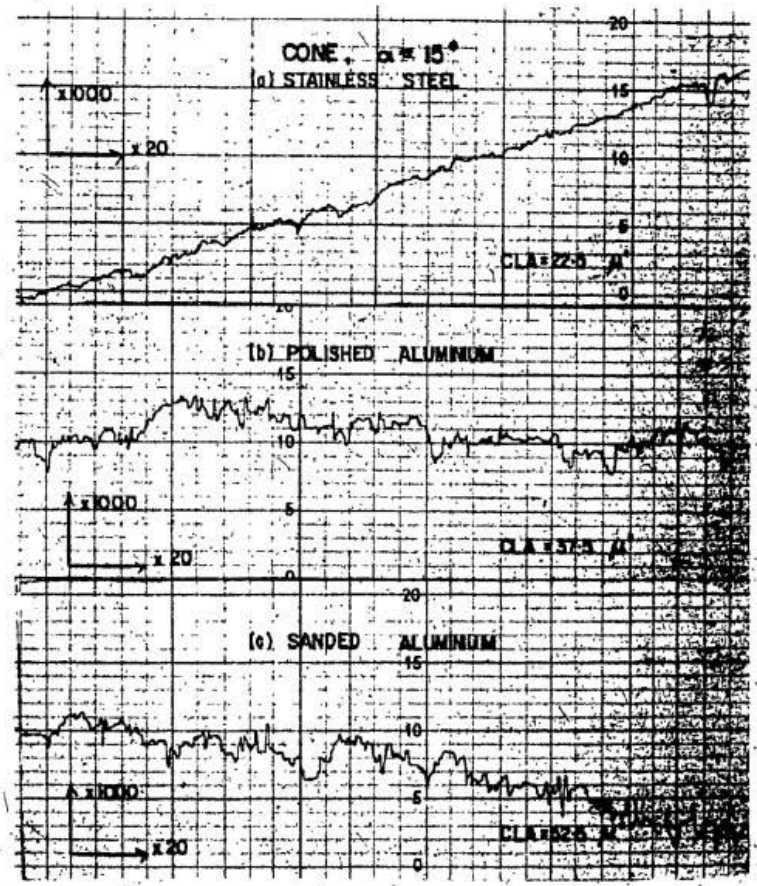


FIG A1. TALYSURF ROUGHNESS MEASUREMENT FOR CONE (α = 15°)

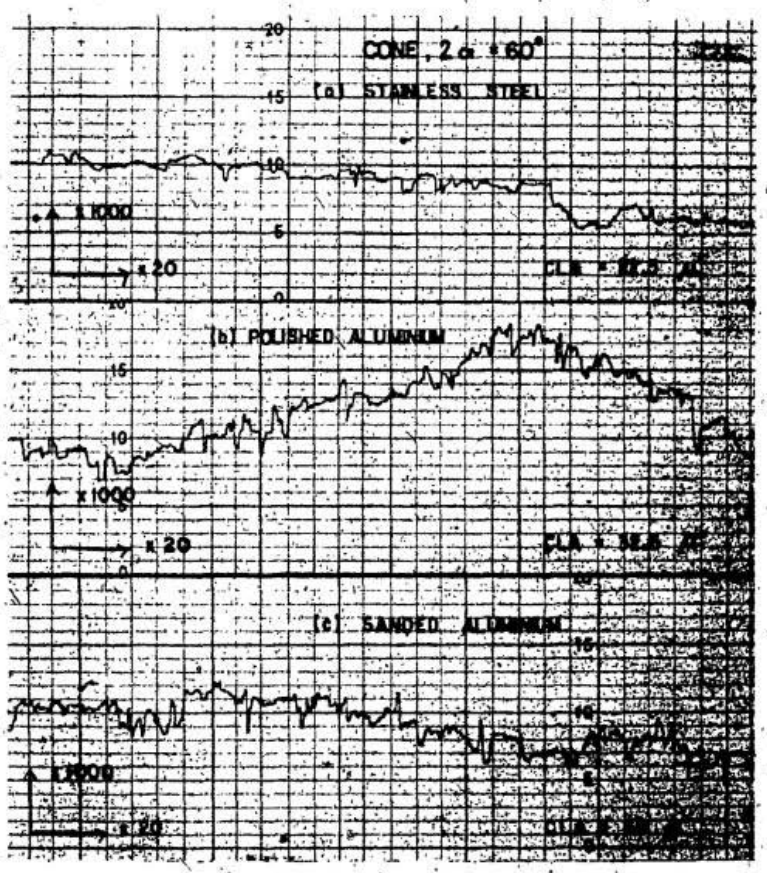


FIG A2. TALYSURF ROUGHNESS MEASUREMENT FOR CONE ($\alpha = 30^0$)

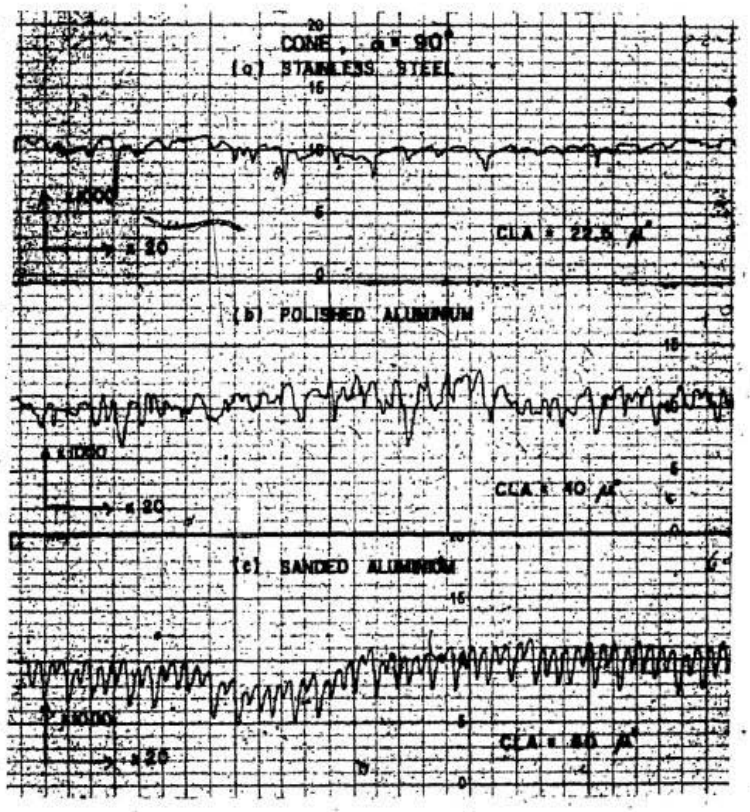


FIG A3. TALYSURF ROUGHNESS MEASUREMENT FOR CONE ($\alpha = 90^0$)

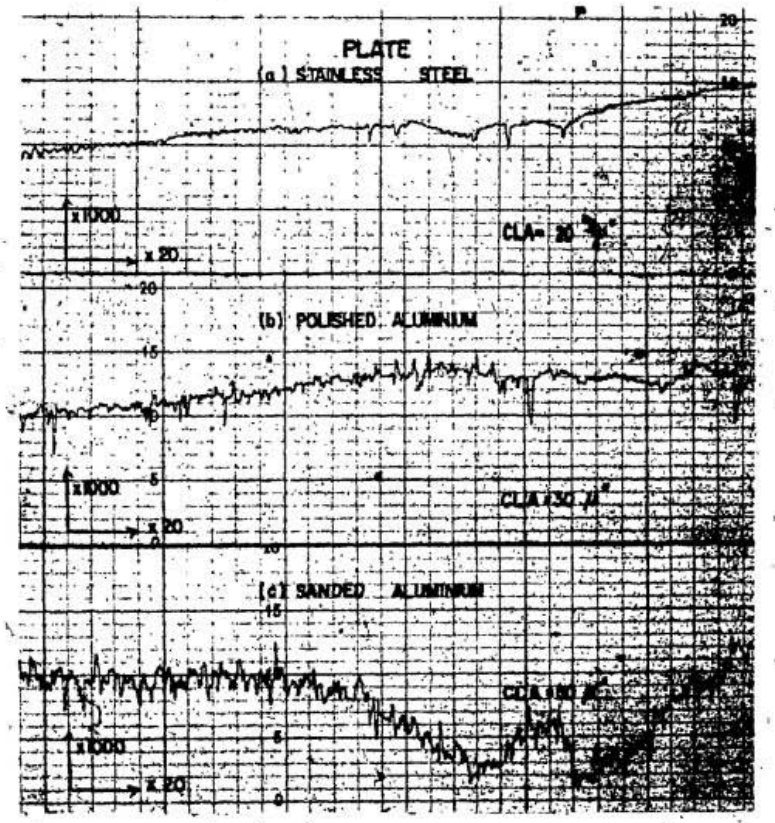
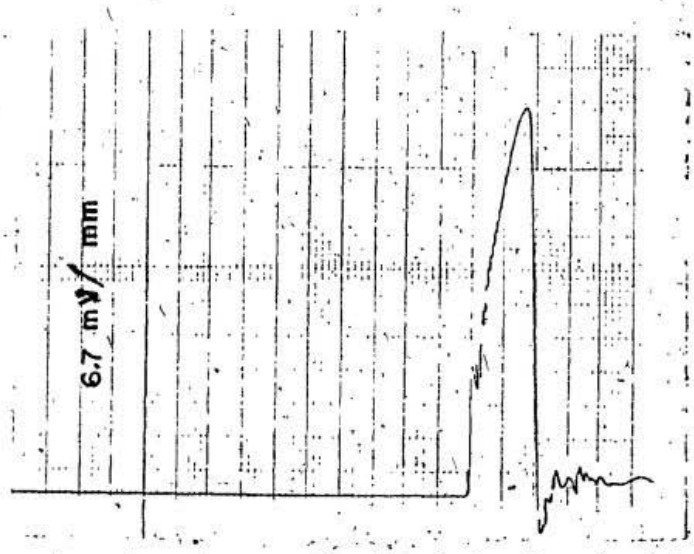


FIG A4. TALYSURF ROUGHNESS MEASUREMENT FOR PLATE

APPENDIX B

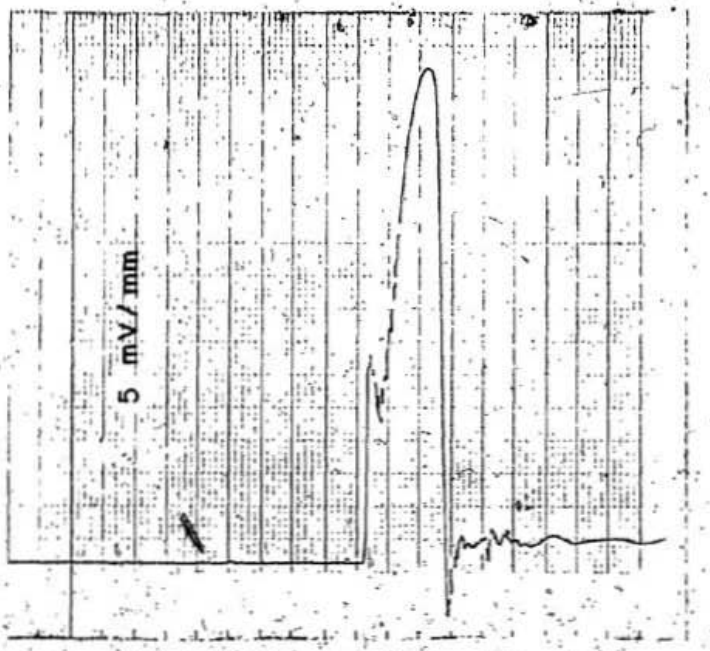
FIGURES SHOWING TYPICAL OUTPUT FROM FREE FALL PENETRATION TESTS



SI TYPE SOIL
PENETROMETER
3.56 cms DIA
CONE
ANGLE 60°
STAINLESS STEEL

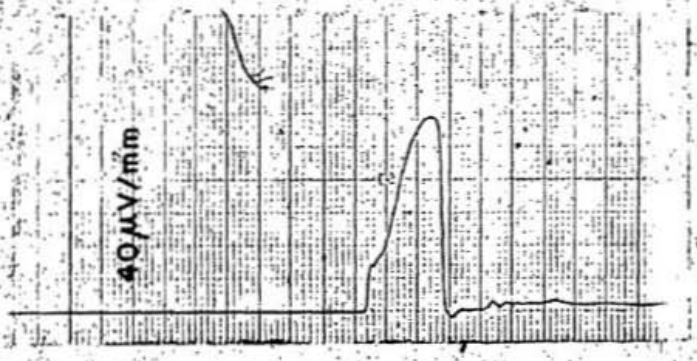
FIG B1. TYPICAL OUTPUT FOR DENSE SAND TARGET

S2 TYPE SOIL
PENETROMETER
3.56 cms DIA
CONE
ANGLE 60°
STAINLESS STEEL

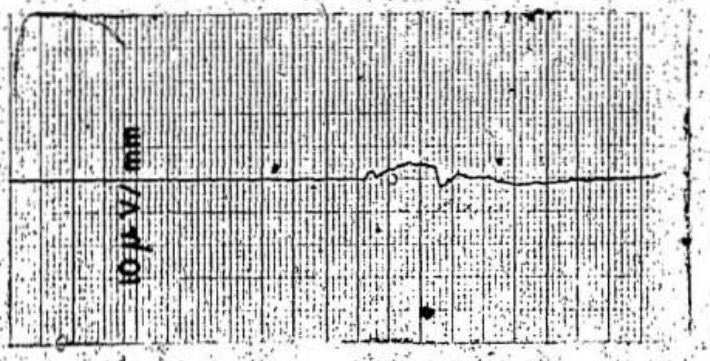


TIME (5 milli sec/mm)

DECELERATION



CONE RESISTANCE



SLEEVE RESISTANCE

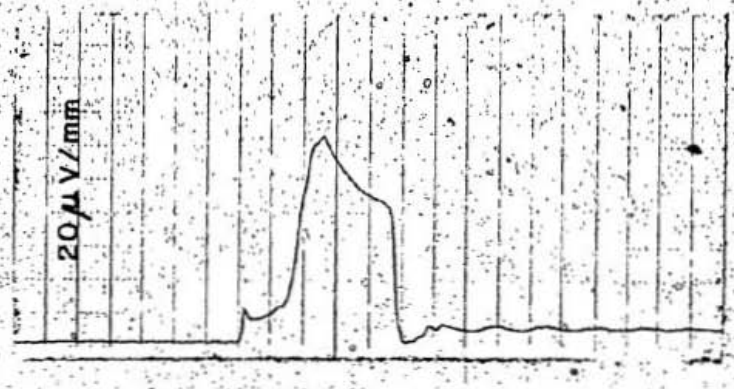
FIG 82. TYPICAL OUTPUT FOR MEDIUM DENSE SAND TARGET



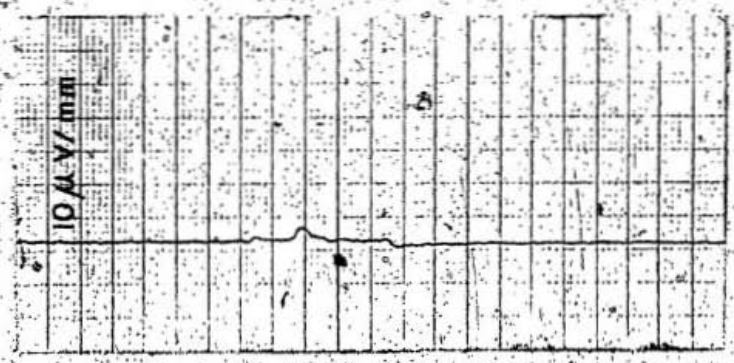
TIME (5 milli sec/mm)

DECELERATION

S3 TYPE SOIL PENETROMETER
3.56 cms DIA
CONE
ANGLE 60°
STAINLESS STEEL

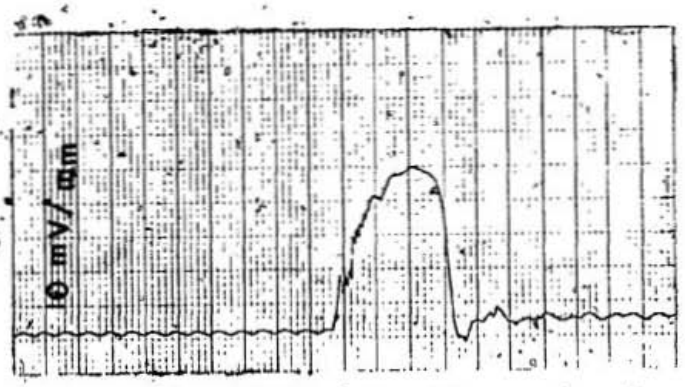


CONE RESISTANCE



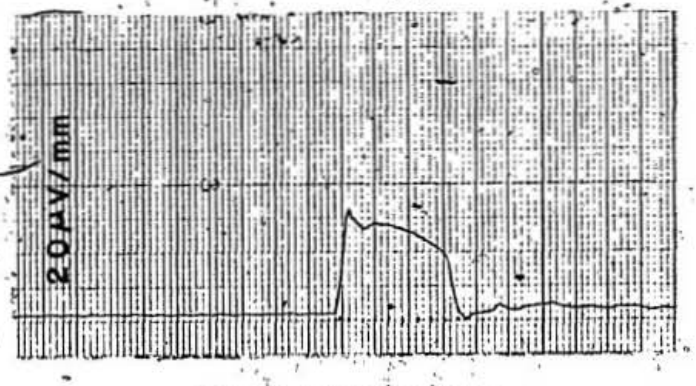
SLEEVE RESISTANCE

FIG B3. TYPICAL OUTPUT FOR LOOSE SAND TARGET

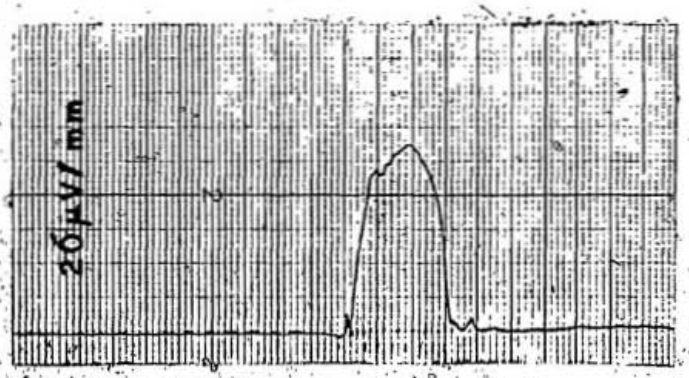


TIME (5 milli sec / mm)

DECELERATION



CONE RESISTANCE



SLEEVE RESISTANCE

C I TYPE SOIL
PENETROMETER
3.56 cms DIA
CONE
ANGLE 30°
STAINLESS STEEL

FIG B4. TYPICAL OUTPUT FOR CLAY TARGET

APPENDIX C

COMPUTER PROGRAM FOR PENETRATION VELOCITY AND DEPTH

```
//E3014603 JOB (3014,603X,1,1),CHAUDHURI,CLASS=X,REGION=100K
//     EXEC FORTGCLG
//FORT.SYSIN  DD  *
C      COMPUTATION OF PENETRATION DEPTH AND VELOCITY FOR A
C      FREE FALL PENETROMETER
       DIMENSION X(15),T(15),V(15)
       REAL NL
   99  FORMAT(//)
       INCT=1
   98  READ(5,50)D,NL,AM,V0,DR
   50  FORMAT(5F8.4)
       C=(96.6-(37.3*(NL/D)))*(D**2.0)*(DR)
       AK=(162.0)*(D)*(DR)
       P=-(23[illegible].0)*(D**2.0)*(DR)
       ALFA=C/(2.0*AM)
       W=(((4.0*AM*AK)-(C**2))**0.5)/(2.0*(AM))
       A=-(P/AK)
       B=(V0+(A)*(ALFA))/W
       TMAX=ATAN(((B*W)-(A*ALFA))/((A*W)+(B*ALFA)))/W
       N=1
       DO 30 I=1,10
       T(I)=(N/10.0)*(TMAX)
       X(I)=((A*COS(W*T(I)))+(B*SIN(W*T(I))))/(EXP(ALFA*(T(I))))+(P/AK)
       V(I)=((B*W-A*ALFA)*(COS(W*T(I)))-(A*W+B*ALFA)*(SIN(W*T(I))))*
     *(EXP(ALFA*(T(I))))
       N=N+1
   30  CONTINUE
       PRINT 99
       WRITE(6,50)D,NL,AM,V0,DR
       PRINT 99
       WRITE(6,60)
   60  FORMAT(5X,'DEPTH IN MTS')
       PRINT 99
       WRITE(6,61)(X(I),I=1,10)
   61  FORMAT(1X,10(2X,F6.4))
       PRINT 99
       WRITE(6,80)
   80  FORMAT(5X,'VELOCITY IN M/SEC')
       WRITE(6,61)(V(I),I=1,10)
       INCT=INCT+1
       IF(INCT.LT.10)GO TO 98
       STOP
       END
/*
//LKED.SYSLIB DD DSN=SYS1.FORTLIB,DISP=SHR
//   DD DSN=NLCS.IMSLLIB,DISP=SHR
//GO.SYSIN   DD  *
/*
//
```